ULTRASONIC TOXICITY: A PRELIMINARY INVESTIGATION OF EFFECTS ON MURINE GONADS AND THE IN UTERO FETUS

BY

JOHN KISSLING BRADY

B.S., University of Illinois, 1970
M.S., University of Illinois, 1973

THESIS

Submitted in partial fulfillment of the requirements for the degree of Doctor of Philosophy in Electrical Engineering in the Graduate College of the University of Illinois at Urbana-Champaign, 1979

Urbana, Illinois

UNIVERSITY OF ILLINOIS AT URBANA-CHAMPAIGN

THE GRADUATE COLLEGE

July 15, 1977

WE HEREBY RECOMMEND THAT THE THESIS BY

JOHN KISSLING BRADY

ENTITLED ULTRASONIC TOXICITY: A PRELIMINARY INVESTIGATION OF EFFECTS ON MURINE GONADS AND THE IN UTERO FETUS

BE ACCEPTED IN PARTIAL FULFILLMENT OF THE REQUIREMENTS FOR THE DEGREE OF DOCTOR OF PHILOSOPHY

Floyd Gunn
Director of Thesis Research

Eb Gordon
Head of Department

Committee on Final Examination†

Floyd Gunn
Chairman

Wm O'Brien

Joseph M. Crowley

M. L. Babcock

C. R. Graves

† Required for doctor's degree but not for master's.

O-517

ULTRASONIC TOXICITY: A PRELIMINARY INVESTIGATION OF EFFECTS ON MURINE GONADS AND THE IN UTERO FETUS

John Kissling Brady, Ph.D.
Department of Electrical Engineering
University of Illinois, Urbana-Champaign, 1979

This thesis reports the initial findings of a study designed to assess the possible effects of ultrasound on the mammalian reproductive tract. The experimental study began as a result of estimates suggesting that appreciable portions of the population will have the opportunity for multiple exposures to ultrasound during the developmental and growth periods of pregnancy. In the design of the study the following objectives were to be realized from the animal experiments:

1) guidance in the selection of parameters for human exposures to ultrasound, and

2) the details necessary for improving observability for detecting ultrasonically related hazardous effects in the human. The fact that deleterious effects have not been reported after nearly a quarter century of clinical involvement is encouraging, but may also be a false security should delayed effects be forthcoming.

The study is divided into two major sections; the first deals with toxicity effects to the in-utero fetus as a function of the day of gestation, the acoustic intensity and the time

of exposure to the acoustic field. The second section addresses the effects of ultrasound on the murine gonads, the testis and ovary, as a function of acoustic intensity, exposure time to the acoustic field and acoustic frequency. The variations in the frequency parameter were confined to the determination of the acoustic absorption coefficient of the testis which was determined experimentally to help elucidate cause and effect of testicular damage.

The exposure parameters for the in-utero irradiations were a frequency of 1.0 MHZ, acoustic intensities in the range of 1 w/cm^2 to 10 w/cm^2 and selected irradiation times of 1 sec to 100 sec.

The exposures were performed using two quartz crystal transducers each having different, well-defined acoustic field patterns. The use of two transducers was dictated by the ultrasonic intensity and time of exposure constraints of the investigation. Calibrations, to determine the acoustic field distribution and peak free-field intensity at the transverse plane occupied by the experimental animal, were carried out weekly. Checks of the entire RF generating system were performed monthly.

The exposure regime for the in-utero insonations were carried out under computer control. The introduction of digital equipment to the procedure allowed all the experiments to be performed in a double-blind fashion, thus minimizing experimenter bias in the study. The computer also permitted a single investigator to carry out the irradiations with no sacrifice in uniformity or limits to experimental capacity.

The testicular and ovarian insonations were performed at a frequency of 1 MHZ (except the exposures performed to determine the acoustic absorption coefficient, which were done over a range of 1.0 - 9 MHZ, predetermined acoustic intensities of 1.0 w/cm^2 to 100 w/cm^2 and exposure times of 1 to 10 sec. A third, focussed transducer was used for these experiments to both limit the tissue volume exposed to the acoustic field, and to obtain the higher acoustic intensities initially thought necessary to obtain testicular damage for characterizations. A reduction in the acoustic intensity was possible after the characterization of the acoustic damage to the tissue.

The calibration and exposure procedures for the testes and ovaries were similar to those for the in-utero fetus, with the exception of computer control, which was found to be unnecessary.

The methods of analyzing the experimental results are unique to each experimental procedure. The observations and data collected from the in-utero exposures have been subjected to a multiple regression analysis and the results are presented as regression equations showing the significant ($P<.05$) statistical relations between experimental variables. The results obtained from the testicular and ovarian exposures are photographic. The photographs are taken directly from the photomicrographs of histologically prepared tissue slides, and demonstrate the range of damage observed in the irradiated tissue.

The results of the statistical analysis of the in-utero ultrasonic exposures are designed to point out any significant difference between the three groups of experimental animals; the exposed group, the sham exposed group and the control group. Within each group of animals, multiple regression curves have been generated to elucidate any effects of acoustic intensity, time of exposure, number of exposures, age, gestation day, etc.

The data obtained in this experimental series, and the statistical analysis of this data have shown that, currently, there is not a simple linear relationship between the acoustic field variables and the effects observable on in-utero irradiated mice. The analysis presented here should form a sound basis for further examination of the complex interaction of ultrasound and fetal development. The analytical methods used in this thesis may also lend themselves to the use of extending the study to other mammalian species and eventually to human effects.

The toxicity data collected on the mouse testes and ovaries was an histological method, and is presented as a series of photomicrographs. Two acoustic intensities, which were used to generate a preponderance of the available data, were chosen to provide the acoustic damage findings from this study. The acoustic intensities chosen, 25 w/cm^2 and 10 w/cm^2, each for a 30 sec duration, produce observable damage in the murine testes which ranges from gross destruction to quite subtle alteration. The amount of observed damage is a function of time. This damage is observable at levels from the subcellular to the whole organ level, and is characterized by cell disruption,

vacuolization, etc. The basic similarities, at the cellular level, among mammalian testicular tissue may permit cross-species inferences as to the interactions of acoustic field and non-murine reproductive tissues. Inferences of this kind would permit the knowledgeable use of clinical ultrasonic devices in diagnostic and therapeutic areas, viz., testicular tumor and cysts, with less risk of damage to the reproductive function.

The current extensive use of ultrasonic devices, e.g., fetal heart monitors and labor monitors, on pregnant women lends immediacy to the need for toxicity information on the female organs of reproduction. During this study the murine ovaries were subjected to acoustic fields having a range of peak intensities from 5 w/cm^2 to over 100 w/cm^2. The exposures were performed both trans-skin and with only the peritoneum between the ovary and the ultrasonic transducers. The ovaries were collected from the animals at various times, post irradiation, and histologically prepared for microscopic examination. No observable, acoustically induced, damage was found in any of the organs. A definitive reason for this seeming immunity to acoustic damage was not found, but speculation on a possible cause involves the physical dimensions relative to the acoustic wave length and the relative acoustic impedance of the tissue. It is possible that exposures over a broad range of acoustic frequencies will resolve this anomaly.

ULTRASONIC TOXICITY: A PRELIMINARY INVESTIGATION OF EFFECTS ON MURINE GONADS AND THE IN UTERO FETUS

BY

JOHN KISSLING BRADY

B.S., University of Illinois, 1970
M.S., University of Illinois, 1972

THESIS

Submitted in partial fulfillment of the requirements for the degree of Doctor of Philosophy in Electrical Engineering in the Graduate College of the University of Illinois at Urbana-Champaign, 1979

Urbana, Illinois

ACKNOWLEDGEMENT

The debt of gratitude owed to the many individuals, both within the laboratory and without is immeasurable. To my advisor, Dr. Floyd Dunn, is due my deepest thanks for his boundless patience, encouragement, assistance and advice in the performance of the work, the writing of this thesis and the expertise applied to all aspects of this endeavor.

The contributions to all aspects of this study by Dr. William D. O'Brien, Jr. have given a breadth and depth to this work that is invaluable. My most sincere appreciation is due to Mrs. Rozsa Kohn for her many long hours of work in the assay procedures of the pregnant animals and the maintenance and care of the animal colony from which samples for the work were drawn.

Mr. Joseph Cobb provided technical assistance to this project without which this work could not have been accomplished, and for which I am most deeply grateful. Mrs. Kay Bailey and Mr. Robert Cicone have my most sincere appreciation for the histological work and many other supportive functions performed. To Mr. Robert Noyes and Mr. Irvin Franklin, I wish to express my sincere appreciation for making the performance of this task possible.

The help and advice of Dr. C. R. Graves in the many aspects of reproductive physiology and the expertise of Dr. H. W. Norton in the intricacies of biostatistics have been both necessary and extensive. This aid is most sincerely appreciated.

To the individuals mentioned above, and to the many other people in this laboratory, I wish to express my most sincere thanks, not only for the specific support given me in performing the work reported here, but for the intangible support, the friendship and the good will expressed in my years in this laboratory.

Without the good will, hard work, expertise and periodic acerbic comments of my typist, Mrs. Lynn Dorner, the task of writing this thesis would have been immensely more difficult. To this patient lady, I owe my sincere thanks.

The debt of gratitude owed to my wife, Amy, and daughter Heather, for their patience, understanding, help and support through the long years of work necessary to arrive at this point, will take a lifetime to repay.

TABLE OF CONTENTS

		Page
ACKNOWLEDGEMENT		iii
LIST OF FIGURES		vi
I.	INTRODUCTION	1
II.	METHODS AND PROCEDURES	8
	A. CALIBRATION METHODS FOR ACOUSTIC FIELDS AND TRANSDUCERS	8
	B. ANESTHESIA TECHNIQUES	21
	C. HISTOLOGICAL PROCEDURES	29
	D. EXPOSURE AND ASSAY PROCEDURES	37
	E. SACRIFICE AND ASSAY PROCEDURES	45
III.	INSTRUMENTATION	49
	A. EXPOSURE INSTRUMENTS	49
	B. ANESTHETIC EQUIPMENT	59
	C. CALIBRATION EQUIPMENT	64
IV.	RESULTS	66
	A. IN-UTERO EXPOSURES	66
	B. TESTICULAR EXPOSURES	82
	C. OVARIAN EXPOSURES	110
V.	DISCUSSION	111
	A. IN-UTERO EXPOSURES	111
	B. TESTICULAR EXPOSURES	120
	C. OVARIAN EXPOSURES	129
VI.	CONCLUSIONS	131
	A. IN-UTERO EXPOSURES	131
	B. TESTICULAR EXPOSURES	133
	C. OVARIAN EXPOSURES	135
LIST OF REFERENCES		136
APPENDICES		142
	A. STATISTICAL PROGRAM LISTING	142
	B. EXPERIMENTAL ANIMAL DATA	148
VITA		172

LIST OF FIGURES

FIGURE		Page
1	Thermocouple Probe	12
2	Representative Acoustic Field Plots	13
3	Free-Body Diagram of Radiation Force Calibrator	14
4	Schematic of Thermocouple Probe - Galvanometer Connections	17
5	Calibration Method for rf Voltage	19
6	Maturation Process of the Spermatid	33
7	Detail of Seminiferous Tubule in the Mouse	34
8	Diagrammatic Representation of the Mouse Ovary	36
9	Animal Identification System	38
10	Mouse and Constraint System	40
11	Irradiation Tank with Mouse in Position for Exposure	40
12	Example of Array Pattern for Exposure of Pregnant Mouse	41
13	Testicular Ligature for the Male Mouse	44
14	Pregnant Female Mouse During Necropsy	46
15	Block Diagram of Exposure System Electronics	50
16	Exposure Tank	52
17	Plane Wave Transducer: Small Aperture	53
18	Plane Wave Transducer: Large Aperture	54
19	Focussed Field Transducer	54
20	Transducer Field Plot for the Small Aperture Plane Wave Transducer	55
21	Transducer Field Plot for the Large Aperture Plane Wave Transducer	55

FIGURE		Page
22	Transducer Field Plot for the Focussed Transducer	55
23	Block Diagram of Computer-Exposure Equipment Interface	58
24	Induction and Short Term Maintenance Anesthetic Equipment	59
25	Animal Constraint System and Long Term Anesthetic Maintenance Equipment	60
26	Animal in Constraint Preparatory to Exposure	61
27	Ball Radiometer	64
28	Thermocouple Probe Calibrator	65
29	Plot of Maternal Survival Regression Equation	70
30	Normal Mouse Testicle Sections	83
31	Mouse Testis Section, High Dose, Immediate Sacrifice, 40X Magnification	87
32	Mouse Testis Section, High Dose, Immediate Sacrifice, 100X Magnification	87
33	Mouse Testis Section, High Dose, 6 Hour Sacrifice, 40X Magnification	88
34	Mouse Testis Section, High Dose, 24 Hour Sacrifice, 450X Magnification	89
35	Mouse Testis Section, High Dose, 24 Hour Sacrifice, 100X Magnification	90
36	Mouse Testis Section, High Dose, 24 Hour Sacrifice, 450X Magnification	91
37	Mouse Testis Section, High Dose, 48 Hour Sacrifice, 40X Magnification	92
38	Mouse Testis Section, High Dose, 7 Day Sacrifice, 40X Magnification	93
39	Mouse Testis Section, High Dose, 7 Day Sacrifice, 100X Magnification	94

FIGURE

		Page
40	Mouse Testis Section, High Dose, 7 Day Sacrifice, 450X Magnification	95
41	Mouse Testis Section, High Dose, 19 Day Sacrifice, 450X Magnification	96
42	Mouse Testis Section, Low Dose, Immediate Sacrifice, 100X Magnification	97
43	Mouse Testis Section, Low Dose, Immediate Sacrifice, 450X Magnification	98
44	Mouse Testis Section, High Dose, 24 Hour Sacrifice, 7X Magnification	99
45	Mouse Testis Section, High Dose, 24 Hour Sacrifice, 100X Magnification	100
46	Mouse Testis Section, High Dose, 24 Hour Sacrifice, 450X Magnification	100
47	Mouse Testis Section, High Dose, 48 Hour Sacrifice, 40X Magnification	101
48	Mouse Testis Section, High Dose, 6 Day Sacrifice, 100X Magnification	102
49	Mouse Testis Section, High Dose, 6 Day Sacrifice, 450X Magnification	102
50	Mouse Testis Section, High Dose, 10 Day Sacrifice, 100X Magnification	103
51	Mouse Testis Section, High Dose, 10 Day Sacrifice, 100X Magnification	104
52	Mouse Testis Section, High Dose, 10 Day Sacrifice, 450X Magnification	105
53	Mouse Testis Section, High Dose, 10 Day Sacrifice, 450X Magnification	105
54	Mouse Testis Section, Low Dose, 19 Day Sacrifice, 100X Magnification	106
55	Mouse Testis Section, Low Dose, 19 Day Sacrifice, 100X Magnification	107

FIGURE Page

56 Mouse Testis Section, Low Dose, 19 Day Sacrifice, 450X Magnification 107

57 Mouse Testis Section, Low Dose, 19 Day Sacrifice, 450X Magnification 108

58 Mouse Testis Section, Low Dose, 43 Day Sacrifice, 450X Magnification 109

59 Mouse Testis Section, Low Dose, 43 Day Sacrifice, 450X Magnification 109

60 Representative Example of Exposed Ovary 110

61 Plot of Acoustic Intensity versus Tissue Temperature Rise 121

62 Plot of Irradiation Time versus Tissue Temperature Rise 122

I. INTRODUCTION

Ultrasound has now been applied as a clinical aid, both diagnostically and therapeutically, for over thirty years and as an experimental tool for an appreciably greater time (1). The areas of the body which have been investigated with the aid of high-frequency sound include the brain, heart, breast, ear, eye and the in-utero fetus, to name only a few.

The central nervous system has received appreciable attention for both the diagnostic and therapeutic application of ultrasound. Considerable work has been performed in establishing threshold dosage ranges for production of irreversible structural changes (2,3), and in studying the physical mechanisms of the interaction of ultrasound with the tissues of the mammalian central nervous system (4,5,6,7,8,9). These investigations include the generation of acoustic tomograms used as diagnostic aids (10), selective placement of deep lesions in the brain (2,3) and dosimetry studies (3,7). Concomitantly, ultrasound was being used therapeutically in the alleviation of the symptoms of Parkinson's disease (11) and related disorders with an encouraging degree of success, and finds application currently in the excision of deep, inoperable brain tumors (12). Diagnostic applications of ultrasound to the central nervous system include the localization of neoplastic growth (12), midline shift from growths or fluid accumulations resulting from

traumatic injury and ventricular abnormalities from pathological processes (13,14).

Examination of the heart and its function has received considerable attention in ultrasonic diagnosis. Among the cardio-vascular parameters measurable by ultrasound are the thickness, velocity and displacement of the cardiac wall (15,16),valvular stenosis and dysfunction (1,16,17), and ventricular and atrial volumes (1,16).

An organ currently receiving a great deal of attention is the human female breast. Due primarily to the large and varied number of abnormalities found in this structure, for example cysts, adenomas, carcinomas, and others, these various types of abnormalities are differentiated with at least the same degree of success as by other currently employed techniques such as palpation or mammography. Ultrasound is well suited to the examination of this organ since there are no intervening bony structures or coverings, and the spector of ionizing radiation is not present so that the efforts of several investigators (18,19,20) are being focussed on the diagnostic capabilities in this area. Among the difficulties encountered in the echographic examination of the mammary gland are the large variabilities found in any age group in the fat/glandular tissue distribution, the changes in tissue constituents as a

function of age and childbearing history and the extreme diversity of pathologies which are common to the breast (19).

Meniere's syndrome is a disturbance of the labyrinth of the inner ear characterized by recurring attacks of deafness, tinnitus, vertigo, nausea and vomiting, and, in some cases nystagmus (21). There are a variety of chemical therapeutics which constitute the first choice of treatment, and these succeed in about three quarters of the incidences and surgical intervention is indicated where these fail. Several surgical procedures have been developed to alleviate the symptoms, among them electrocoagulation of the labyrinth, however, these have the disadvantage of possibly producing total loss of hearing, as the eighth cranial nerve must be avoided in these procedures. Two ultrasonic techniques (22) have been developed which accomplish the necessary destruction of the labyrinth without the accompanying destruction of the cochlea. The first of these involves considerable surgery in requiring a mastoidectomy, whereas the second technique uses an approach through the round window and may be done under local anesthesia. These techniques (21,22) are becoming established procedures in the treatment of this type of inner ear dysfunction.

The increasing use of doppler fetal monitoring and tomographic scans (10,16,23,24,25,26) have raised the question of the safety of ultrasound, as employed diagnostically.

Detection of the fetal heartbeat (16), the identification of multiparity (10,25), anatomical defects, and uterine and placental abnormalities (16) and fetal biparietal diameters (27) are among the aspects of obstetrical examination in current use. Thus, the current applications of diagnostic ultrasound may provide continued opportunities for series of ultrasonic exposures, beginning shortly after conception (25), extending through infancy, childhood (28) and maturity. The male reproductive system is also being exposed to high frequency acoustic fields for diagnostic purposes (29,30). A proposal to use ultrasound as a male contraceptive has been suggested (31).

The applications of ultrasound outlined above constitute only a fraction of the current clinical uses (1). The abdominal organs, including liver, kidney, spleen, bladder and lower gastro-intestinal tracts are also targets of acoustic investigation (24,32).

Estimates suggest that very appreciable portions of the population (33) will have the opportunity for multiple exposures to ultrasound during developmental and growth periods (28). However, definitive information providing guidance and allowing intelligent, safe employment of this modality is generally lacking (26,27). Although some information regarding

possible damaging effects of ultrasound have been reported (34,35,36,37,38,39,40,41,42,43), complete systematic study has not yet been undertaken. Effects on the in-utero fetus of murine species have been examined for exposures to frequencies in the low (1 to 3) megahertz region (26,39,41,44,45). The acoustic intensities and exposure times employed range from the low milliwatt region (26,41), to hundreds of watts per square centimeter (44) for times of minutes to hours (41,45). These exposures included both pulsed (39,44) and continuous wave regimes (26,41). The results from these studies have been generally negative (41,44).

Experiments have been performed to elucidate the effects on the ovary of the rat (46) with the results demonstrating no effect on gestational support in the pregnant animal.

The testes of the rat have been used to explore the possibility of ultrasound as a male contraceptive (31). Damage to the organ of both a reversible and irreversible nature has been shown, but the information regarding the proposed site of interaction has not emerged. It was felt that initiating such a study was essential and that results from animal experiments should provide:

1. guidance in the selection of parameters for human exposures to ultrasound, and

2. details necessary for improving observability for detecting ultrasonically related hazardous effects in the human. The fact that deleterious effects have not been reported (nor have they specifically been looked for) after nearly a quarter century of clinical involvement is encouraging, but may also be a false security should delayed effects be forthcoming.

The present study was undertaken with these ideas in mind.

As the term toxicity is most often referred, in medicine, to agents administered in weight or volumetric form, its employment with regard to a wave phenomenon may require definition. Ultrasonic toxicity, as employed herein refers to any effect which proves deleterious or debilitating to the animal or the organ system under consideration, in response to exposure to ultrasound of quantitatively describable conditions. Thus, in the case of the female ovaries and the male testes, toxicity may imply sexual nonviability, and with respect to the in-utero fetus, toxicity can denote fetal death, teratological manifestations or a broad range of abnormalities of organ systems,

skeleton, musculature, etc. Though the usage may appear vague, selection of specific endpoints for observation of experimentally induced effects removes doubts for specific investigation.

This study deals with the toxic effects of ultrasound to the in-utero fetus, the male gonads (testes), and the female gonads (ovaries), of the mouse. The exposure of the developing embryo and fetus within the uterus is performed at two different gestational periods, viz., at the beginning of organogenesis (day 6/7 of the pregnancy); and prior to, and during, limb bud formation (day 10/11 of pregnancy). These periods were chosen to coincide with periods of liability to known teratogenic agents, such as drugs, ionizing radiation, foods, smoking, alcohol, nutrition, etc. The results tabulated from a post mortem necropsy of the dam are submitted to standard statistical procedures (47,48), chosen to establish and identify relationships between the experimental observations and the irradiation parameters in order to delineate causative factors as opposed to group differences without cause-effect data.

Testes of the mouse have been exposed to acoustic fields both in-vivo and in-vitro in an effort to provide both toxicity information and some insight into the interaction mechanisms between ultrasound and germinal tissue. Preliminary data concerning propagation properties of ultrasound in this organ

has been reported (49), and is applied here to help eliminate some toxognomonic aspects of acoustic exposure.

A range of acoustic intensities and exposure times, 1 w/cm^2 - 100 w/cm^2 and 1 sec to 60 sec, have been investigated in an effort to elicit a toxipathic reaction in the exposed organ. Animal death is an unacceptable result of ultrasonic exposure, and was a predominating occurrence at acoustic intensities above 25 w/cm^2 and exposure times greater than 20 seconds. Exposures at 1 and 2 w/cm^2 when applied as specific organ exposures, produced no observable histological results, contrary to results reported elsewhere (31) as producing irreversible sterility, and are not discussed with respect to organ exposures in this paper. The two testicular exposure conditions, 25 w/cm^2 and 10 w/cm^2 for 30 sec, included in this thesis are designed to elucidate the temporal aspects of acoustic toxicity, the cellular involvement and site of action data as a basis for subsequent investigation.

The ovary, because of its anatomic placement, is liable to acoustic insult under many ultrasonic diagnostic procedures involving the abdominal contents in the female (10). Despite the obvious importance of toxicological data for this organ, very little work has been published on effects (46,50). The first of these papers discusses the effects of acoustic exposure of rat ovaries on the developing fetus; the second examines, in

a superficial manner, the gross reactions of the ovary in rats to ultrasonic exposures. Histological work was not done in either investigation. This study attempts to provide histological data relating ovarian response to acoustic insult.

The thesis comprises chapters on the Methods and Procedures; Instrumentation; Results; Discussion; and Conclusion. The Methods and Procedures section describes the calibration exposure, anesthetic, assay and histological methods used to perform the experiments and collect the data reported here. The equipment and instruments used in connection with this study are described in the Instrumentation section. The section reporting the Results includes the statistical analysis of the in-utero assay procedures and the morphological findings of the testicular and ovarian exposures. The Discussion and Conclusion sections respectively contain a presentation of the findings and discussion of their meaning, for all three aspects of the study under a single heading. The implications and directions of this study are reviewed and discussed with respect to the objectives obtained and areas of future fruitful endeavor.

II. METHODS AND PROCEDURES

A. CALIBRATION METHODS FOR ACOUSTIC FIELDS AND TRANSDUCERS

This chapter includes descriptions of the methods and procedures developed and adapted

1. to perform the calibration of the acoustic fields, transducers and associated electronics,

2. for the ultrasonic exposure procedures, including the anesthesia techniques (and background), the animal constraint method and computer control of the irradiation, and

3. for the necropsy and assay procedures and the histological techniques.

The calibration of acoustic intensity and the determination of the field distribution of the ultrasonic transducers used in this study are performed in two stages, viz., the measurement of the acoustic field intensity at the peaks of the distribution using a primary standard, and the relative distribution in space as measured by a secondary standard, respectively. The primary method employs the radiation force acting on a

small stainless steel sphere (51) suspended in the acoustic field, and the secondary standard uses the transient thermo-electric technique (52,53). The two methods are necessary as the radiation force technique requires a special set-up, as employed in this laboratory, to reach acceptable accuracies, and cannot be moved about to all exposure systems (54).

The transducer being calibrated is mounted in the end wall of the calibration tank opposite the castor oil absorbtion chamber, which fills the rear portion of the tank, and is separated from the coupling medium by a Rho-c window. The medium through which the acoustic wave propagates is distilled, degassed water. The degassing is performed by autoclaving the distilled water for 30 minutes and subsequently sealing the completely filled containers with rubber stoppers to establish and maintain a vacuum as the water cools. The complete exclusion of air from the hot containers ensures an excellent vacuum upon cooling which allows for storage of the liquid for extended periods in a degassed state. A thermocouple probe, shown in Figure 1, is attached to a coordinate system used to plot the acoustic field in all three dimensions.

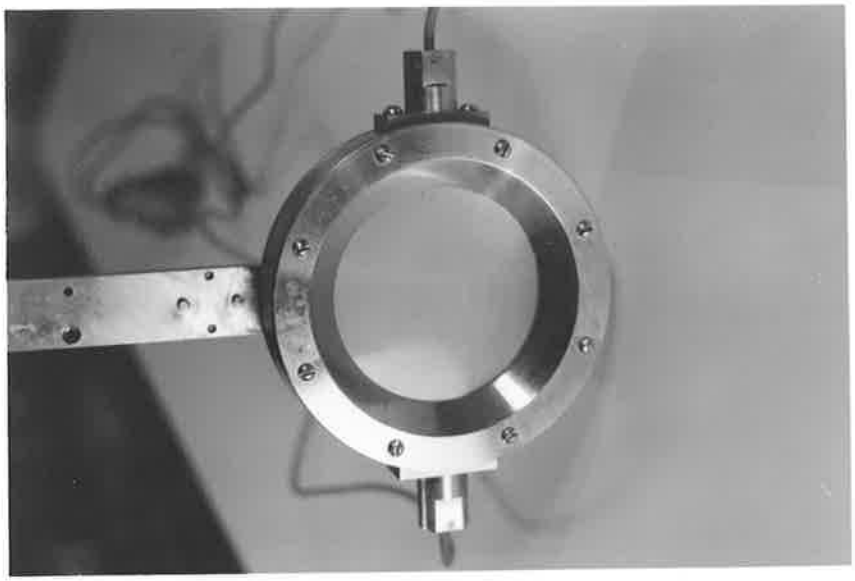

Fig. 1. Thermocouple Probe Calibrator

The transducer is excited electrically to emit a short acoustic pulse of the order of 0.1 sec. The thermoelectric output of the iron-constantan thermocouple junction imbedded in the Dow Corning 710 acoustic absorbing fluid, is displayed on an oscilloscope screen. This pulse, representing a rapid heating at the thermocouple junction, is the result of viscous forces between the thermocouple wire and the surrounding medium. The height of this pulse is proportional to the acoustic intensity(54,55). As the thermocouple probe is moved in steps along one of the three axes in the field, the varying heights of the peaks are plotted to arrive at the field cross section, or a longitudinal slice, of the acoustic field. Examples of the types of plots which may be generated are displayed in Figure 2.

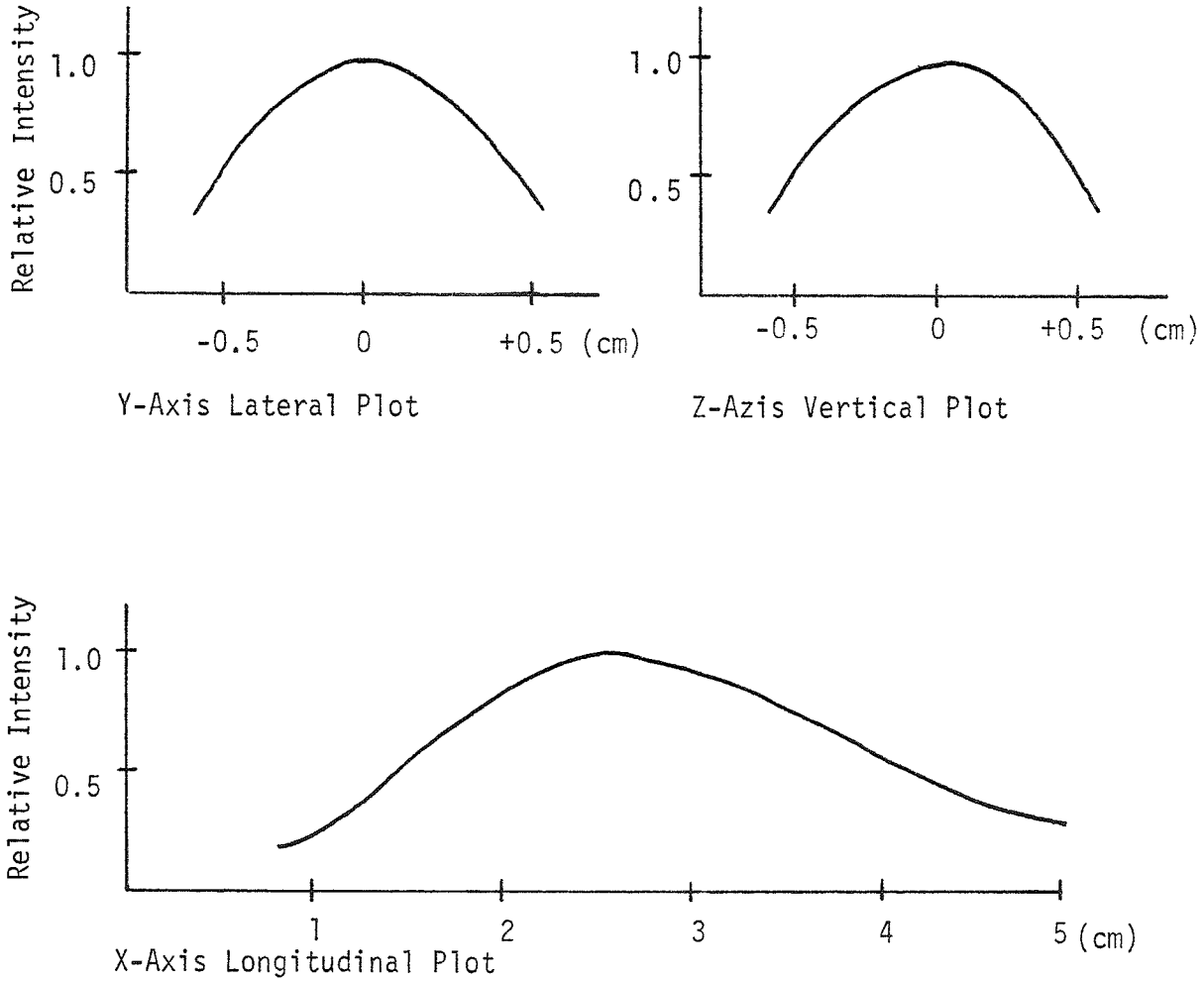

Fig. 2. Representative Acoustic Field Geometries

The field cross sections depicted in Figure 2 are desirable, from the consideration of spatial uniformity, as this will allow specimens of approximately 1 cm. in extent to be irradiated with less than 10% variation in acoustic intensity.

The intensity at the peak of the spatial distribution is then determined by the radiation force method. Here a stainless steel

ball, supported by a bifilar monofilament nylon suspension, is placed in the acoustic field with its geometric center at the position previously occupied by the thermocouple probe. In practice, the peak region of the field is calibrated by electrically exciting the transducer to emit a continuous wave (CW) signal and allowing the radiation force (51) to deflect the stainless steel ball a small distance, compared to the length of the suspension, along the axis. The coordinate system to which the ball is attached is adjusted to return the sphere to the original point in the acoustic field, as observed with the aid of cross-hairs in a traveling microscope. Upon removing the acoustic field, the ball returns to an undeflected position, now some known axial distance from the position of interest in the acoustic field being examined. The free-body diagram showing the forces involved is shown in Figure 3, and the equation governing this relation in Equation 1.

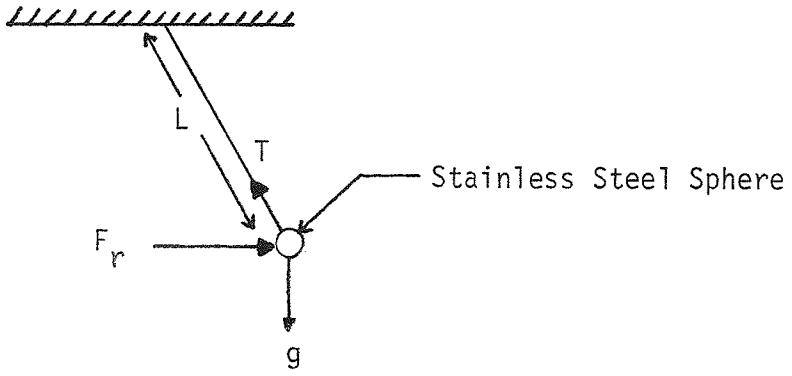

Fig. 3. Free-Body Diagram of Radiation Force Calibrator

$$F_r = \frac{\Delta\chi(m_s - m)g}{L}$$

EQUATION 1

In the equation F_r is the force on the stainless steel sphere, $\Delta\chi$ is the measured deflection; $(m_s - m)$ is the weight of the sphere in water, g is the gravitational constant, and L is the known length of the suspension system. All the quantities in this equation are known except $\Delta\chi$, which may be readily measured to 0.1 mm.

Equation 2 relates the radiation force to the acoustic intensity or energy density at the point of interest in the field (54,55,56).

$$I = \frac{FrC}{\pi a^2 y}$$

EQUATION 2

In this equation C is the velocity of sound in the imbedding fluid medium, a is the radius of a sphere and y is the radiation force per unit cross section and unit mean energy density. King (54) first considered the value of y assuming a perfectly rigid sphere.

The values obtained by Yosioka and Hasagawa (56) take into account the elasticity of the sphere by use of two material constants, as opposed to the compressibility alone. The degree of error between the two values is dependent upon the wave number ka, the sphere material, dimensions and the acoustic frequency employed. Examination of the Yosioka equations, over a wide range of ka values, has provided tabular values of y for ka of less than 0.5 to greater than 40, and these values are used with Equation 2, to determine this dosimetrically fundamental quantity, viz., the acoustic intensity in the field at the point where the specimens are positioned (57).

The deflection of the stainless steel sphere is recorded for a number of different driving voltages applied to the acoustic transducer, enabling a plot of the acoustic intensity versus the square of the transducer driving voltage to be constructed and to fit to a straight line by the least squares method. The data points are supplied to a program residing in the laboratory computer and are treated as follows: an integral is performed over the surface of the sphere to provide the relationship of the peak intensity, on the axis of the beam, to the average intensity over the surface of the ball. The necessary physical data concerning the distribution of the acoustic field in the medium is supplied from the field plotting obtained with the thermocouple probe. The computer program computes the "peak" acoustic intensity at the site of the ball in the field. Computational assumptions are that

the field is symmetrical about the peak and that it decreases in a smooth, continuous, monotonic fashion as the radial distance increases away from the axis. For the field distribution chosen and the limited lateral extent involved, the assumptions are good.

The result of this calibration procedure is a quantitative relationship between the peak acoustic intensity at the point of interest in the field and the rf voltage applied to the X-cut quartz crystal in the transducer assembly. This relationship and the knowledge that the acoustic intensity is proportional to the square of the applied voltage (55) may be used to calibrate a secondary standard, the thermocouple probe, at any frequency and ambient temperature. The theory of the thermocouple probe is well documented elsewhere, (52 , 53). The calibration of this secondary standard is accomplished by connecting the output of the thermocouple probe to a sensitive recording galvanometer as shown in Figure 4, and placing the thermocouple junction at the previously calibrated point in the acoustic field.

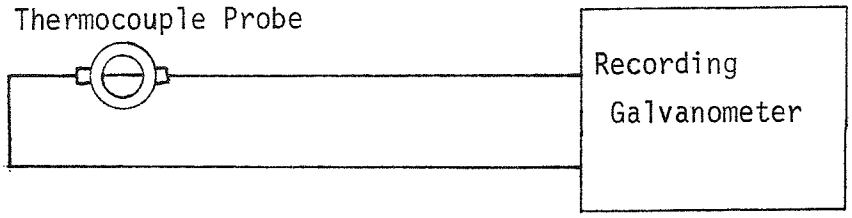

Fig. 4. Connection Diagram of the Thermocouple Probe and Galvanometer

The fluid contained in the thermocouple probe, in which the thermocouple junction is embedded, is Dow Corning Fluid No. 710, which has a pressure absorption coefficient, α, of about 0.29 n/cm at 1 MHz and 37^{o} C. and an acoustic impedance closely approximating that of water. Thus, reflections occurring at the interface between the probe fluid and the coupling medium, usually degassed water, are minimal. Reflection or refraction is not a consideration if the probe is used as a secondary standard, calibrated by the radiation pressure method.

As the acoustic field propagates through the fluid of the thermocouple probe, the fluid in the vicinity of the thermocouple junction is heated in proportion to the local intensity of the field. This heating is manifest by the concomitant change in output of the thermocouple and is recorded as the galvanometer deflection. The procedure is repeated for several different intensities at the junction and a plot of the galvanometer deflection versus the square of the transducer voltage is constructed. Assuming thermal conduction processes are negligible, linearity of the acoustic intensity with respect to the square of the voltage across the faces of the quartz crystal, then accurate knowledge of the rf driving voltage provides an acceptable knowledge of the acoustic intensity at the field point of interest.

The necessary information to relate the values of external controls to the rf voltage impressed upon the quartz crystal is

provided by commercial rf voltage standards. A block diagram of the voltage calibration system is provided in Figure 5.

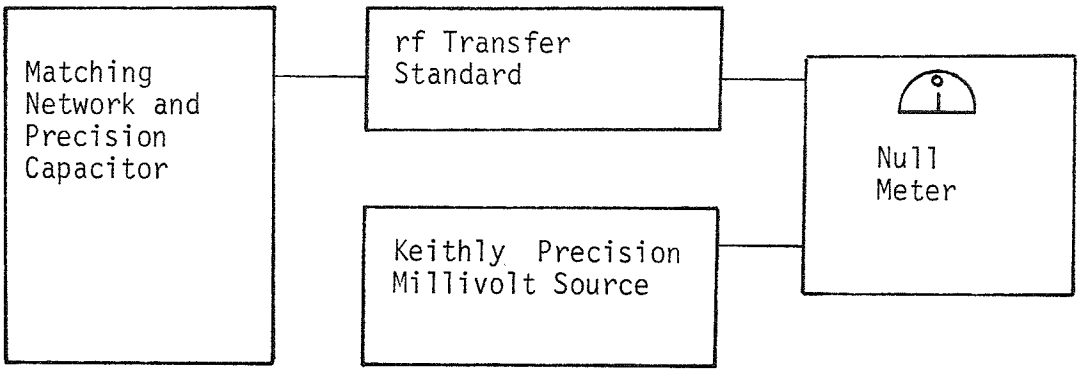

Fig. 5. Calibration Method for rf Voltage

The transfer standards have a D.C. voltage output which is proportional to the RMS rf voltage input. To avoid electrical loading on the relatively low-power thermocouple output, the D.C.voltage is applied to a sensitive null-meter, which is then balanced using an accurate (0.5%) Keithly millivolt D.C. source. Since the transfer ratio of the standards is known very accurately (1%), a close correlation may be established between the transducer driving voltage and the external controls used to vary the magnitude of the voltage applied to the acoustic transducer. Extremely accurate (.01%) tabular data relating the value of a precision capacitor, located in a divider network, to the voltage applied to the acoustic transducer is generated by a least-squares linear fit program residing in the in-house computer.

Measurement of these values is made periodically to ensure the accuracy, within 5%, of the acoustic intensities applied to the experimental animals. This combination of calibration procedures and instrumentation, i.e., the radiation force method of absolute calibrations, the thermoelectic, or thermocouple secondary standard, and accurate knowledge of the transducer driving voltage provides a system for determination of the acoustic field parameters (intensity), within 3%, necessary to this investigation.

The disadvantages of these calibration methods lie in the lack of phase and harmonic information. The suspended sphere and thermocouple probe both respond to total incident energy and provide no information regarding either the relative phase or spectral content of the field. An interesting and informative comparison of several calibration methods may be found in the literature (58).

B. ANESTHESIA TECHNIQUES

The field of anesthesiology may be considered more art than science. In order to comprehend its intricacies, to utilize its technology, or simply to put an animal to sleep with reasonable expectation of its awakening, it is necessary to appreciate the art as well as understand the science. The history associated with the final selection of the anesthesia used in this study is considered informative to the understanding of the action and interaction of these agents with other pertinent variables of this investigation. General anesthetics may be divided into two broad categories, viz., inhalation anesthetics and parenteral (including injectable) anesthetics. Each has advantages and disadvantages which may be species dependent, as, for example, administration to the adult human and the cat. The former will usually tolerate an intramuscular or intravenous injection and the latter must be restrained for the intramuscular and the intravenous is virtually impossible in the awake animal. For obvious simplicity, the discussion of anesthetics will be confined to the mouse, the subject of the experiments described herein.

The advantages to the use of an injectable anesthetic in the mouse lie in the relative ease of administration, the ability to maintain a given anesthetic level for long periods of time (on the order of hours if necessary), and the lack of exposure of the experimenter to the anesthetic agent, assuming reasonable

dexterity. A primary disadvantage of parenteral anesthesia for the small rodent is the single practical route of administration, viz., intraperitoneally, which is very imprecise due to the physiological variabilities associated with body cavity injection such as membrane transport rates, metabolic rates, etc., and the inability to decrease the dose following administration (59).

The barbiturate anesthetics have been used extensively, but it has been demonstrated that sodium pentabarbital (trade name Diabutal or Nembutal), if administered intraperitoneally to pregnant rats early in pregnancy, induces a significant increase in the number of teratologies in the offspring (59). As the physiology of the rat and the mouse are sufficiently similar, the use of this drug was considered inappropriate in a study having a teratological endpoint. Further, the barbiturate anesthetics may cause tissue sloughing if brought into contact with mucus membranes, muscle or facia outside the vascular system. The introduction of a needle into a body cavity, the contents of which are the object of study, combined with the injection of a possibly tissue damaging agent into this cavity, provides unacceptable chemical and mechanical risks.

The alternative to parenterally administered anesthetics are the inhalation anesthetics and analgesics. The advantages to the inhalation anesthetics are the ease with which one may

regulate the anesthetic depth, the non-invasive method of administration, the non-accumulation of high concentrations in any single organ or locale in the body, and the large range of solubilities allowing for individual selection of the rapidity of induction, depth of final anesthesia stage and speed of recovery. Disadvantages to gaseous anesthetic agents lie mainly in the delivery systems, which may be classified as closed systems, semi-open systems or open systems (60). The closed system is designed such that the gases occupying the system may not escape freely into the surrounding atmosphere, and when properly used, provides excellent control of anesthetic depth and pulmonary ventilation while permitting only minimal quantitites of anesthetic gases to escape to the atmosphere. Unfortunately, this system does not lend itself readily to use on animals having small tidal volume, such as the mouse, due to the inherent system dead-space. The semi-open system is designed such that a small amount of the gas mixture escapes into the atmosphere and is constantly replaced, the remainder being recirculated as in the closed system. The open system employs no recirculation and in its simplest form may be a piece of cotton or gauze soaked in the anesthetic liquid and placed on, or in the the vicinity of, the specimen's nose and mouth. The open anesthetic system is usually provided with a primitive air mover and a mask to fit over the air passages with anesthetic soaked material at some location between the air (or gas) source and the mask (60).

A distinct disadvantage of the latter two systems is that considerable amounts of the anesthetic gas mixture may escape into the atmosphere and, under certain circumstances, could prove hazardous to the laboratory personnel. Additionally, some inhalation anesthetics are potentially explosive in nature, such as ether, there is difficulty in quantitatively determining the delivered dose, and the effect upon material used in close proximity to the escaping vapors, such as interaction with some plastics which are soluble in some anesthetic liquids, are also disadvantages.

At the outset of this investigation serious consideration was given to choosing the appropriate anesthetic agent for effect and efficacy for the mouse. The experimental series began with the readily available injectable drugs, such as sodium pentabarbital (tradename - Diabutal, 60 mg. per ml), which was considered undiluted and diluted with injectable, sterile saline. Undiluted administrations were found to be unacceptable due to the extremely small volumes, on the order of 0.03cc, needed to kill virtually 100% of the animals.

A 1:3 dilution with injectable sodium chloride using a dose of 0.3 to 0.45 cc for induction followed by a 0.1 cc maintenance dose if the procedure required anesthesia for greater than 30-45 minutes was found acceptable.

Chloral hydrate was considered a desirable anesthetic as it could be prepared in a variety of concentrations, boiled for sterility, and provided a broadened dividing line between deep stage III surgical anesthesia, as determined from respiratory function, and terminal stage IV. However, a disadvantage was the instability of the prepared solution, even with refrigeration, rendering it unusable in less than 3 weeks. The variability of response from specimen to specimen was only slightly less than that with the barbiturate drugs, induction was slower, but the recovery period faster, with greater excitability. Chloral hydrate is, in general, a good, low toxicity, reasonably safe general injectable anesthetic for the mouse.

The relatively new analgesic-anesthetic Innovar-Vet (a phenlanyldehydrobenz peridol mixture) was examined because of reported (personal communication: Dr. R.H. Bubar) successful use with some small rodents, notably guinea pigs. Diluted and undiluted at a variety of strengths ranging from 1:1 to 1:20 resulted in the animals either being lightly narcotized or killed, and the dividing line between these two unacceptable states was consistently narrow. Since neither light analgesia nor a moribund state were suitable for the proposed work, this agent was discarded.

Among the inhalation anesthetics reviewed were chloroform, diethyl ether, nitrous oxide, ethylene, cyclopropane, Halothane and Metofane. The first five were rejected because of their explosive

nature or undesirable side effects to rodents. As an example, though chloroform is a very good general anesthetic for most mammals, it is highly toxic to mice. Metofane was selected as the anesthetic to be used for the following reasons: it is not flammable with all mixtures of air and oxygen; there is no confirmed record of hepatic damage, no sensitization of the cardiac conducting muscles with repeated exposure, use of it does not effect uterine contractibility, its saturation concentration in dry air is only 3%, and it is lipid soluble, thereby providing analgesic action for a long period after the administration of the agent ceases. Though Halothane is an equally efficacious anesthetic, it has a few disadvantages for this particular study. Anesthetic induction is slightly longer as compared to Metofane, as it is not lipid soluble there is virtually no analgesic action, and it is slightly more difficult and expensive to administer since it is about twice as volatile a liquid as Metofane.

The use of a gaseous anesthetic required the design and construction of a special instrument for administration, which is described in detail in the Instrumentation section.

The anesthetic procedures are identical for males and females and are independent of the organ system studied. Induction of anesthesia is accomplished using the semi-cylindrical induction chamber shown in Section III. The animal is presented to the semicircular opening of the chamber with the experimenter maintaining a

firm grip on the animal's tail and exerting a slight backward tension, which causes the vast majority of animals to move forward into the chamber, whereupon the gate is inserted into the appropriate slot. The stainless steel container holding anesthetic soaked cotton is then moved to connect the chamber holding the mouse to that holding the anesthetic. The partition between these two compartments is a perforated wall backed by copper screen wire to prevent the animal from coming into physical contact with the soaked cotton.

A stage III surgical anesthesia will usually be obtained in two to four minutes depending upon individual weight, age, sex and inclination to hold breath. This anesthesia depth is usually obvious, from observable respiratory function; but, since the excitability phase of Metofane induction is so mild and short-lived, a problem of distinguishing a mouse under deep stage II or early stage III from one which is merely quiescent for a moment may occur. This is easily resolved by attempting to proceed to the next step of the routine, short-term maintenance anesthesia of the animal. This involves removing the animal from the induction chamber and placing the head, from the ears forward, into the small cylinder shown in the equipment section. The cotton pads at the end farthest from the opening are wetted with approximately 0.2 cc of Metofane and the intervening space between these pads and the nose of the animal provides a reservoir of breathable air-anesthetic mixture. Although this is referred to as an intermediate, or short-term anesthetic

device, any depth of anesthesia may be maintained for hours, if necessary, by adjusting the amount of room air allowed to flow between the rim of the cylinder and the animal's head.

The intermediate anesthetic procedures were used in this study for the clipping, shaving, and depilating the animal, and for mounting in a constraint. Two anesthetic procedures were used in administering maintenance anesthesia. A semi-open method was used for the vast majority of specimens requiring anesthesia for varying periods of less than one hour. Procedures requiring over one hour of continuous anesthesia required an open system incorporating oxygen delivery capabilities and variable oxygen-gas ratio mixtures.

Methods discussed above have provided an extremely simple, non-traumatic and effective anesthetic procedure for the mice used in this study. The deleterious effects which some anesthetic agents produce appear to be absent or minimal, and recovery and continued health of the subjects has been excellent, as virtually no loss of animals occurred due to anesthetic procedures. Areas of improvement may lie in the long-term maintenance anesthetic equipment and procedures. The two delivery systems could be combined to improve flexibility necessary in the regulating arrangements of a semi-open system for the anesthesia of small rodents.

C. HISTOLOGICAL PROCEDURES

1. Staining Techniques

The preparation of the tissues for histological examination begins with the excision of the organ, diffusion fixation in a 10% formalin in Ringers Solution and embedding in paraffin. The paraffin embedded organ was sectioned at 10 μ for ovarian tissue and 6 μ for testicular tissue.

Three separate stain techniques were used in studying the morphology of testes and ovaries, viz., Trichrome (62) for the connective tissues, hematoxylin and eosin (H&E) (61) for nuclear and cytological details, and periodic-acid-Schiff (PAS) for acrosomal details in the seminiferous tubules of the testes (62). The Trichrome was found redundant, since the H&E gave sufficient connective tissue detail, and was later abandoned. The H&E makes visible the nuclear and the cytoplasmic structures, and a reasonable degree of detail is visible in connective tissue components of the testes. This same stain is used alone to prepare the ovaries for examination, since this stain-counter-stain technique delineates all structures of interest therein. Thus, the strongly anionic structures, such as nuclear material, stain a deep blue while the cytoplasmic organelles vary from pink to red.

The PAS stain is used on a second testicular sample to enable the experimenter to count, or otherwise determine the

presence of, all the stages of spermiogenesis. PAS strongly stains polysaccharides, cartilage, some mucins and DNA (62) and since the acrosomal head cap is high in carbohydrates (63), it is exhibited clearly. The counter stain is Metanil yellow, giving all the background a faint yellow to yellow-orange tint, further highlighting the deeply stained acrosome.

A third histological procedure used in the laboratory is an alizarin-Red-S technique for cartilaginous structure examination. This technique follows a standard routine of ethyl alcohol hardening, 1% KOH clearing, alizarin-Red-S staining of cartilage and the subsequent infiltration with glycerin (61). This provides a whole-body specimen of relative clarity having the cartilaginous bony precursors appearing as bright red structures. This technique is used to examine post mortem fetuses for skeletal structural anomalies induced by exposure to ultrasound.

2. The Testis

a. A Brief Description of Testicular Tissue

The sequence of events in the mouse testicle, at any single location in a seminiferous tubule, requires approximately 35 days for completion (64). This cycle begins with the first maturation division of a spermatogonium, or stem cell, and ends with the release of a spermatozoon into the lumen of the tubule. The entire process is divided into three distinct phases; the maturation of the spermatocytes during which the mitotic activity occurs; the meiotic

phase which produces the haploid germ cells, and the spermiogenic phase in which the spermatid progresses to an immature spermatozoon. The final maturation of spermatozoa is completed during the journey through the epididymus and vas deferens prior to expulsion during ejaculation.

The first phase of spermatogenesis is a construct of several mitotic activities (65,66) initiated by the first division of a dormant spermatogonial cell, and continues for 5 subsequent division. During this process one of the daughter cells does not continue to divide, but becomes a resting stem cell, thus replacing the stem cell and maintaining the original spermotogonial population. The end point of this mitotic activity is the production of primary spermatocytes and the beginning of the second phase of spermatogenesis. This phase is the meiotic stage of germ cell production. During this stage of spermatogenesis, the future spermatozoon acquires its haploid complement of chromosomes and its sex determination through the possession of an X or Y sex chromosome. The post-meiotic germ cells, spermatids, undergo an 8.5 day maturation process called spermiogenesis.

The development of the spermatid may be divided into four sections; the Golgi, the cap, the acrosomal, and the maturation phase. The Golgi phase begins with the formation of the proacromsomal granules in the Golgi apparatus of the cytoplasm.

The coalescence of the proacrosomic granules to form the acrosomic cap is the transition from the Golgi to the cap phase of spermiogenesis. During this phase the single proacrosomic granule applies itself closely to what will become the anterior pole of the nuecleus, and begins to spread, resembling a bowler hat perched on the nuclear "head". The cap phase of spermiogenesis persists through spermatid stage 8. As the acrosome is forming in close association with the nuclear membrane, the entire nucleus is migrating from a central position in the cell to the periphery.

Stage 9 of the maturation of the spermatid demonstrates the transition from the cap phase to the acrosomal phase. During this phase the spermatid completes the rotation to orient the developing flagellum toward the tubule lumen and the nucleus completes the motion to abut itself against the cell membrane nearest the basement membrane. The nucleus and the acrosomal cap are now undergoing a transformation as shown in Figure 6. The nucleus flattens and becomes elongated, with the developing acrosome providing a close fitting cap surrounding it. A concomitant change is taking place at the opposite pole of the spermatid as the flagellum develops. The details of this development are not visible in the Histological preparations used in the study.

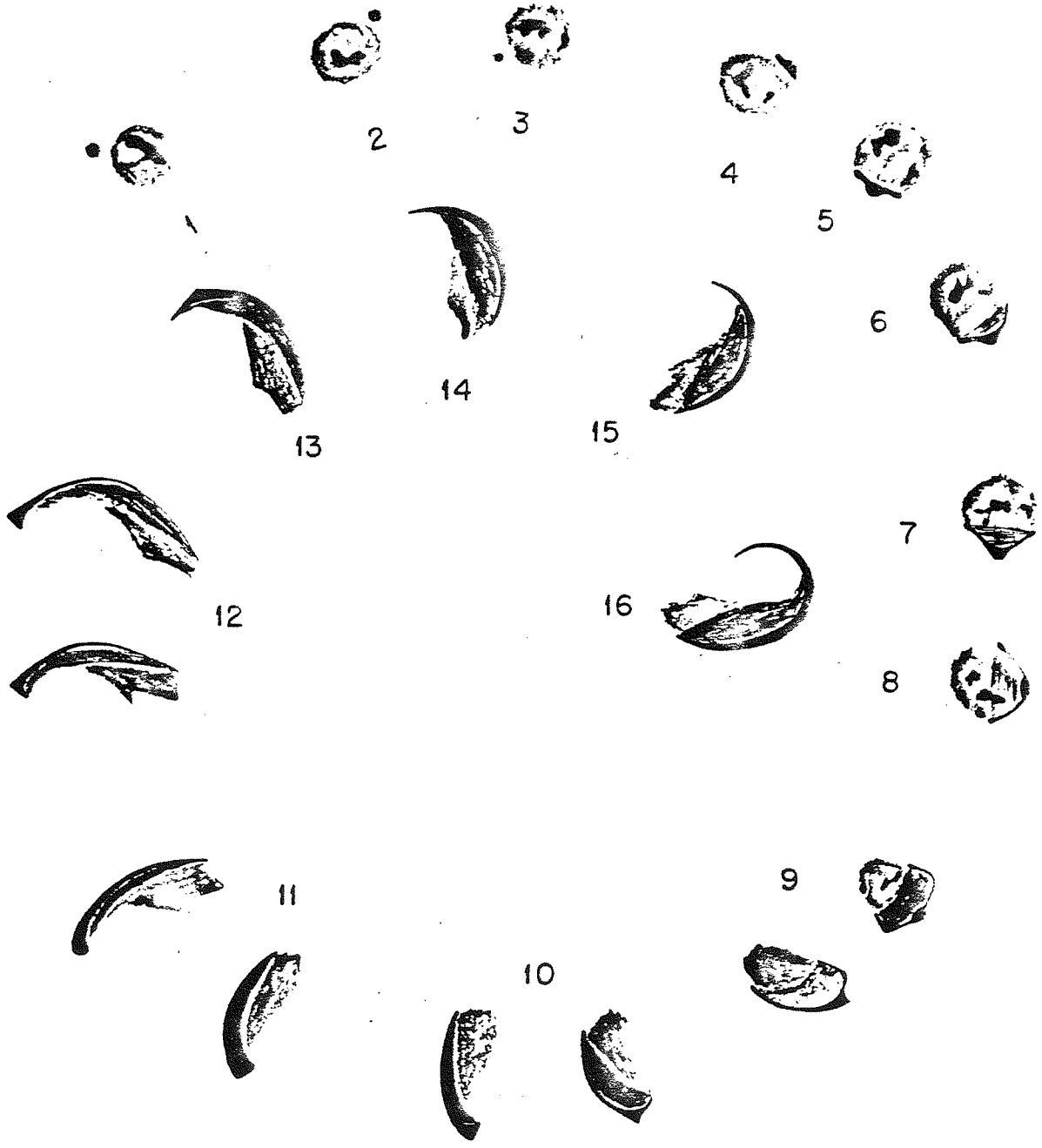

Fig. 6. Maturation Process of the Mouse Spermatid (from Oakberg, 1956) (63)

The flagella of the late spermatid is visible as it emerges from the wall of the tubule into the lumen. The diffuse fimbriated mass visible in the center of the tubule lumen in Figure 7, demonstrates the normal appearance of the free spermatozoan tails. The fine cytoplasmic details of spermatid maturation are discernible only in electron micrograph studies which is beyond the scope of the present work.

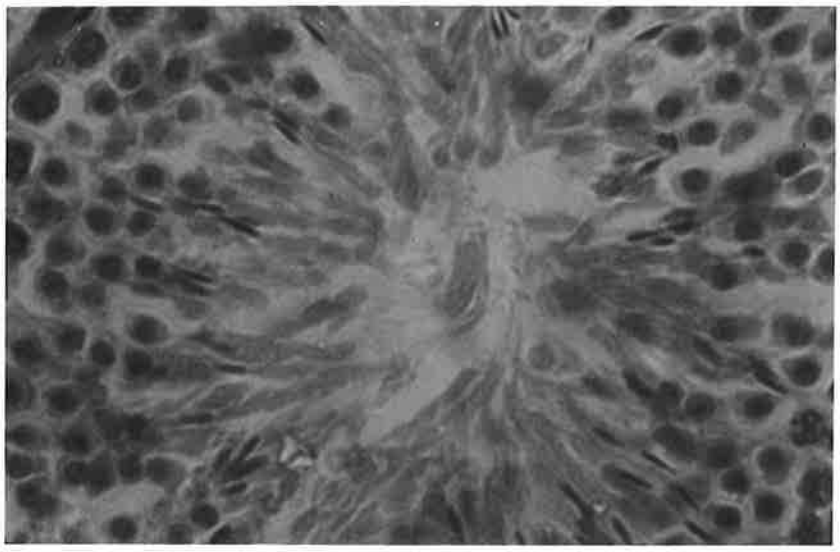

Fig. 7. Detail of the Seminiferous Tubule in the Mouse, Showing Appearance of Spermatozoan Tails in the Lumen

Upon reaching spermiogenic stage 16, the mouse spermatid is ready for ejection into the lumen of the tubule as a young spermatozoon. As the new germ cell leaves the tubule wall it loses a globular mass of cytoplasmic debris. This cytoplasmic debris includes ribosomes, degenerating mitochondria, lipid droplets and Golgi membranes.

This leaves only a small cytoplasmic droplet attached to the spermatozoon at the base of the tail section. This droplet disappears during the final maturation of the germ cell in the epididymus. The discarded residual body is phagocytized by the Sertoli cells at the same time that the mature spermatid is released from the cytoplasmic embrace of these cells.

b. Observation Procedure

In evaluating the normal progression of the germ cells from the stem cell, or spermatogonial stage to young spermatozoa, two examination procedures are employed as exemplified by the histological stains utilized. The above spermatocytogenic details may all be observed by the use of the H & E stain on a single section. The cytological details of nuclear size, chromatin distribution and density, abnormal mitotic activity and abnormal cytoplasmic structures or inclusions are easily identified in this preparation. The location of the spermatogonia, spermatocytes and Sertoli cells are noted relative to the basement membrane and tubule lumen. This latter aspect is important if the normal movement of the maturing germ cell from basement membrane to lumen is not occurring. A perceptible radial distance should exist between the primary spermatocyte and the basement membrane, whereas the stem cells should all adhere closely to the membrane. The sole indication of normal development for the remaining lifetime of the germ cell is the temporal and spatial relations of acrosomic development and visible microanatomic features of this structure.

3. The Ovary

a. Stain Technique

A single stain procedure is sufficient to permit the exploration of all the morphological aspects of the ovary. A hemotoxylin and eosin stain, as described in the preceding section, permits ready identification of the ovarian stroma, primordial germ cells, oogonia, developing follicles, corpora lutea and corpora albicans. All these aspects may be seen diagramatically in Figure 8. In contrast to the testicle almost all stages of oogenesis may be visible in a single ovary at any time during the four day estrous cycle of the mouse.

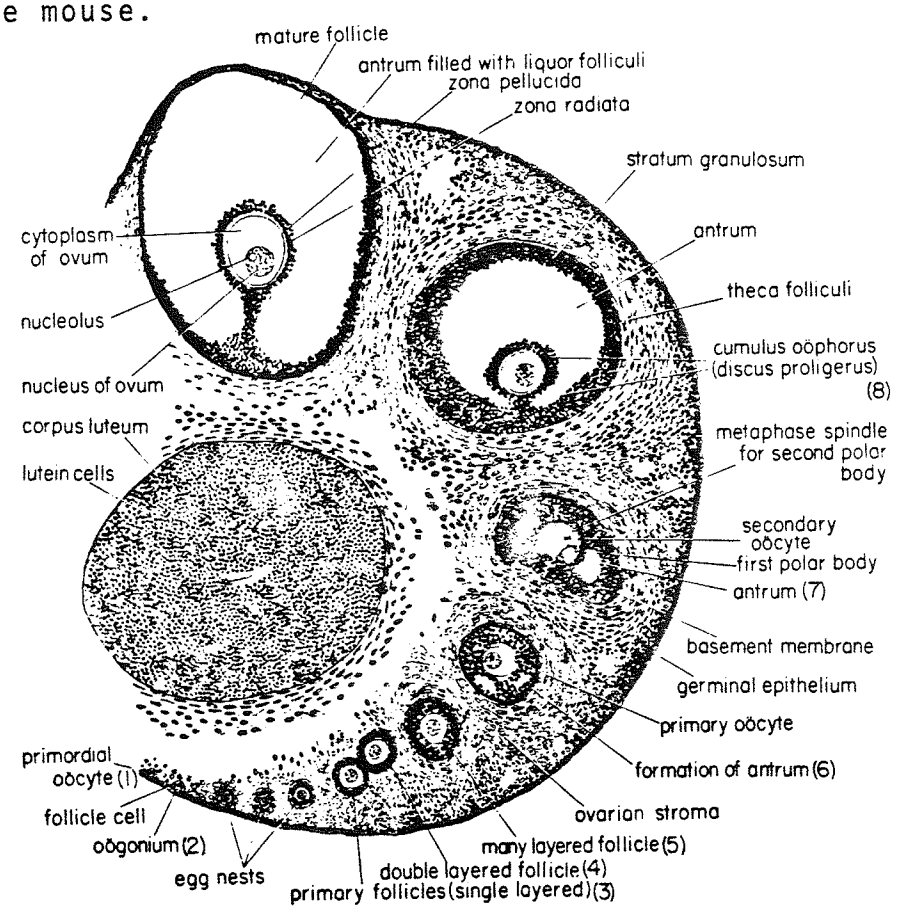

Fig. 8. Diagrammatic Representation of the Mouse Ovary (from Rugh, 1968) (64)

b. Observation Procedure

In the course of microscopic examination of the ovary, the structures examined for indications of ultrasonic anomalies or damage are the Graafian, developing, and primordial follicles; corpora lutea; blood vessels and ovarian stroma (interstitial cells). The examination begins at low magnification to detect gross morphological changes and progresses to increasingly higher magnification to identify any changes in cell structure. The ovaries are mounted such that a series of six, ten μ thick serial sections cut from the center of the ovary are mounted on a single microcope slide. Three slides are prepared, but only one is stained. The relative sizes of the ovary and the acoustic beam are such that there is less than a 5% variation of intensity across the entire organ. Thus, any damage produced acoustically should be evident in any section through the ovarian tissue. Based on this supposition, only one stained slide, containing six to eight sections, is examined microscopically, unless some evidence of abnormality is located at which time the remaining slides are stained and reviewed. This procedure is more than adequate to establish if ultrasonic damage has been done to the organ.

D. EXPOSURE AND ASSAY PROCEDURES

When anesthesia has progressed to the point that the animal may be manipulated, the identifying punch marks are placed in the ear. The values of these punches are shown in Figure 9.

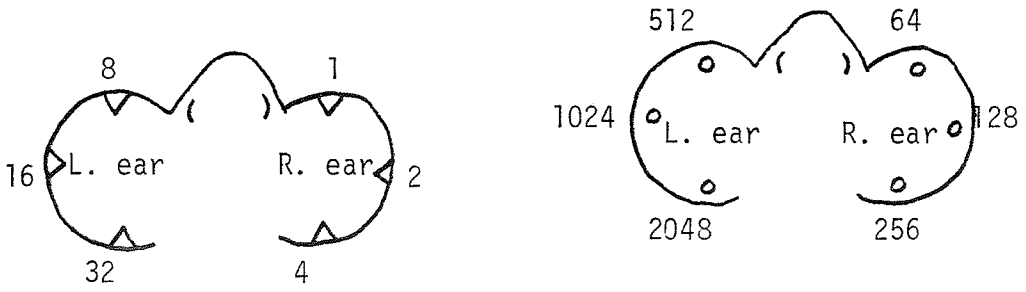

Fig. 9. Animal Identification Markings

Six discrete positions can be identified and two punch markings, viz., one round and one v-shaped notch, can be produced at each location. Combinations of these punches allow 4096 (2^{12}) individual animals to be numbered without repetition. The numbering may be done without the benefit of anesthesia, as it is relatively non-traumatic, but in the interest of speed and greater placement accuracy, it is performed after anesthetic induction.

After number identification, the animal is sheared with a commercial clipper, having a No. 40 shaving head which leaves a very short stubble to be removed using a readily available depilatory, NEET ®. The depilatory in the form of a paste, is applied to the skin for approximately 3 minutes which is sufficient to remove all remaining hair. The liquid is thoroughly wiped off and the mouse is

immersed in a detergent solution to remove any vestiges of the depilatory and to wet completely the skin surface. This procedure eliminates the entrapment of small air bubbles on the skin surface, which if introduced into the sound field would serve as cavitation nuclei and/or scattering centers. Surplus detergent is rinsed from the animal by dipping in a beaker of warm tap water.

The animal is now mounted, dorsal surface uppermost, into the animal holder and the anesthetic headpiece is fitted as shown in Figure 10. The holder and experimental animal are then transferred to the irradiation tank where the ensemble is positioned for the particular exposure regime. The position for the exposure of the pregnant female is illustrated in Figure 11, showing the relative positions of the mouse, acoustic asorber, transducer and positioning pointer, which is swung to the side and out of the acoustic pathway prior to irradiation. The pointer is positioned with the upper edge of the 1 cm. diameter disc just touching the xiphoid process of the mouse on the vertical center line, i.e., on the linea alba. As seen in Figure 12, the lateral field distributions of the transducers are such that only small areas can be exposed with uniform distribution of the acoustic field parameters. As relatively large areas of the mouse must be exposed in the case of the pregnant female irradiations, it was necessary to utilize exposure arrays to achieve uniformity of exposure conditions over the area of interest.

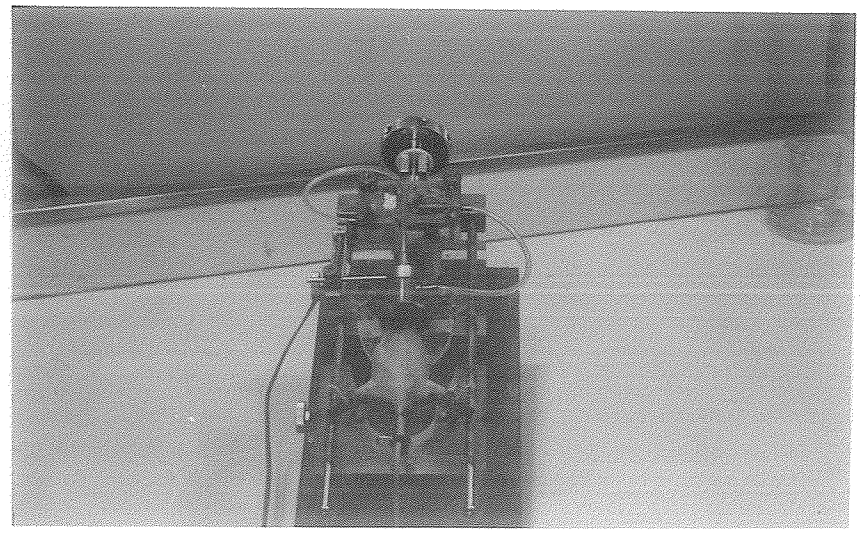

Fig. 10. Experimental Animal Mounted in Constraint System

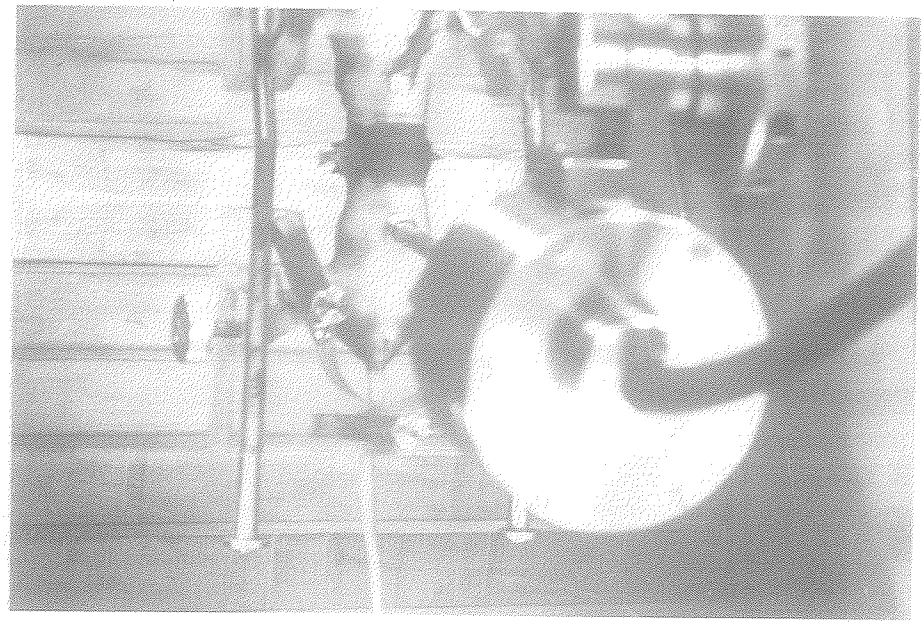

Fig. 11. Irradiation Tank and Experimental Animal Positioned for Exposure

The two dimensional array used to provide uniform acoustic illuminations of the abdominal cavity is shown in Figure 12. The data for this array, together with the associated acoustic intensity and exposure time, is stored in the PDP-8 mini-computer, and may be given the specific dimensions desired for individual animals.

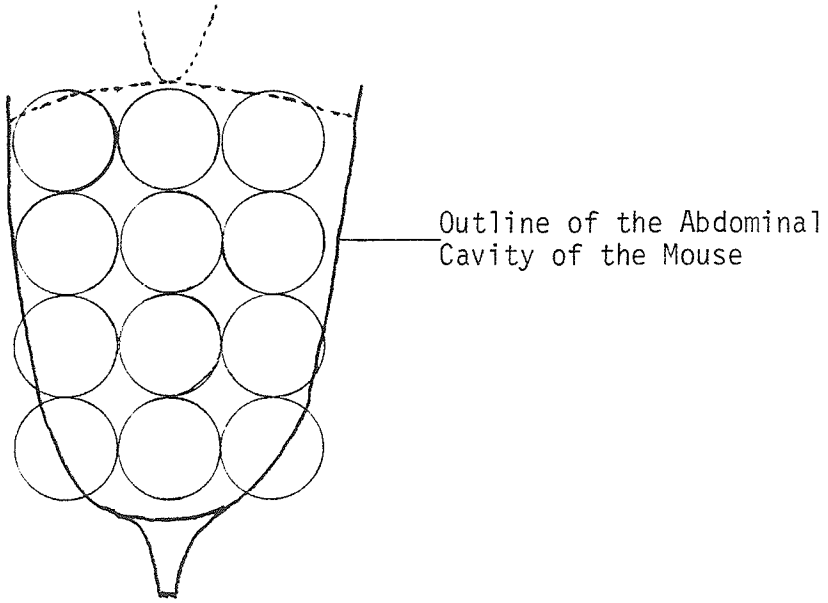

Fig. 12. Example of Exposure Array Employed to Irradiate the Abdominal Region of the Pregnant Mouse

Upon completion of the mouse positioning procedure, the start signal is sent to the computer to initiate the exposure sequence. The termination of the sequence is signaled by the computor via a teletype message, as are procedural errors such as equipment settings which permit an erroneous dose, failure of the electrical or mechanical sequences, and operator error in setting the exposure variables. A second class of computer output lists the animal number, exposure array size, and specified dose given the specimen.

The computer has been incorporated in an interactive mode in the study to facilitate the implementation of a double blind mode of operation while allowing a single investigator to carry out the irradiation routines. This computer-experimenter interaction provides for the machine to move the animal relative to the acoustic beam, switch and alter the power to the transducer in complex sequences, monitor equipment function and respond to both automatic and operator initiated interrupts. The procedure to bring the computer on line begins with the input of the exposure parameters, viz., the acoustic intensity, time of each "shot" in the array, the dimensions of the array, and the number of the animals which are to be controls, or "sham" irradiated animals. The computer selects the animals to be sham irradiated by a pseudo-random number technique utilizing the numbers given to the first mouse in the sequence. The data listing the sham animals is outputted by the computer on either the teletypewriter or on punched paper tape, with the latter form being advantageous in implementing the double-blind aspects of the procedure. This exchange of information terminates the initialization procedures for the computer.

After the animal preparation is complete, and the acoustic beam has been located at the designated anatomical stucture, the computer is supplied with a start signal via the TTY. The computer, through appropriate interface equipment, performs the mechanical sequences necessary to irradiate the subject. This is repeated for each animal in the group undergoing irradiation. This exposure

sequence, as described above, is repeated 24 hours later on the same animals to provide a higher total dose delivered to each subject, over a greater portion of the gestation period. This exposure procedure provides another dose related variable which may aid in elucidating the processes of tissue -- ultrasound interaction.

The procedure employed in exposing the testicles in the male differs in several significant points from that of pregnant females, viz., the shaving is restricted to the scrotal sac and inguinal region, no depilatory is used, and the organs are constrained, dependent, in the scrotum. The relative scarcity of hair on the scrotum and the possibility of localized irritating action of the depilatory suggest the first two differences. The third difference in procedure is necessitated by the reaction to stimulus of rodents to retract the testes into the inguinal canal. Such retraction may place the organs well into the abdominal cavity making them relatively inaccessible to an acoustic field of known intensity. The photograph in Figure 13 shows the testes of a mature mouse restrained in the scrotal sac by a ligature. It should be noted that the ligature does not include the preputial area. The animal is anesthetized and contrained in the holder in the same way as the pregnant female and a single exposure is performed for each testis. After the exposure, the animal is allowed to recover from the anesthetic and is caged and fed as normal colony animals until the time for sacrifice, which is accomplished by cervical dislocation. The

Fig. 13. The Use of a Ligature in the Constraint of the Testes of the Mouse in the Scrotal Sac

testes are removed and immediately immersed in a 10% formalin in Ringer's solution after which they are ready for histological preparation following 48 to 72 hours of fixation.

The procedure employed in exposing the ovaries of non-pregnant, proven reproductively capable females follows the course of the pregnant females through the anesthetic sequence. Stage III surgical anesthesia is then maintained while an incision is made through the lateral skin surface and the skin flap reflected dorsally, to expose the peritoneum overlying the ovary. The animal is then mounted in the holder, placed in the exposure tank and oriented

such that the peritoneum lies in a plane orthogonal to the axis of the acoustic beam, with the ovary centered precisely on the axis. The exposure of the ovary is then carried out while the tissue-water boundary is closely observed for signs of cavitation or off-axis movement due to radiation force effects, either of which would invalidate the animal.

After the exposure sequence is completed, and the animal removed from the holder, the wound is closed with No. 11 wound clips, and the animal allowed to recover, as with the testicular exposure, until the time of sacrifice. The sacrifice procedure is identical to that used with the males, and the ovaries are carefully removed and fixed. The exposed ovary is differentiated from the unexposed by removing all the surrounding fat from the irradiated organ. The tissue is suitable for histological preparation within 24-48 hours of sacrifice.

E. SACRIFICE AND ASSAY PROCEDURE

Necropsy of the pregnant females occurs on the 18th day of gestation. The sacrifice is performed by cervical dislocation providing quick, efficient dispatch of the animal, entailing a minimum of trauma to both the female and the fetuses. The corpse is tacked to a paraffin block, ventral side upward and the abdominal cavity is exposed by a U-shaped incision beginning at the lowest rib on the left side, extending downward to the hip joint, traveling

laterally to the opposite hip joint, then upward to the lowest rib on the second side. The skin flap resulting from this incision is reflected to provide unimpeded access to the abdominal contents, viz., the uterine horns, fetuses, and all other digestive and reproductive organs, see Figure 14.

Fig. 14. View of the Abdominal Contents of the Pregnant Mouse at Necropsy: Distribution of Fetuses in the Abdomen

The uterine horns are spread laterally to facilitate access to the contained fetuses and placentae, which are removed for examination. The maternal organs are examined for gross pathologies or abnormalities such as vascular aneurysms, liver petechiae, stasis of the urinary or gastrointestinal tract, excessive bleeding, implantations or resorptions in the uterine horns, diaphragmatic hemorrhages and

renal atrophy or necrosis. The ovaries are removed to permit a count of the corpora lutea. The animal is then discarded.

Each fetus is examined for gross anatomical defects or teratologies inclusive of defects of paws and limbs such as polydactyly, missing toes, clubfoot or limb malformations. The skin is examined for hemorrhagic conditions or pigment defects. The eyes and ear flaps are checked for non-fusion or growths. The naso-palatinic region is non-surgically inspected for cleft lip or cleft palate conditions. The sex of each fetus is recorded and the weight of each litter is measured to ± 0.05 gms. These data which are to be subjected to statistical analysis are recorded on a single data sheet for each mouse and includes the animal's identifying number, dates for breeding and sacrifice, strain of mouse, number of live fetuses, their sex and physical condition and any pathologies, the number of resorptions (early and late), the number of stillborn, implantation sites, corpora lutea, and litter weight. Comments concerning any unusual pathologies associated with the female are appended.

The procedures developed to gather numerical data on the acoustic properties of the ovaries and the testes, are the same with regard to the acoustical aspects. The animal to supply the organ of interest is sacrificed by cervical dislocation and the gonad excised speedily and mounted in specially designed support cups attached to the animal holder, described above. A thermocouple constructed of

0.003 in. copper and constantan wires is threaded through the tissue with the aid of a 30 ga. hypodermic needle to center the junction in the organ. The free ends of the thermocouple are soldered to large diameter copper wires which drive a recording galvanometer having a sensitivity of approximately 1 μamp per cm deflection. The possibility of interchangable galvonometer elements provide a sensitivity range of 0.792 μ amp per cm to 1.34 μ amp per cm.

The modified holder with the organ in place is mounted in the irradiation tank, the total circuit impedance is measured, and an approximate positioning of the transducer is performed, by means of the locating pointer, which is refined by performing a beam plot, as described in the section on calibration procedures, with the substitution of the tissue-thermocouple system for the thermocouple probe. A series of exposures are performed, the time duration of each being 1 sec, and the acoustic intensities adjusted to give galvanometric deflections in the range of 2 to 10 mm. The 37 degree C. water bath serves as the reference temperature for the thermocouple thus avoiding the large DC offset which would be generated should a standard ice bath be utilized.

Following the exposure sequence, and the photographic development of the galvanometer recording film, the tissue is removed from the exposure tank and an incision is made above the thermocouple to verify the position of the junction in the tissue. The organ is then discarded.

III. INSTRUMENTATION

A. EXPOSURE INSTRUMENTS

Much of the equipment and instrumentation used in this study for the generation and calibration of ultrasonic fields has been in existence for a number of years and is adequately described elsewhere (54,55). Consequently, only a brief description is given. Where additions and modifications to the conventional devices make it necessary, more detail is provided.

A block diagram of the system is presented in Figure 15. A crystal oscillator (International Crystal, Model FO-1), provides the rf signal at the nominal resonant frequency of the quartz crystal transducer, 1.0 MHz in this case. This low level signal is presented to a series of amplifiers, through an attenuator having a maximum output of 2 KW from the final stage, into a nominal 50 ohm load. The high input impedance of the ultrasonic tranducers is matched to the low impedance of the final amplifier by a tuned LC matching network. Incorporated in the matching network is a precision capacitor which appears as one leg of the voltage divider providing for variation of the intensity of the acoustic field over a wide range. The divider network also provides a feedback path to the screen grid of the final amplifier via stabilzing circuits which insure a predetermined rectangular envelope of the rf signal applied to the transducer. A Philbrick Research's R-100B dual regulated

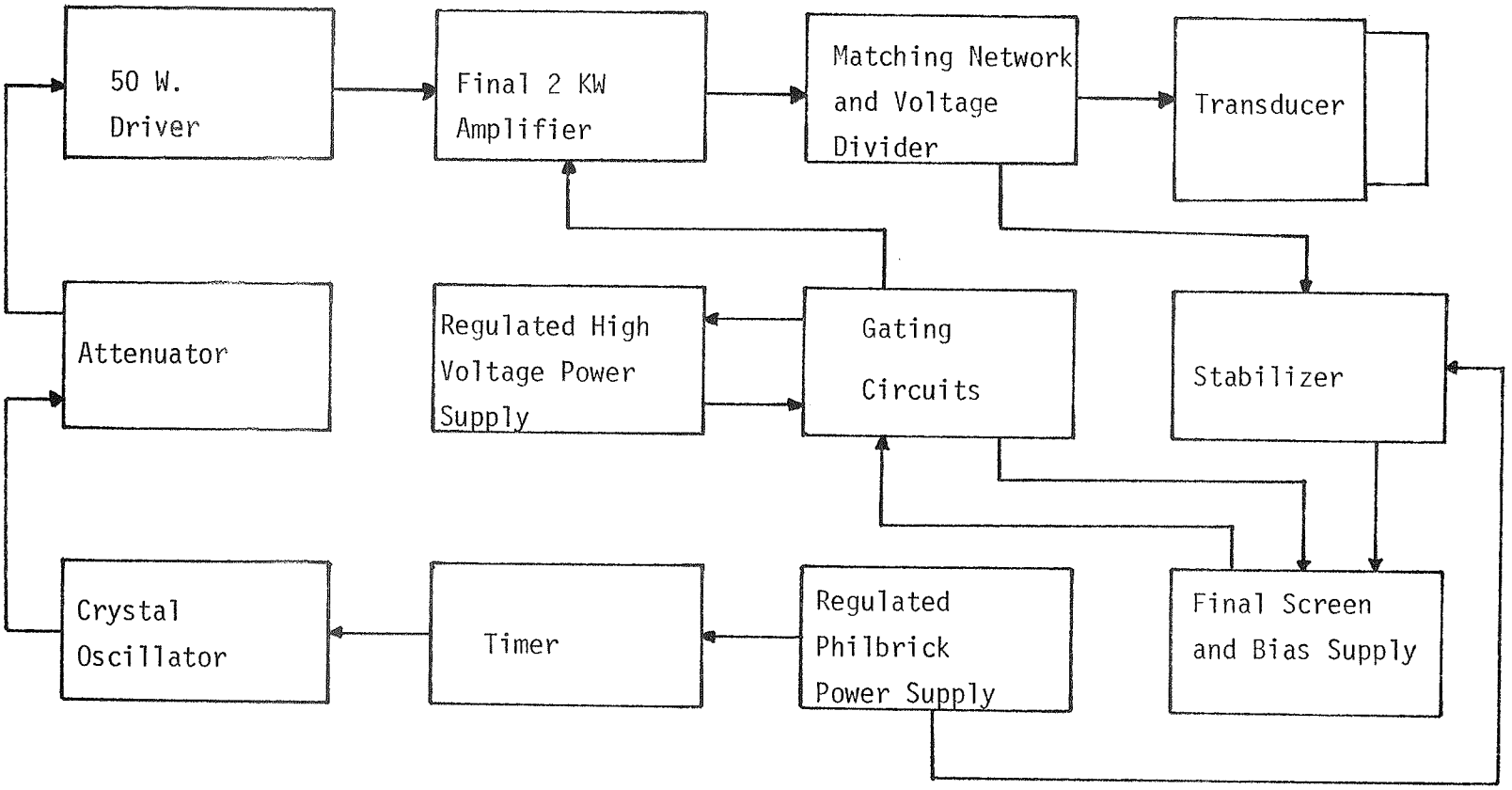

Fig. 15. Block Diagram of Exposure System

power supply serves as a precision reference voltage source for the stabilizer network. A relative indication of rf voltage is supplied by a Hewlett-Packard model 410-C VTVM monitoring the matching network through a second divider. The timing and gating signals are provided by a Computer Measurements Co., Model 786-C dual preset counter and clock (when not operating under computer control). The clock circuit which may be manually set to provide rf bursts ranging from 1 msec to hours, recycles automatically for repetitive bursts. Rise and fall times of the acoustic pulse subsequently generated are typically 10 μsec.

Three dimensional positioning of the animal relative to the transducer is made possible by means of a Bridgeport mill base (Model 96463) modified to provide support surfaces for both the irradiation tank and the acoustic transducer. Figure 16 is a photograph of the irradiation tank with transducer in place. Movement in all three dimensions may be accomplished manually or by use of precision drive motors associated with each axis. The motors provide step movements in 0.001 in. increments. The relative position of each point on all three axes is provided by a Digipoint (Janus Control Corp,. Model 6373) digital position readout. This position indicator displays the position of the mill base bed to the nearest ten thousandth of an inch, exceeding the positioning capability of the stepping motors by one order of magnitude.

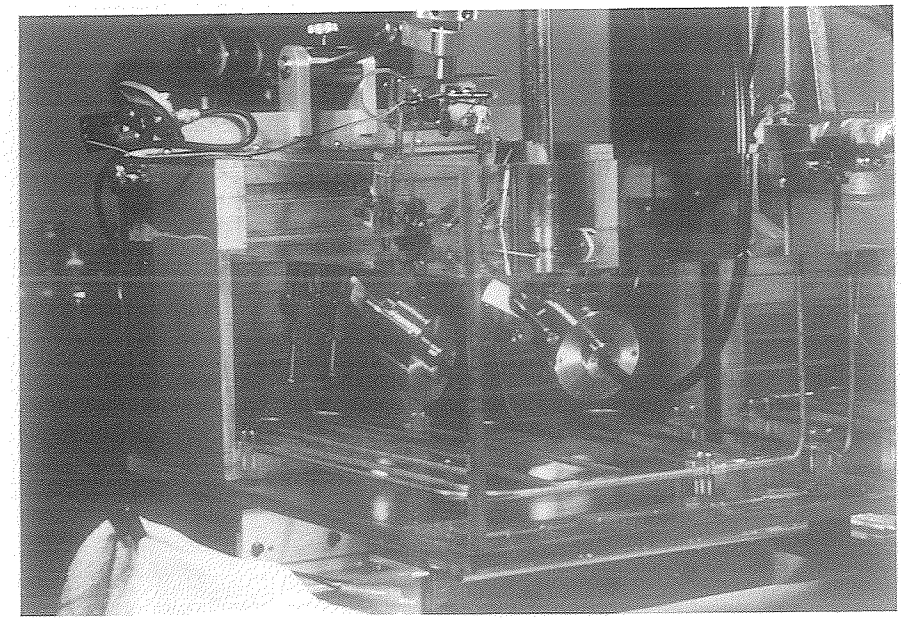

Fig. 16. Exposure Tank and Related Equipment

The ultrasonic irradiation tank, shown in Figure 16 is constructed of one inch thick plexiglas sheets bonded by means of a cloroform-plexiglas shavings solution. The end wall opposite the transducer is lined with angled strips of SOAB (TM) acoustic absorbing material to minimize standing waves in the ultrasonic field. Circulation of the Ringer solution bath and minimization of thermal gradients is provided by a magnetic bar stirring system working through the floor of the tank. The desired temperature of the bath is maintained by the circulation of warm water through stainless steel tubing laced across the bottom on one inch standoffs, with the bath temperature maintained to within $\pm$ 0.5^{o} C. by means of a proportional temperature controller. The tank is rigidly fixed to

the Bridgeport mill base by two stainless steel dowel pins and locking screws. The fixture visible at the top of the tank above the acoustic absorbing material is the mounting bracket for the animal holder which provides both rectilinear and angular variability of specimen orientation in the left half-volume of the exposure tank.

Three transducers were assembled for this project, in order to provide the necessary range of acoustic intensities and geometries. Figures 17 through 19 are photographs of these instruments; one focussed and two plane-wave field generators. Each transducer is capable of a unique range of intensities and field geometries, and a representative sample of the field geometry of each transducer is illustrated in Figures 20 through 22 shown with normalized relative acoustic intensities.

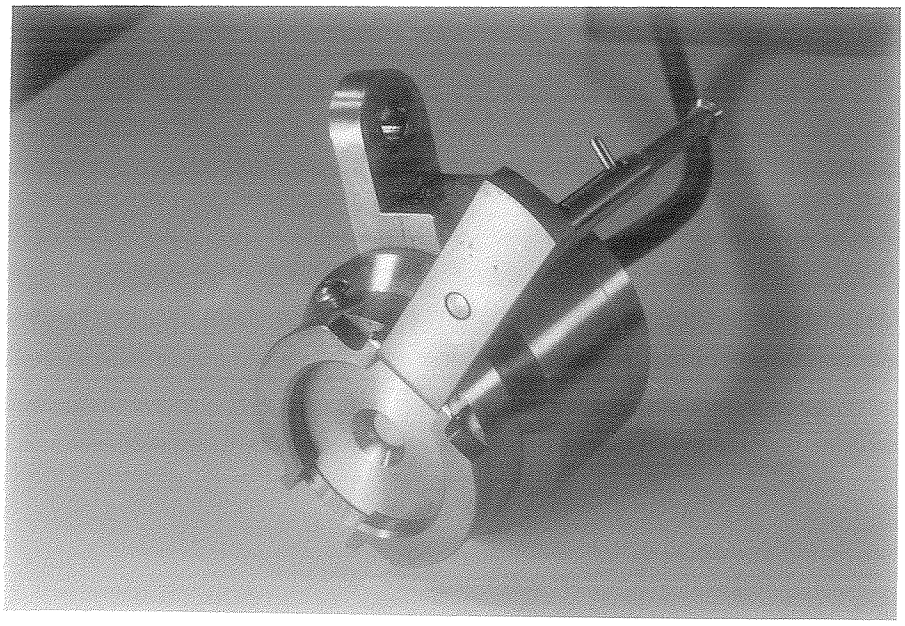

Fig. 17. Transducer No. 1: Small Aperture, Plane Wave Acoustic Source

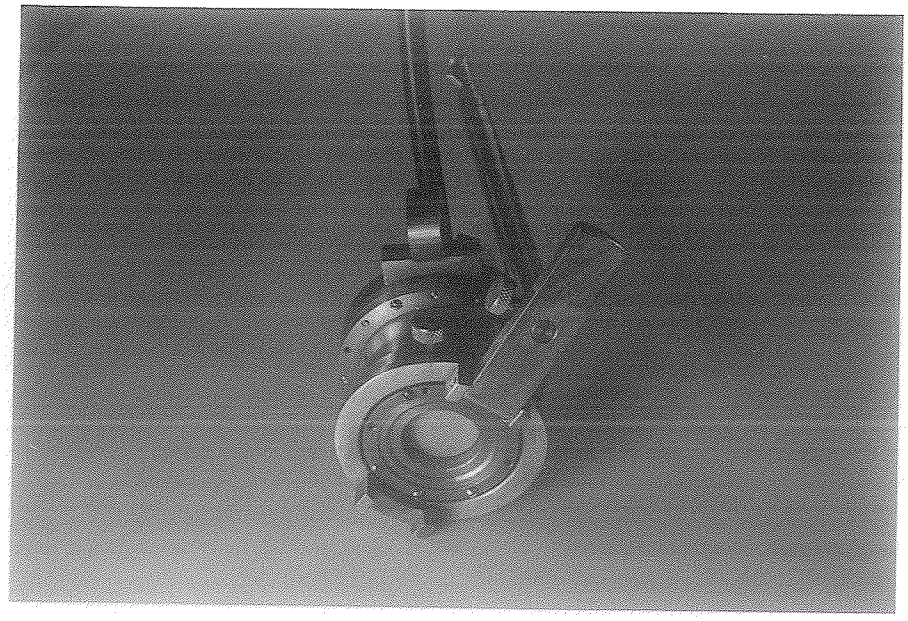

Fig. 18. Transducer No. 2: Large Aperture, Plane Wave Acoustic Source

Fig. 19. Transducer No. 3: Focussed Field Acoustic Source

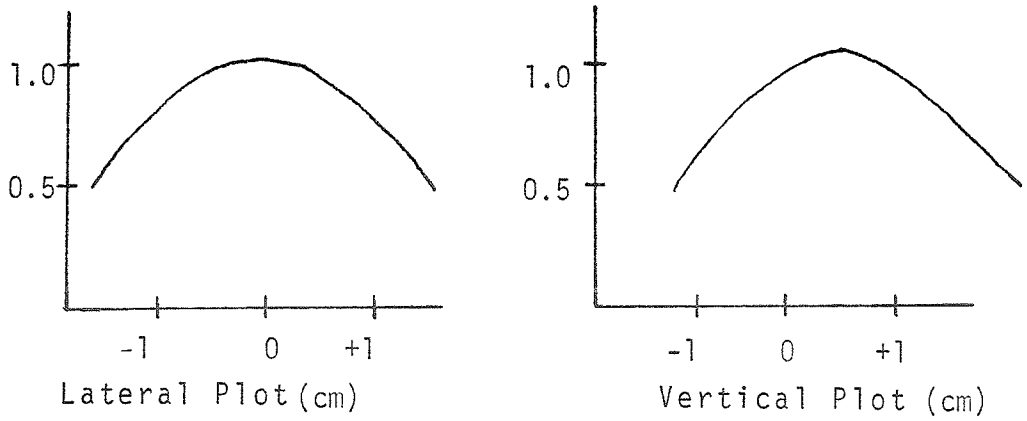

Fig. 20. Geometry of the Acoustic Field Generated by Transducer No. 1

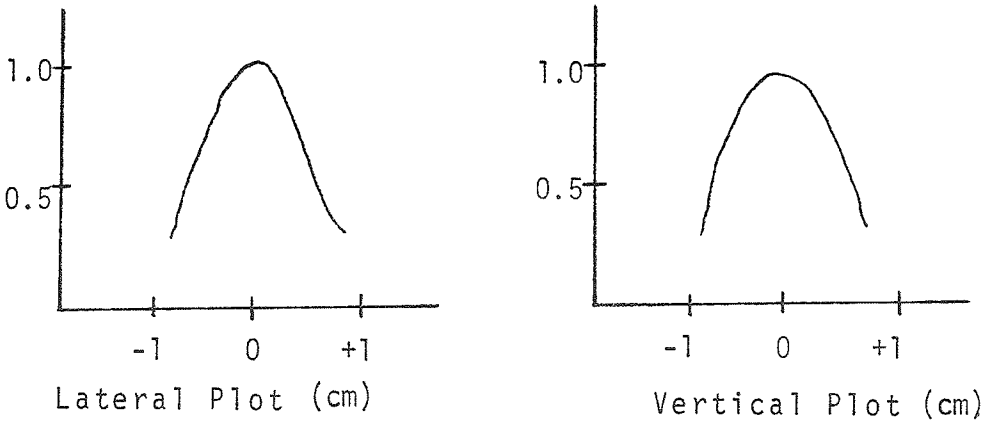

Fig. 21. Geometry of the Acoustic Field Generated by Transducer No. 2

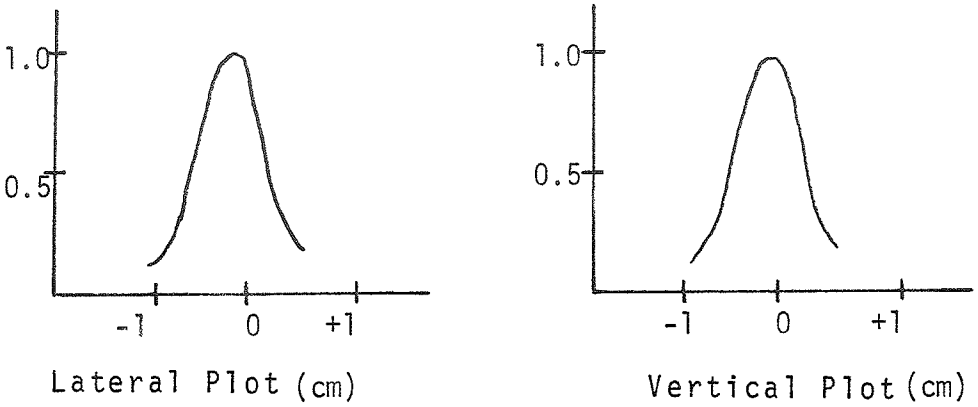

Fig. 22. Geometry of the Acoustic Field Generated by the Focussed Transducer

The development of the three transducers resulted from project requirements for variable geometries and/or field intensities. For example, the ideal transducer for the pregnant animal exposures would deliver the predetermined ultrasonic exposure in a single pulse having an intensity distribution across the abdomen (of approximately 3 x 6 cm) of less than 5%. Since a transducer design, to accommodate this requirement may be impossible to achieve, the three transducers were used as required by the exposure parameters. Table 1 illustrates the maximum available acoustic intensities and attendant field geometries for each transducer.

TABLE 1 - TRANSDUCER PARAMETERS

Transducer No.	1/2 Power Beam Width	Maximum Usable Peak Intensity
1 (Plane-wave)	3.0 cm	2.5 W/cm
2 (Plane-wave)	1.5 cm	10.5 W/cm
3 (Focussed (f≈3.5 cm)	.5 cm	125.0 W/cm

As an example of the limitations imposed by the contraints of maximum available peak acoustic power versus acoustic field width; transducer No. 1 is used for exposures involving intensities of no more than 2 W/cm^2, but achieves complete abdominal coverage with a 2 x 3 shot array, spaced 1 cm apart. Transducer No. 2 may be employed at acoustic intensities of 10 w/cm^2 and a 4 x 5 shot array. The necessity for a numerically larger array (not spatially larger) requires more exposure time due to the limited positioning speed of the computer controlled mill base.

The progressive incorporation of digital processing equipment into the study to provide control and monitoring capabilities was both gradual and necessary. During the developmental period of the project, two men were fully occupied in performing the exposures and implementing the double-blind aspects of the program. The first step toward automation was taken when the automatic sequencing capabilities of the CRC counter and the stepping motor controls were tied together to perform a portion of the array motions of the irradiation. This step did not eliminate any personnel, but did reduce the work load.

The integration of the full capabilities, both computational and machine control, of the in-house computer facilities permit one individual to perform the exposure routine and a second person necessary only to provide safekeeping of the double-blind information. Figure 23 is a block diagram of the computer-exposure equipment tie in. The teletype provides the usual user-equipment link for low-speed data exchange. The high-speed paper tape reader-punch provides both program loading facilities as well as animal exposure status in a form not readily read by the experimenter. The digital to analog and analog to digital interface circuitry provides the monitoring, control and bookkeeping functions necessary to fault free operation of the exposure equipment. This last capability makes superfluous a second individual for the irradiations.

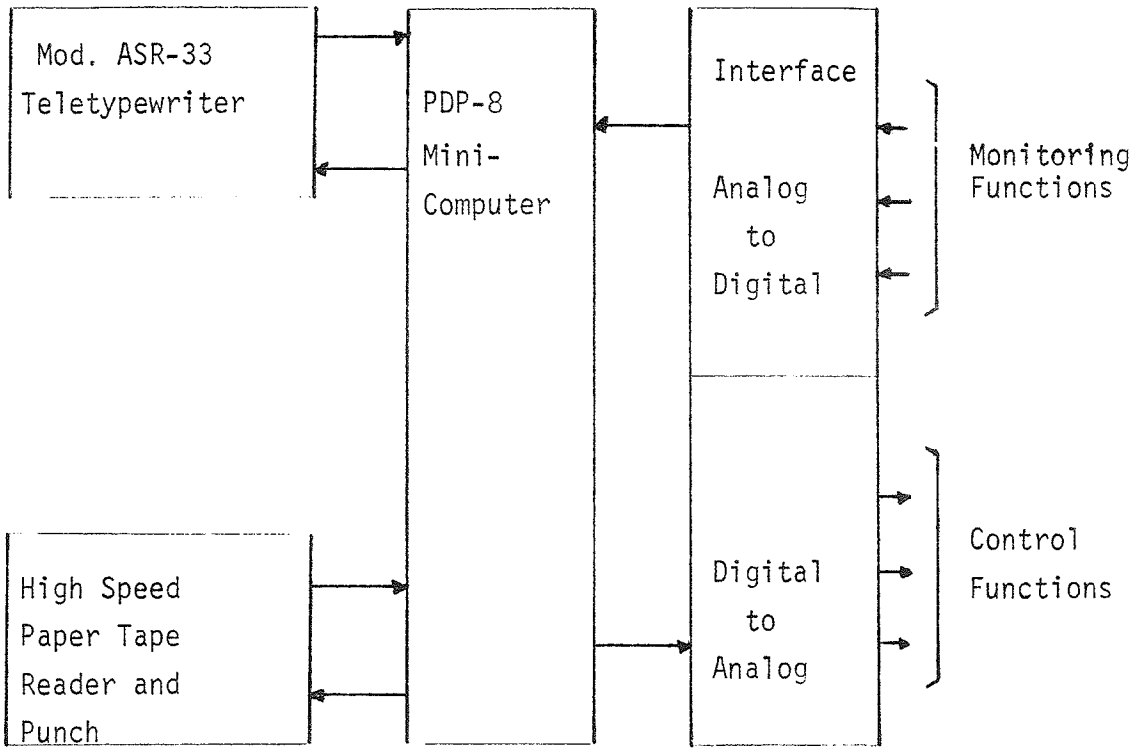

Fig. 23. Block Diagram of the Computer-Exposure Equipment Interface

The full hierarchical interrupt capabilities of the PDP-8 computer provide for complete operator control at all points of the exposure sequence in the event of emergency or error conditions. These interrupts are designed to halt in a state which will minimize danger to the equipment, animal and operator in the event of equipment malfunction. The software package consists of an assembly language program, occupying 8K of core and implementing the procedural alternatives discussed in the preceding section with a reasonable degree of flexibility.

B. ANESTHETIC EQUIPMENT

The anesthetic delivery equipment was designed and built specifically for the needs and exigencies of this procedure and anesthetic medium. Figures 24 and 25 show, respectively, the various articles of equipment for 1) induction; 2) short term maintenance; and 3) long term maintenance of a mouse under the gaseous anesthetic.

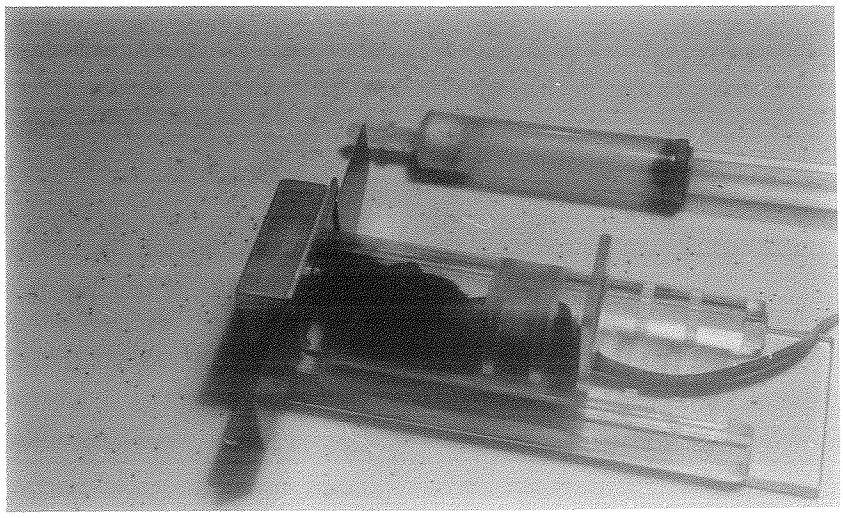

Fig. 24. Anesthetic Equipment for the Induction and Short Term Maintenance of Anesthesia in the Mouse

The induction chamber, Figure 24, employs several novel concepts in the design, viz., the ability to regulate the delivery of the anesthetic agent to the animal, the passive restraint to avoid physical injury to the subject during the excitable phase of induction and the adaptability for the size of the animal. This last feature is essential since a grip on the tail of the animal must be maintained until the excitable stage terminates, to prevent the animal from turning end for end in the chamber. The short term maintenance of anesthesia is accomplished utilizing the small cylinder device shown in Figure 24. This tube was constructed from a standard 10cc plastic syringe barrel, and cotton wadding inserted to fill the closed end.

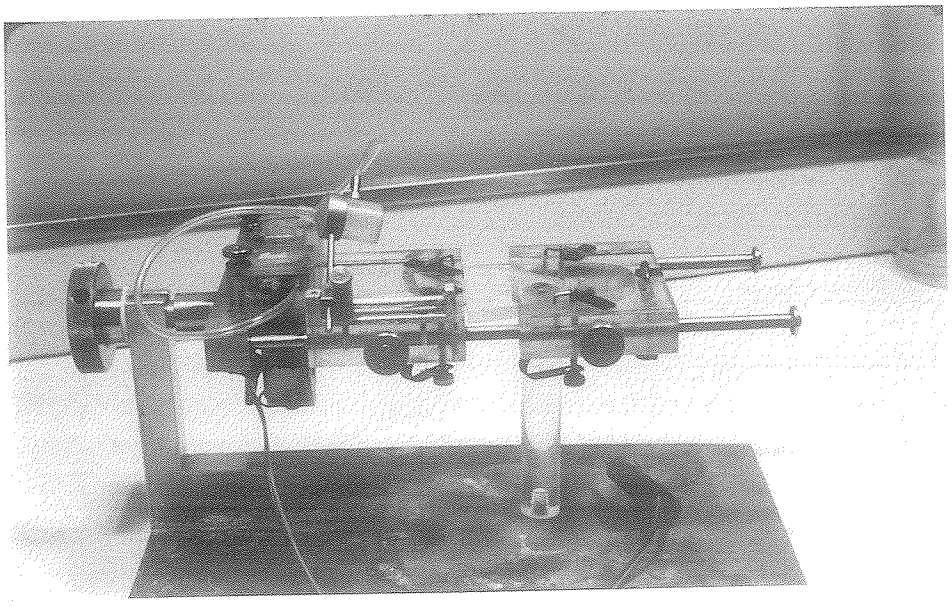

Fig. 25. Anesthetic Equipment for the Maintenance of Anesthesia in the Mouse for Extended Time Periods

The head of the mouse or any small rodent, just occupies the opening in the syringe barrel, making it an ideal device for the short term maintenance of anesthesia, while allowing manipulative freedom of the subject.

The mechanism for maintaining anesthesia for periods exceeding one hour is an integral part of the animal restraint system. Figure 25 shows the holder and anesthetic machine and Figure 26 shows this instrument with the animal in place, preparatory to the exposure sequence. The animal holder is constructed of stainless steel and lucite, to resist the effects of corrosion by the Ringers solution. The feet and tail are gripped by clamps designed to minimize movement by the animal, yet do no injury to the limbs.

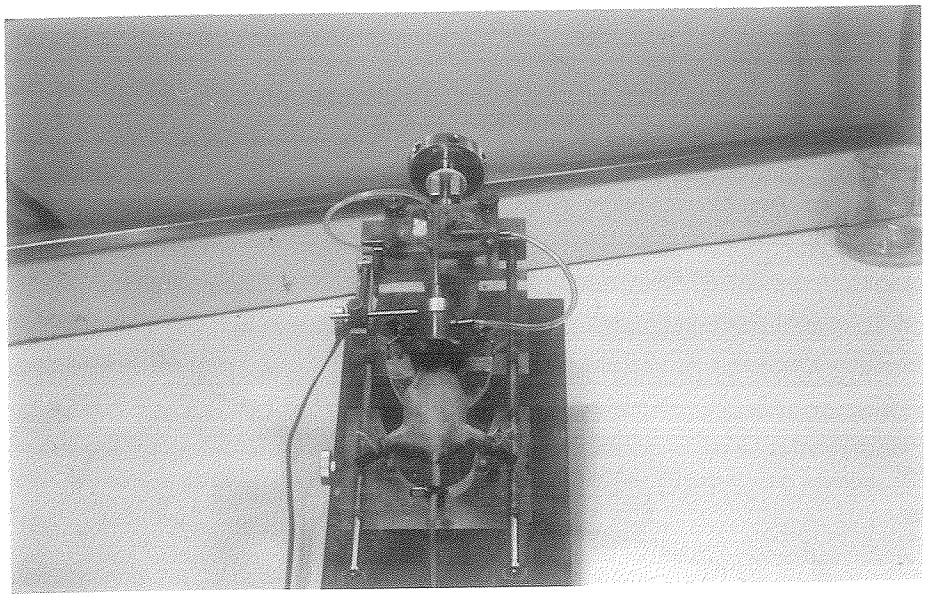

Fig. 26. An Experimental Animal in the Constraint System, Preparatory to Exposure

Differing physical dimensions of the mouse are accommodated by the lower sliding block. The anesthetic device is part of the upper mounting fixture of the animal holder with a connecting plug for electrical power, which can be connected to a mating plug mounted on the exposure tank to drive the circulating fan. The soda lime CO_2 absorber is standard with any closed or semi-closed anesthetic system to minimize the rebreathing of expired CO_2. The anesthetic diffusing element is a reservoir supplying evaporatable anesthetic liquid to replenish that consumed by the animal. The centrifugal fan provides a constant motion of the gases past the animal's nose and mouth through the head cup. The cup loosely fits the animal's muzzle and provides for leakage of room air to the animal preventing death by hypoxia. A limitation of this device is the CO_2 build-up after approximately 1 1/2 hours and which requires periodic removal of the head piece, and reoxygenation of the subject. As times longer than one hour of anesthesia were unnecessary, this device proved to be quite satisfactory.

The second model of a long term anesthetic machine corrects some of these problems. Here, an open type of administration system having no provision for recirculating the gases, provides means of closely regulating the gas flow, either air or oxygen to the animal, as well as valving to alter the ratio of anesthetic to gas. This ratio may be adjusted from zero to

saturation for a wide range of flow rates. Volatile drugs may be administered by mixing with the fluid in the flow-rate chamber, or the gas humidity may be adjusted by the use of water in this chamber. This anesthetic machine allows a greater degree of control over the anesthesia depth of the animal and the maintenance of a satisfactory homeostatic condition for long periods. A disadvantage is the open aspect of the administration which may release significant quantities of gas to the room atmosphere. Fortunately, the low saturation concentration of Metofane combined with reasonable room ventilation precludes any harm to personnel except in cases of gross negligence.

C. CALIBRATION EQUIPMENT

The acoustic calibration methods and instrumentation utilized in this study have been completely described elsewhere and are only briefly discussed herein.

Figure 27 shows an example of the stainless steel sphere and bifilar suspension system used in the radiation force method of absolute calibration.

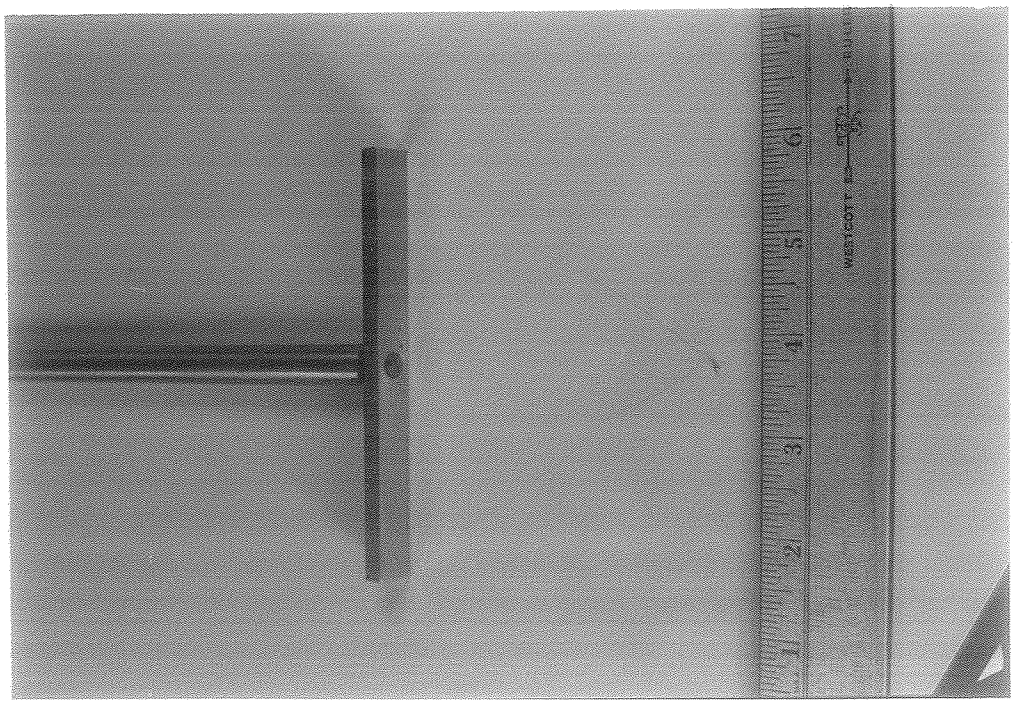

Fig. 27. The Acoustic Radiometer and Bifilar Suspension System

The absolute values for the acoustic intensity derived from the stainless steel ball deflection data are transformed to a secondary standard, the thermocouple probe, shown in Figure 28. This use of a transfer standard in the determination of acoustic field parameters provides an accurate, portable, stable and repeatable method of assuring accuracy in the determination of acoustic field intensity over an extended period of time.

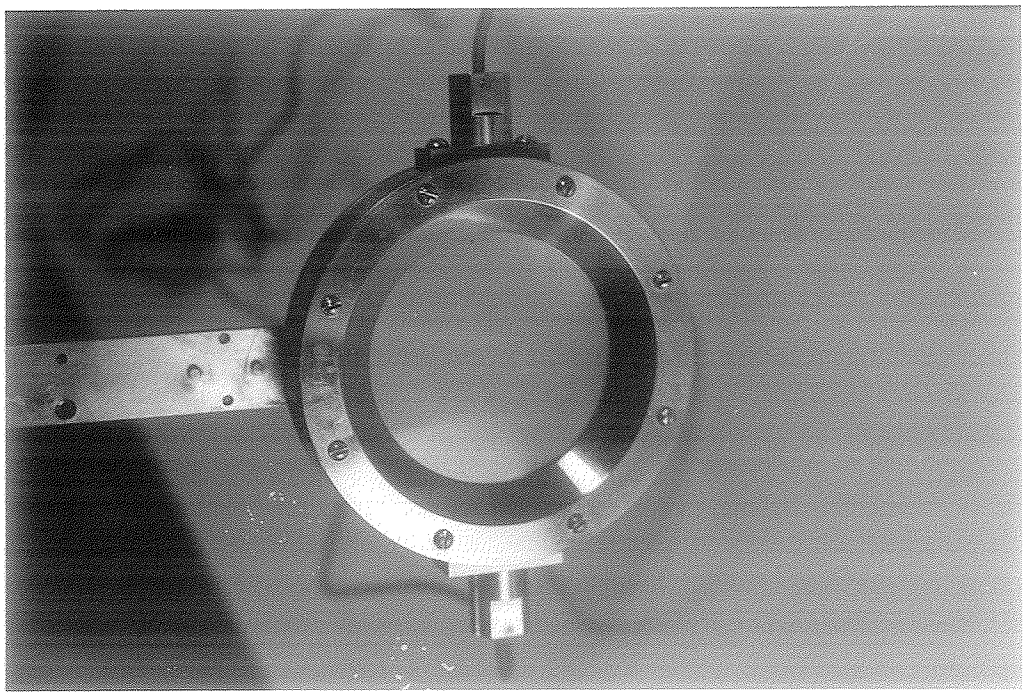

Fig. 28. The Thermocouple Probe Calibrator Uses as a Secondary Standard for Acoustic Field Calibration

IV. RESULTS

A. IN-UTERO EXPOSURES

The in-utero fetal exposures were performed at selected intensities, times and repetitions designed to elicit a toxophilic reaction. In this preliminary work the number of repetitions was either one or two and the intensities and associated time of exposure are listed in Table 2. The sham irradiated animals would constitute a zero intensity with an associated time for each group reported and are therefore not listed in the table.

TABLE 2 - ACOUSTIC INTENSITIES AND ASSOCIATED TIME OF EXPOSURE

Intensity (W/cm^2)	Time (Sec.)
1.0	50.0
1.0	100.0
2.0	50.0
2.0	100.0
5.0	10.0
6.0	10.0
8.0	5.0
10.0	5.0
20.0	1.0

Each of these groups contains 30 or more animals, except the last, and each has a corresponding sham exposed group as

detailed in the Procedures Section on the "double blind" aspects of the experiment.

The analysis of the data utilized the multiple regression programs contained in the SOUPAC statistical package, which is in residence with the IBM 360/75 computer library at the University of Illinois Digital Computer Laboratory. Eighteen dependent variables were chosen from the experimental observations and these were examined as a function of up to 29 independent variables. Table 3 lists these variables. The average value for each of the experimental, independent variables is provided in each of the following sections, as is the standard error of estimate, to provide some indication of the goodness of fit of the model.

The first three dependent variables in Table 3 refer to the probability of an effect of the procedure or acoustic exposure on the dam. The probability of an anomaly is treated to examine the significance of the number of occurrences and the significance of the type of anomaly occurring. The litter variables, implants, size, etc., examine the significance of changes in the magnitude of these experimental variables as functions of the independent variables. Average fetal weight analysis constructs a relationship between the average weight of a fetus (total litter wt./ total no. live fetuses) and the exposure parameters. The proportion of males in a litter is related to the exposure variables to examine preferential sex susceptibility.

The independent variables were selected to supply causative factors for all experimental observations and include the possibility of non-linear relationships. The first four independent variables in Table 3 involve the acoustic exposure parameters, viz., acoustic intensity, time of exposure and the number of times the animal was subjected to the exposure procedure. The next four independent variables concern assessment of damage due to the handling procedure. The sinusoidal terms concern cyclic responses of the animals, in the event this cyclic behavior masks results. The term "dip constant" is included to account for possible detrimental effects upon maternal fertility of a miticidal chemical treatment used temporarily during the study. The next four independent variables concern animal selection data. The number of corpora lutea was included as an independent variable in the analysis of variables related to litter observations. Implants and resorptions are included as independent variables for fetal weight and proportion of males to account for the decrease of fetal weight with increasing litter size and the relatively high proportion of male fetal deaths in-utero as a function of increasing resorptions (67).

In Table 3, and in all subsequent tables, "I" is the peak, free field intensity; "T" is the time of exposure; and "R" is the number of repititions of the procedure.

TABLE 3 - LIST OF DEPENDENT AND INDEPENDENT VARIABLES

Dependent Variables	Independent Variables
P (Maternal Damage)	I T R
P (Maternal Survival)	I^2 T R
P (Pregnancy)	I T^2 R
P (Anomalies):	I T R^2
Hemorrhagic	T
Eyelid Fusion	R
Giant	T^2
Stunted	TR
Exencephaly	COS θ ($\theta = 2\pi\frac{D}{365}$)
Unspecified	SIN θ
Litter:	COS 2θ
Implants (Total)	SIN 2θ
Implants (Empty)	⋮
Litter Size	COS 6θ
Resorptions (Early)	SIN 6θ
Resorptions (Late)	Miticidal/Dip Constant
Resorptions (Total)	Maternal Age
Average Fetal Weight	(Maternal Age)^2
Proportion of Males Per Litter	Day of Gestation
	Irradiated/Sham Control
	No. of Corpora Lutea*
	No. of Total Implants**
	No. of Total Resorptions**

*Analysis of Litter Parameters only

**Analysis of fetal weight and proportion of males only

1. Probability of Maternal Survival

As in maternal damage, adult mortality was only appreciable at intensities exceeding 5 or 6 w/cm^2 and Table 3 lists the independent variables of significance here.

Independent Variable	P
I^2 T R	< .001

$\bar{y}$ = 0.953

Standard Error of Estimate = 0.208

This produces a regression equation of the form:

$$y = 1.239 - .00159\ ITR - 3.250 \times 10^{-4}\ I^2\ TR.$$

EQUATION 3

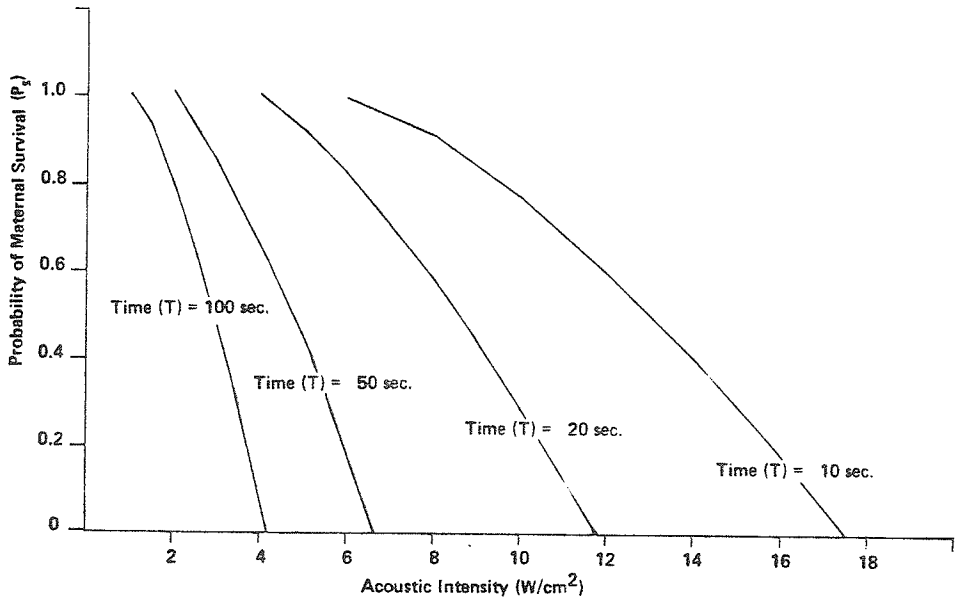

Figure 29. Plot of the Probability of Maternal Survival vs. Acoustic Intensity (w/cm^2) With Exposure Repetitions as a Parameter

Fig. 29 shows a family of smooth curves generated by regression equation 3 relating the probability of maternal survival to acoustic exposure variables considered pertinent, viz., the acoustic intensity and time of exposure, for two repetitions of the irradiation sequence. The points plotted represent the percent survival of the exposed animals.

It should be noted that the smooth curves in Fig. 29 shown as an example of the use of the equations, reflect the data more accurately in the regions where irradiation damage was observed than in low intensity regions, where little or no damage occurred. This illustrates both the limitations and advantages of this equation. To extend the usefulness of the equation as a prediction to low intensity, long exposure time conditions, acoustically related damage must be encountered in these areas. Conversely, the equation is useful in its present form in predicting damage at acoustic intensities in the region of 10 w/cm^2.

2. Probability of Maternal Damage

The assessment of maternal damage comprised observations of paralysis, skin slough, urinary dysfunction, intra-abdominal bleeding, and/or internal organ anomalies. Table 4 lists the independent variables with the associated level of significance (Student's T-Test).

TABLE 4 - INDEPENDENT VARIABLES AND ASSOCIATED LEVELS OF SIGNIFICANCE FOR THE PROBABILITY OF MATERNAL DAMAGE

Independent Variable	P
I^2 T R	< .001
I T^2 R	< .05
I T R	< .01
T	< .05
T^2	< .001

$\bar{y}$ (Avg. value of ind. variable) = 0.0148

Standard error of estimate = 0.286

The combination of these variables results in the regression Equation 4, below, which describes the probability of maternal damage in terms of the independent variables.

$$y = 0.06828 + .003545\ ITR + .00161\ I^2TR + 2.77 \times 10^{-5}\ IT^2R$$
$$-.00428\ ITR^2 - .0232\ T + 1.453 \times 10^{-4}\ T^2$$

EQUATION 4

These values are consistent with experimental data in that infrequent, grossly observable damage was done to the dams below an intensity of 6 w/cm^2 and this consequence of exposure was assiduously avoided as an undesirable side effect to the question of reproductive toxicity.

3. Probability of Pregnancy

The probability of an animal being pregnant at the time of necropsy carries implications which extend beyond the necessity of having parturient animal for analysis. Among these implications is the absence of observable gravidity which may be indicative of a toxic process. Table 5 lists the significant independent variables and associated P values for this case.

TABLE 5 - SIGNIFICANT INDEPENDENT VARIABLES AND ASSOCIATED P VALUES FOR THE PROBABILITY OF PREGNANCY

Independent Variable	P
I T R	< .001
I T^2 R	< .001
I T R^2	< .01
T	< .02
T^2	< .01
Dip	< .05
Age	< .02
$(Age)^2$	< .01

$\bar{y}$ = 0.764

Standard error of estimate = 0.410

The regression equation constructed from these independent variables is Equation 5 below:

$$y = 0.2906 + .0237\ ITR - 7.3207 \times 10^{-5}\ IT^2R - 6.535 \times 10^{-3}\ ITR^2 + .0332\ T - 1.506 \times 10^{-4} T^2 - 4.651\ (Dip) + .055A - 1.501 \times 10^{-4}\ A^2$$

EQUATION 5

Note that two variables appear in this regression equation which are not related to exposure conditions, viz., age and the chemical dip. The age variable was included to account for decreasing fecundity with maternal age and the chemical dip constant was included to account for reproductive side effects of the miticide or traumatization by the treatment.

4. Probability of Fetal Anomalies

Six classifications (See Table 3) of fetal anomalies were used as dependent variables in a single pass through the regression routine, which served to give both individual analysis of each dependent variable and correlation analysis between dependent variables. Of these six categories, only subcutaneous hemorrhages were found to be significant with respect to number and type. Table 6 lists the independent variables of significance.

TABLE 6 - INDEPENDENT VARIABLES OF SIGNIFICANCE - HEMORRHAGIC ANOMALIES

ANOMALIES

Independent Variable	P
Number	
Exposed/Sham	< .01
Control	< .001
I T^2 R	< .02
T	< .05
T^2	< .01
R	< .02
Gestation Day	< .05

$\bar{y}$ = 0.102

Standard error of estimate = 0.208

Type	
Exposed/Sham	< .05
Control	< .01
I T^2 R	< .01
T^2	< .02
R	< .01

$\bar{y}$ = 0.133

Standard error of estimate = 0.390

These two sets of independent variables produce two regression equations describing the probability of having an occurrence of this type of anomaly. For the number of hemorrhagic incidences:

$$y = 0.26 - 1.003\ E/S + .421\ C - 2.036 \times 10^{-3}\ ITR + 3.907 \times 10^{-5}\ IT^2R - .024T + 1.128 \times 10^{-4}\ T^2 - .0111R - 3.805 \times 10^{-2}\ G.D.$$

EQUATION 6

The regression equation for type of anomaly is Equation 7 below:

$$y = 0.3711 - 1.030\ E/S + .483\ C - 9.724 \times 10^{-4}\ ITR + 5.778 \times 10^{-5}\ IT^2R + 1.357 \times 10^{-4}T^2 - 1.217\ R$$

EQUATION 7

No correlation greater than ± 0.10 was found between the dependent variables.

5. Litter Characteristics

Two of the dependent variables were found to be a significant function of the independent variables, viz., total number

of implants and number of live fetuses per litter. Table 7 lists the independent variables of significance for each of these dependent variables with the associated $\bar{y}$ and standard error of estimate. Table 8 lists the correlation coefficients between the dependent variables of significant correlation.

The variables presented in the two columns of Table 8 are obtained by taking the sum and difference of each dependent variable for the two uterine horns of the specimen. The correlation of the Column I variable with the adjacent Column II variable is listed in the third column as a signed correlation coefficient.

TABLE 7 - SIGNIFICANT INDEPENDENT VARIABLES - TOTAL IMPLANTS/NUMBER OF LIVE FETUSES

Independent Variables	P
Total Implants	
I T R^2	< .05
Sum of (Σ) Corpora Lutea	< .001
$\bar{y}$ = 4.09	
Standard error of estimate = 2.93	
Number of Live Fetuses	
I T R	< .001
I T^2 R	< .05
I T R^2	< .001
COS(2π day/365)	< .05
Sum of (Σ) Corpora Lutea	< .001
$\bar{y}$ = 2.97	
Standard error of estimate = 2.33	

Two independent regression equations may be written for the two observations as Equation 8 and Equation 9 below:

$$y = -0.907 + .041\ ITR - .146\ ITR^2 + .411\ \Sigma\ C.1.$$

EQUATION 8

$$y = -1.684 + .077\ ITR - 1.413 \times 10^{-4}\ IT^2R - .029\ ITR^2 + .660\ Cos\ (2\pi \frac{D}{365}) + .387\ \Sigma\ C.1.$$

EQUATION 9

TABLE 8 - PAIR OF DEPENDENT VARIABLES AND CORRELATION COEFFICIENTS

Δ = sum of Dependent Variable I	Σ = difference of Dependent Variable II	r
Σ Total Implants	Σ Total Resorptions	0.58
Δ Total Implants	Δ Early Resorptions	0.61
Δ Total Implants	Σ Total Resorptions	0.69
Σ Total Implants	Δ Late Resorptions	0.78
Σ Total Implants	Σ Late Resorptions	-0.75
Δ Total Implants	Σ Total Resorptions	-0.51
Σ Early Resorptions	Σ Total Resorptions	0.61
Δ Early Resorptions	Δ Total Resorptions	0.89
Σ Late Resorptions	Σ Total Resorptions	0.51
Σ Late Resorptions	Δ Late Resorptions	-0.89
Σ Late Resorptions	Δ Total Resorptions	-0.71
Δ Late Resorptions	Σ Total Resorptions	-0.75
Δ Late Resorptions	Δ Total Resorptions	-0.78
Σ Total Resorptions	Δ Total Resorptions	-0.51

The remaining dependent variables either had no significant relationship to the independent variables or, as in the case of early resorptions and total resorptions, the standard error of estimate exceeded the variable mean by a great amount, or both.

6. Average Fetal Weight

The average fetal weight was obtained, for each litter, by dividing the litter weight by the number of live fetuses. Two independent variables, total implants and total resorptions, have been summed for the regression analysis of fetal weight and proportion of males. Total live fetuses was introduced as a statistical weight.

Table 9 lists the independent variables for fetal weight and the associated significance levels.

TABLE 9 - SIGNIFICANT INDEPENDENT VARIABLES - FETAL WEIGHT

Independent Variables	P
T	< .01
T^2	< .001
Total Implants	< .05

$\bar{y}$ = 1.107 gms.

Standard error of estimate = 0.252

The regression equation constructed from the variables is Equation 10.

$$y = 1.285 - .0119\ T + 1.28 \times 10^{-4} T^2 - .031\ (\text{No. Implants}) \text{gms.}$$

EQUATION 10

7. Proportion of Males

The proportion of males, obtained by sexing each fetus, is tested against the extended independent variable list as in the fetal weight test. Table 10 lists sifnificant independent variables.

TABLE 10 - SIGNIFICANT INDEPENDENT VARIABLES - PROPORTION OF MALES

Independent Variables	P
Total Implants	< .001
Total Resorptions	< .001

$\bar{y}$ = 0.804

Standard error of estimate = 0.530

The regression equation constructed from these variables is Equation 11 below.

$$y = 0.434 + .122 \text{ (No. Implants)} - .187 \text{ (No. Resorptions)}$$

EQUATION 11

B. TESTICULAR EXPOSURES

Figures 30a through c present three different magnifications of normal mouse testes sections. All magnifications reported are the three original microscope magnifications used for all the figures (except Figure 44 which is 7X) in this section: 40, 100, and 450 power. The original microscopic magnification with the photographic magnification are combined to provide the reference scales which accompany the three normal testis figures below.

Table 11 presents the key for the symbols used in this section to identify structures or cells of particular interest.

TABLE 11 - SYMBOL KEY FOR TESTICULAR AND OVARIAN RESULTS

A - A Type Spermatogonia

B - B Type Spermatogonia

BM - Basement Membrane

BV - Blood Vessel

CA - Corpora Albicans

CL - Corpora Lutea

G - Germinal Cell Gaps

GF - Graafian Follicle

I - Intermediate Spermatogonia

L - Tubule Lumen

N - Sertoli Cells

OS - Ovarian Stroma

TABLE 11 (continued)

P - Primary Spermatocyte

PF - Primordial Follicles

S - Spermatid

T - Seminiferous Tubules

TA - Tunica Albuginea

TW - Tubule Wall

V - Vacuole

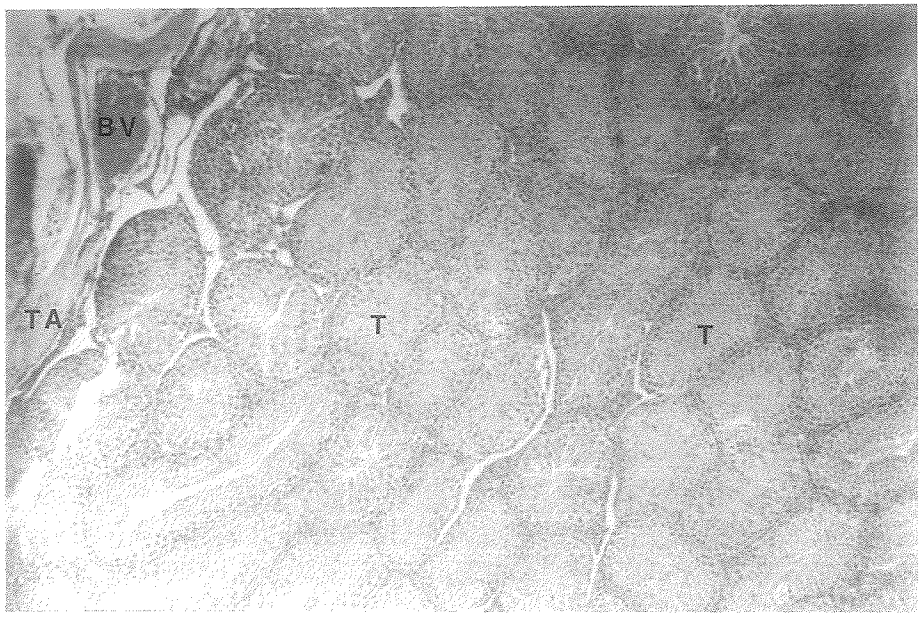

Fig. 30a. A 40 Power Micrograph of Normal Mouse Testis, H&E Stain (100 μ)

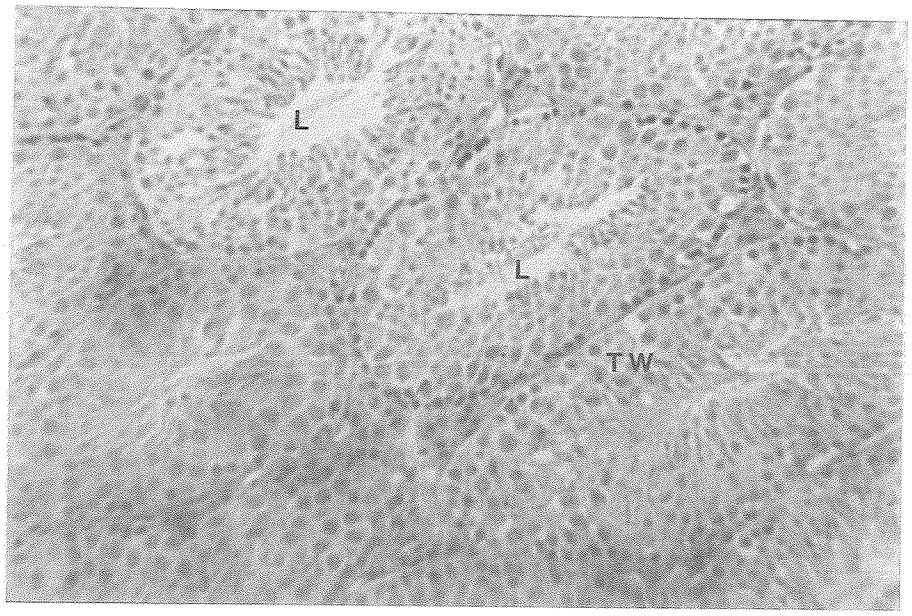

Fig. 30b. A 100 Power Micrograph of Normal Mouse Testis, H&E Stain (50 μ)

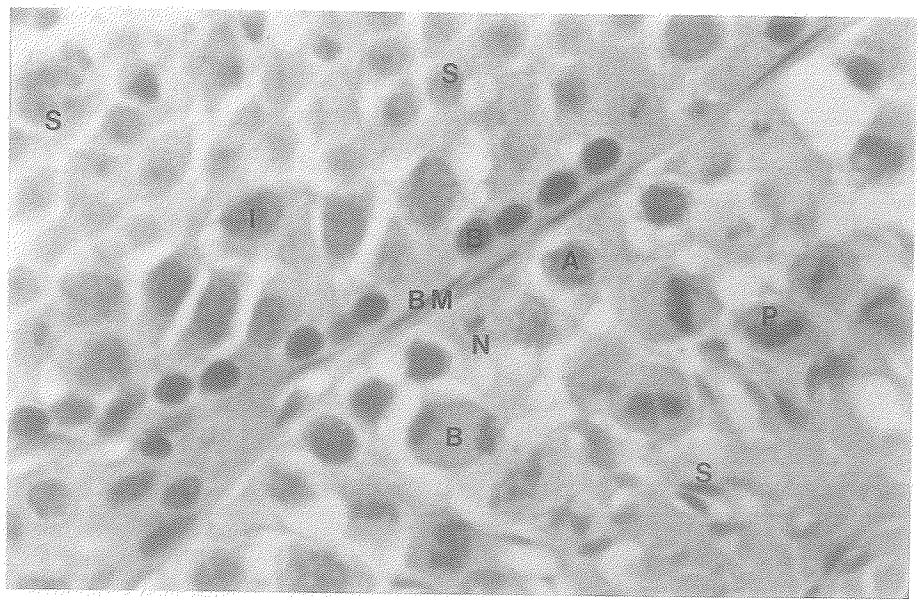

Fig. 30c. A 450 Power Micrograph of Normal Mouse Testis, H&E Stain (10 μ)

Figure 30a is a 40X micrograph of the testes illustrating the gross organization of the seminiferous tubules, embedded in a matrix of interstitial cells and the whole surrounded by a tough, connective tissue capsule, the tunica albuginea. Figure 30b is a 100X view of the same section showing the densely packed interstitial cells, the ordered complexity of the tubule walls, the basement membrane surrounding the tubule and the tubule lumina in detail. The structure of a tubule, at the cellular level, is shown in Figure 30c, which is a 450X micrograph of a portion of two tubules. Here two stem cells are visible, adjacent to and just below the basement membrane which forms a diagonal in the figure. On the opposite side of this membrane the curving line of deeply stained cells are the type B spermatogonia, which are the mitotic offspring of the stem cells via the intermediate stage. The mitotic figures visible in the lower tubule are also type B spermatogonia dividing to form primary spermatocytes. The remaining cells visible in the lower tubule are pachytene primary spermatocytes which have a mottled appearing nucleus, and the thin, tapered shapes of stage 15-16 spermatids which will be released into the tubule lumen as immature spermatozoa.

Histological appearance, at all magnifications, of tissues from sham irradiated animals were indistinguishable from that of normal animals, as discussed above.

The histological effect of the two exposure conditions are employed for exposing testes, viz., 25 w/cm^2 for 30 sec and 10 w/cm^2 for 30 sec, are presented separately in order that the time course of development of the damage can be followed. The two exposure conditions are referred to as the high dose and the low dose conditions, respectively.

1. High Dose

The lacework appearance at the top right in Figure 31, obtained immediately after irradiation, represents what has been found to be characteristic of the early stages of gross, acoustically induced damage, i.e., vacuolization of the tubule wall and sloughing of the germinal epithelium from the basement membrane. These processes are seen in greater detail in Figure 32, which shows a portion of three different tubules, each having large areas devoid of cells, large gaps along the basement membranes, and many cells free from an attachment and floating into the lumen. A thickening of the tunica albuginea is visible in the lower right corner of the figure. The paucity of spermatozoan tails in some lumina is evident.

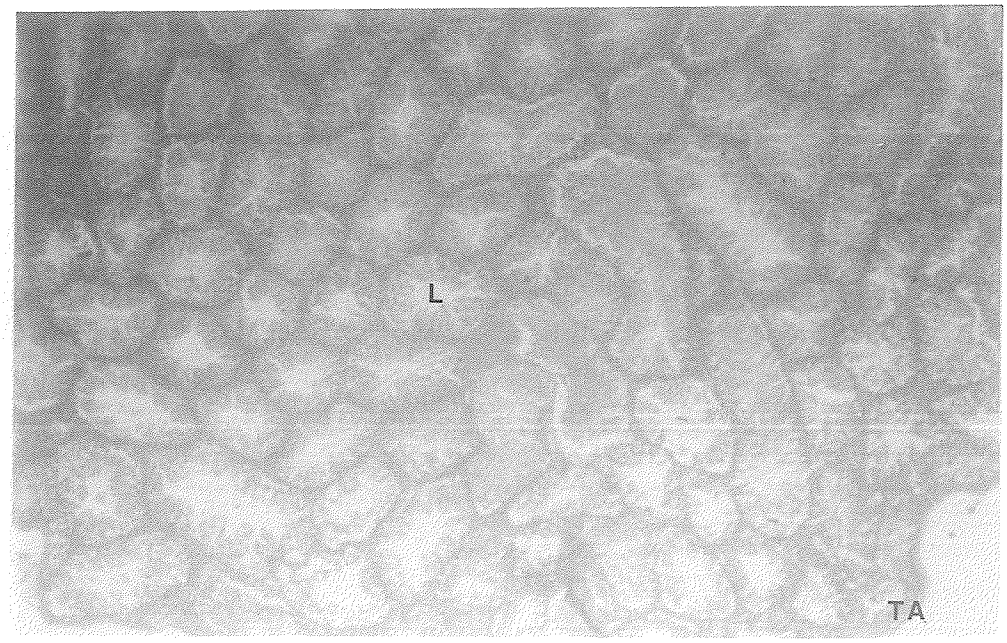

Fig. 31. A 40 Power Micrograph of Exposed Mouse Testis, Immediate Sacrifice, High Dose, H&E Stain

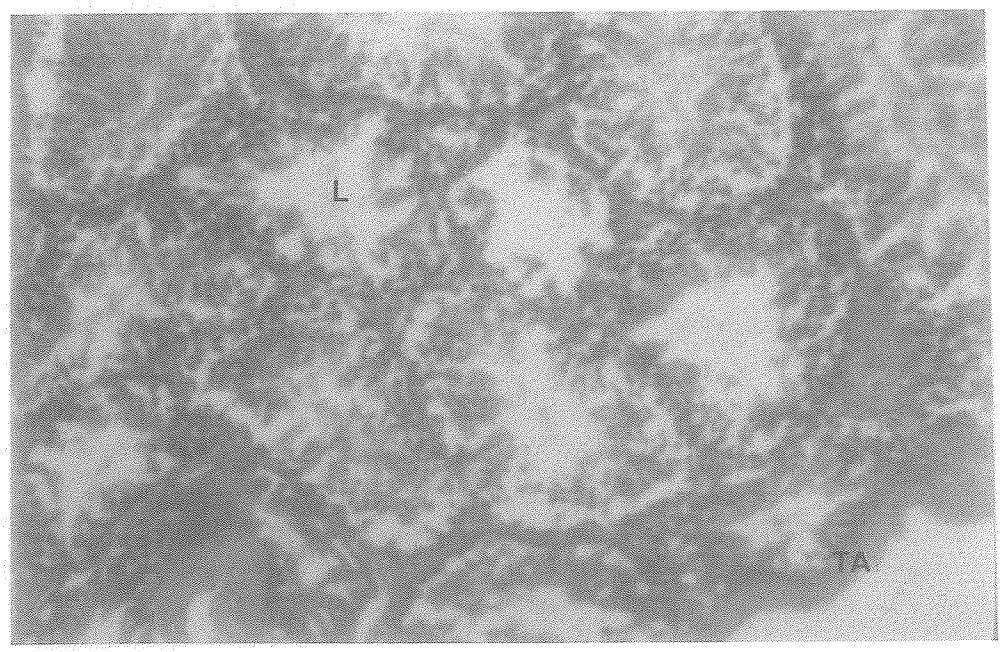

Fig. 32. A 100 Power Micrograph of Exposed Mouse Testis, Immediate Sacrifice, High Dose, H&E Stain

Figure 33 is a 40X micrograph of a testes from an animal sacrificed six hours after exposure. The disintegration of tubule structure and interstitial cells may be observed in the lower half of this figure. This damage is characterized by the lack of continuity of tissue between tubules, the loose debris around tubules, and the variety of tubules clogged with cellular debris. The organization characteristic of the germinal tissue is completely absent here as evidenced by the mixture of cell bodies and fluid within the tubules.

Fig. 33. A 40 Power Micrograph of Exposed Mouse Testis, 6 Hour Sacrifice, High Dose, H&E Stain

The appearance of the testicular tissue at 24 hours post irradiation is shown in Figures 34 and 35. Figure 35 shows sloughing of the germinal epithelium from the basement membranes, and the extensive damage to the interstitial tissue in the upper right portion.

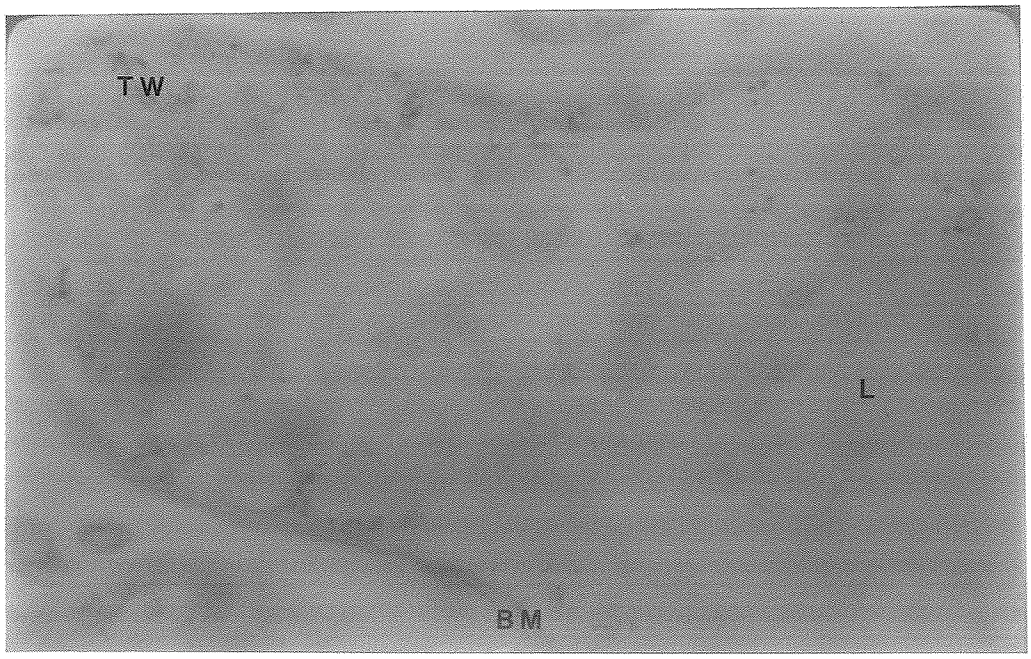

Fig. 34. A 450 Power Micrograph of Exposed Mouse Testis, 24 Hour Sacrifice, PAS Stain

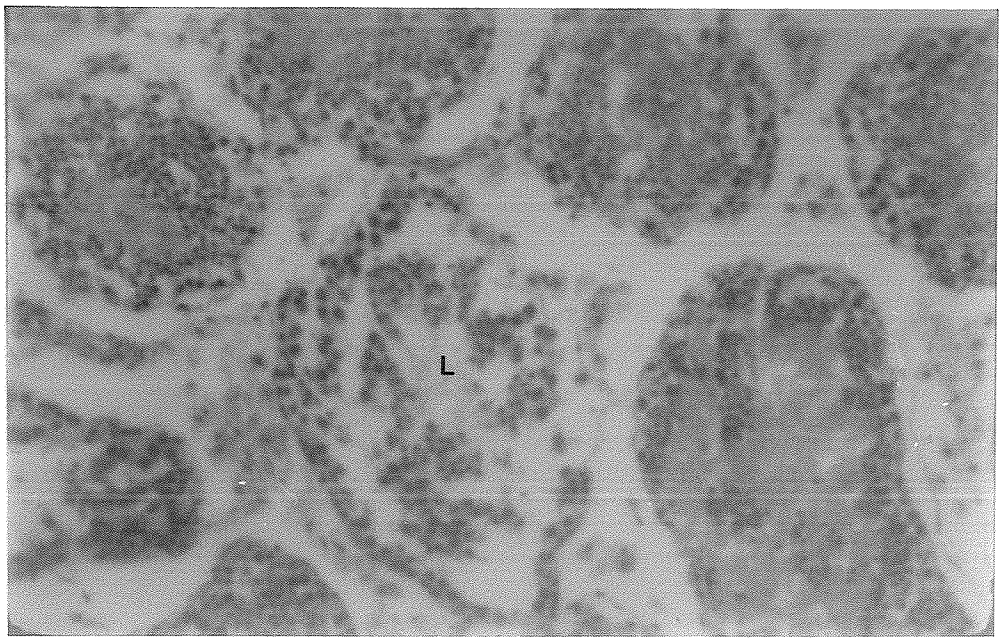

Fig. 35. A 100 Power Micrograph of Exposed Mouse Testis, 24 Hour Sacrifice, H&E Stain

Figure 36 is PAS stained, 450X magnification of a tubule illustrating further vacuolization of the tubule wall and the existence of dead spermatids in the dissolving tissue. The spermatids appear as pale-staining, irregularly shaped, dark masses spotted throughout the section. No normal morphology is visible here.

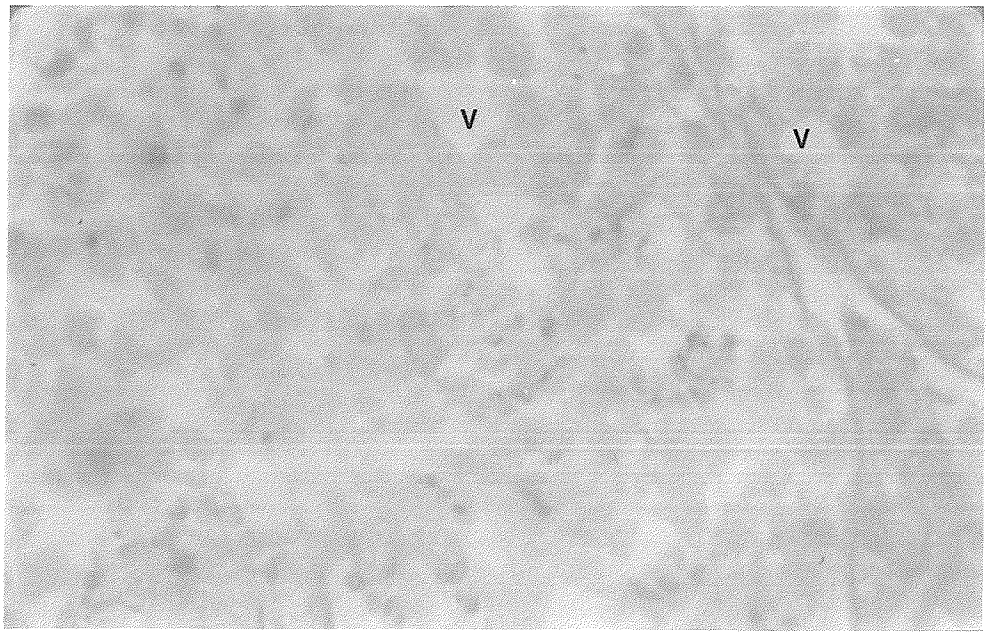

Fig. 36. A 450 Power Micrograph of Exposed Mouse Testis, 24 Hour Sacrifice, PAS Stain

Figures 37a and 37b show one section each of the two testes from a single animal at 48 hours post irradiation. Figure 37a exhibits three areas of differing morphological appearance, viz., an approximation to gross normalcy at the left, a disrupted appearance at the middle, and a tapered band of tissue at the right edge consisting of tubules presumably filled with an amorphous slurry of fluid and cell debris.

Figure 37b, on the other hand, does not show an excess of fluid, though many tubules are completely denuded of the germinal epithelium, having broken basement membranes, a thickened tunica, visible top left, and the total lack of interstitial cells (right of center).

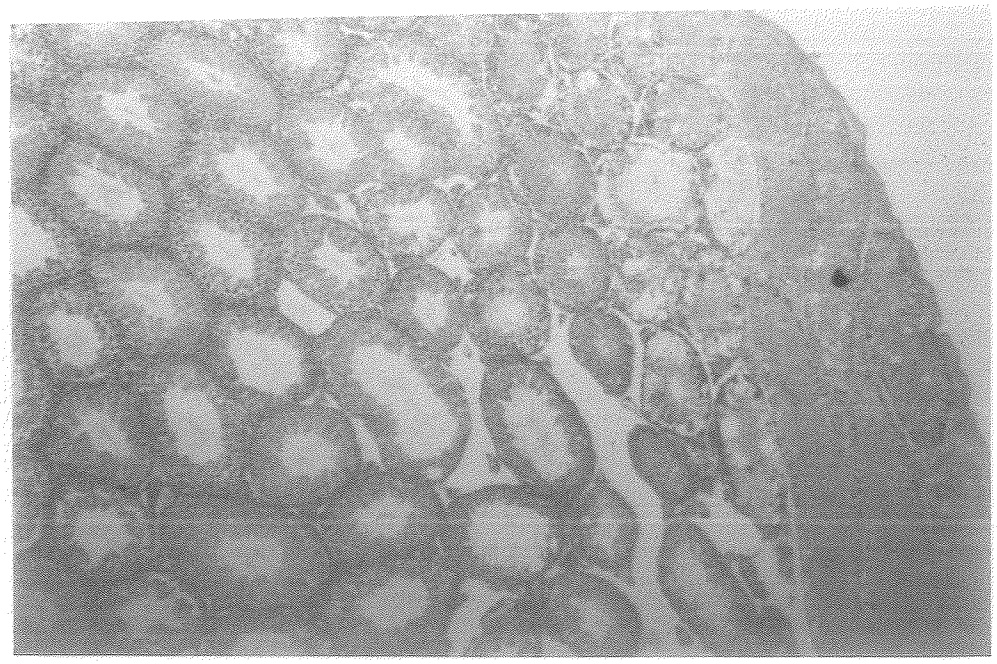

Fig. 37a. A 40 Power Micrograph of Exposed Mouse Testis, 48 Hour Sacrifice, H&E Stain

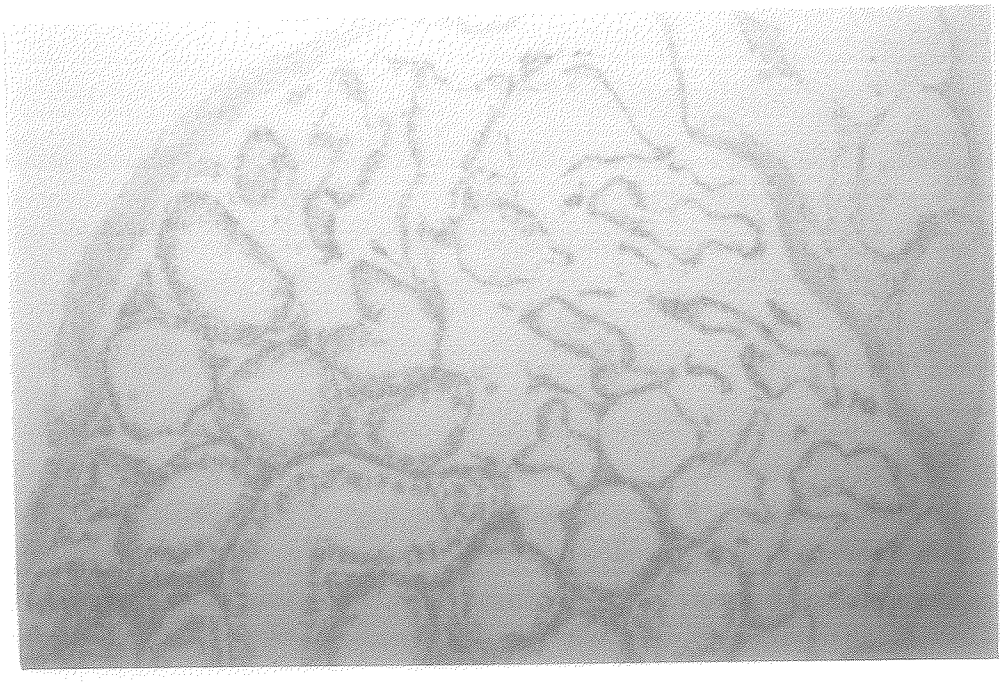

Fig. 37b. A 40 Power Micrograph of Exposed Mouse Testis, 48 Hour Sacrifice, H&E Stain

Figures 38, 39, and 40 are from a single testicle from an animal sacrificed seven days post irradiation. Figure 38 is a 40X micrograph of the testis showing a varying appearance of damage from top to bottom. A grossly thickened and delaminating tunica albuginea is visible at the very top of the figure as a pale, spotted band of tissue. Directly below the tunica is a group of fluid-filled tubules with no discernible organization, and almost no remaining germ cells. A third tissue bank, immediately below consists of empty, or clear fluid-filled, tubules, the walls of which are absent. These last tubules show vestiges of germinal epithelium. The abrupt and varied changes in tubule damage seen in this figure are characteristic of the discontinuities observed throughout the exposed tissues.

Fig. 38. A 40 Power Micrograph of Exposed Mouse Testis, 7 Day Sacrifice, H&E Stain

Figure 39, a 100X micrograph, shows details of the denuded tubules of the third band shown in Figure 38. The tubules have begun to collapse since there is no longer a wall to maintain the normal rounded shape.

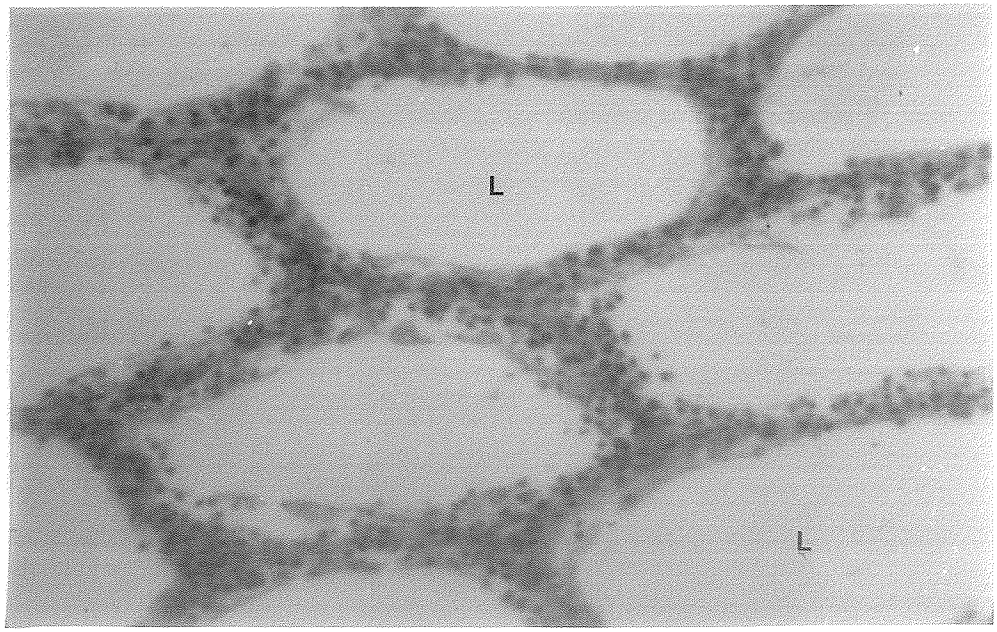

Fig. 39. A 100 Power Micrograph of Exposed Mouse Testis, 7 Day Sacrifice, H&E Stain

Figure 40 is a PAS section showing spermatids appearing to undergo liquifaction, and illustrating the gross disruption of the germinal epithelium which extends to relative numbers of cells and to cellular morphology, which is abnormal except for the appearance of the acrosomes.

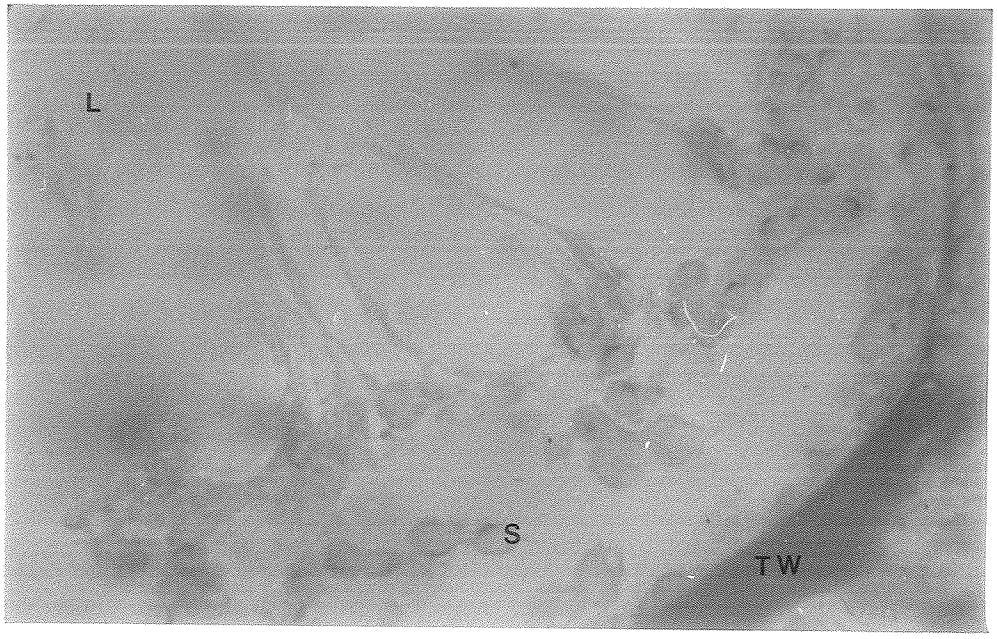

Fig. 40. A 450 Power Micrograph of Exposed Mouse Testis, 7 Day Sacrifice, PAS Stain

Figure 41 is a 450X micrograph of a testes section obtained 19 days post irradiation and illustrates the ongoing degeneration of the germinal epithelium by the large numbers of dead and liquifying cell remnants within and bordering the tubule lumen.

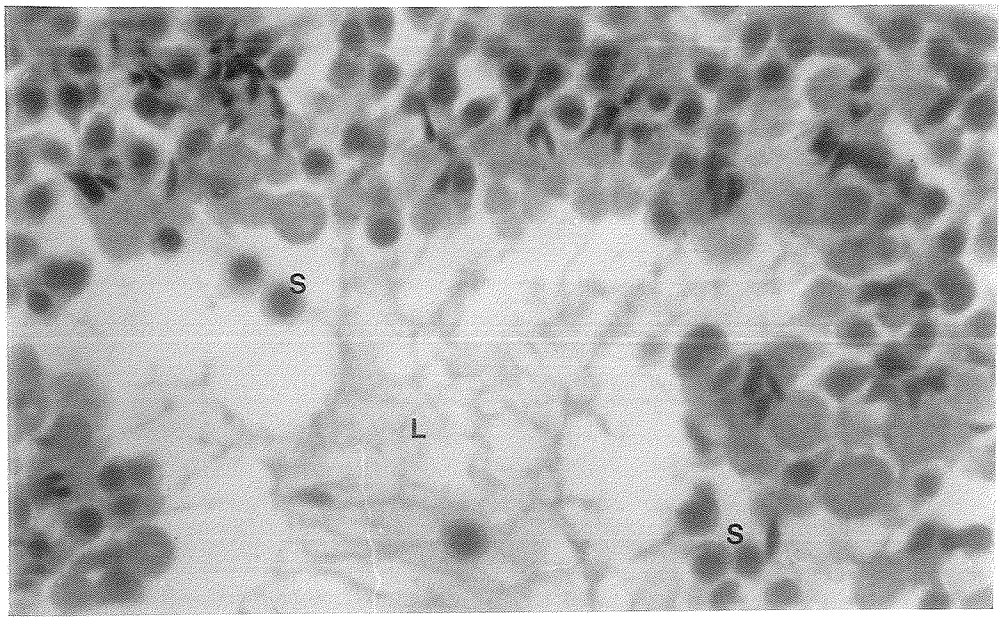

Fig. 41. A 450 Power Micrograph of Exposed Mouse Testis, 19 Day Sacrifice, H&E Stain

Study of the time dependency of damage to the testicle at the high dose terminated at day nineteen since no animal survived longer. The majority of the animals which died in the course of the experiment did so from severe damage to the lower gastrointestinal tract. In view of the gross nature of this destruction, a lower dose was chosen, viz., 10 w/cm^2 for 30 sec, and the experiment repeated. Only two animals died during this exposure regime, and these from causes not determined. This allowed the experiment to be pursued to 49 days post irradiation.

Figures 42 and 43, 100 and 450X respectively, show some vacuolization and excess fluid accumulation immediately after exposure. In particular in Figure 43, abnormal amounts of fluid may be observed at the lumen boundary, and slight vacuolization within the tubule wall. No grossly disrupted or liquifying cells are visible.

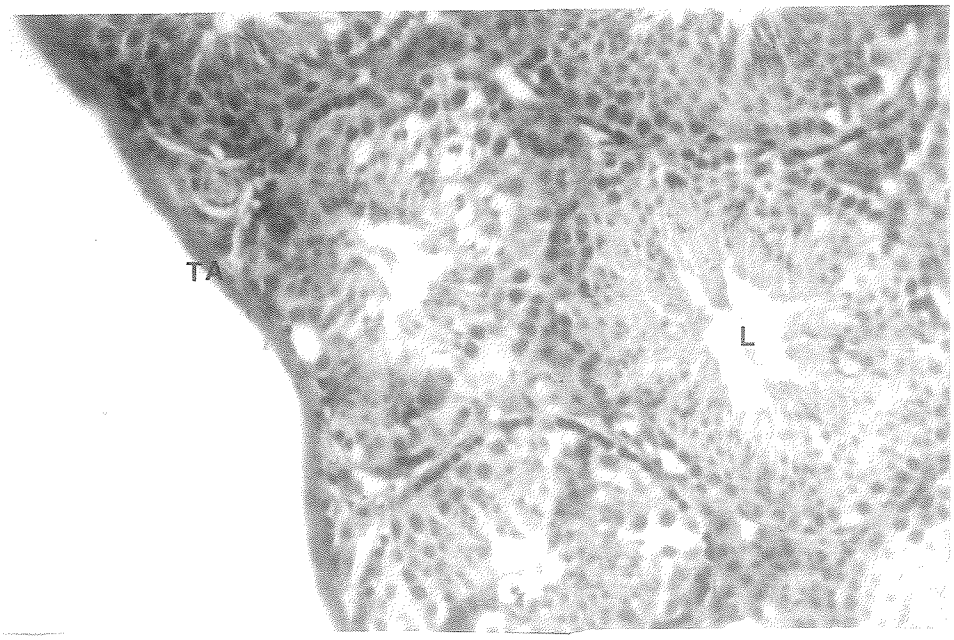

Fig. 42. A 100 Power Micrograph of Exposed Mouse Testis, Immediate Sacrifice, H&E Stain

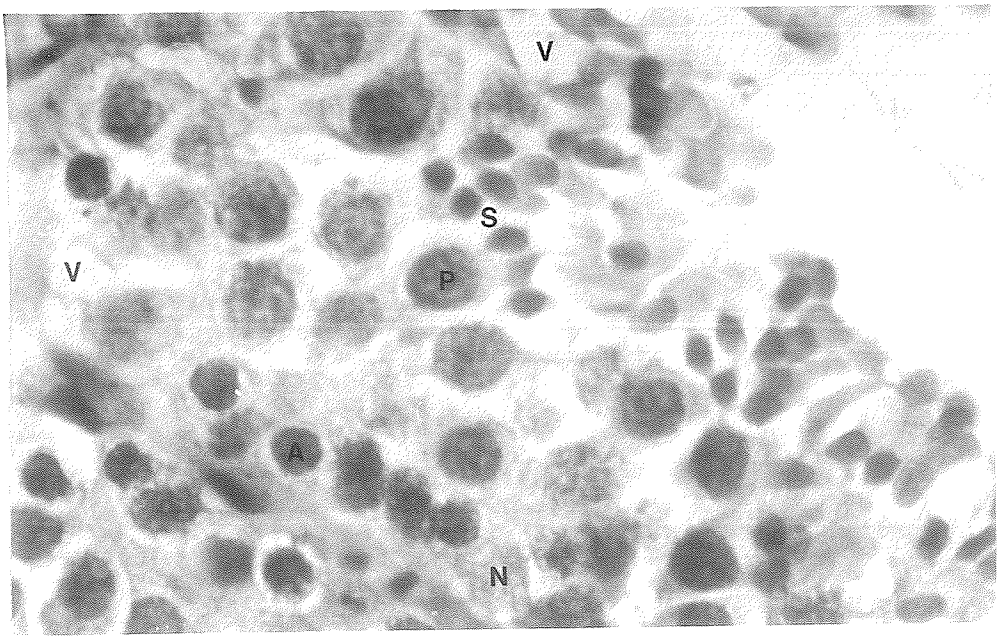

Fig. 43. A 450 Power Micrograph of Exposed Mouse Testis, Immediate Sacrifice, PAS Stain

Figure 44 (7X) obtained 24 hours post irradiation, shows both testes, wherein the acoustic field was incident from the bottom of the figure. The testis on the right shows an area of destruction extending from the bottom half around the left edge with the remaining portion of the organ exhibiting the majority of interstitial cells missing, while the tubules appear morphologically normal.

Fig. 44. A 7 Power Micrograph of Exposed Mouse Testis, 24 Hour Sacrifice, H&E Stain

Figure 45, at 100X magnification, shows the boundary region between the two types of damaged tissue. The gross morphology on the left shows some of the types of disruption observed at the higher intensity immediately after exposure, and the abnormal mixture of cells and cellular fragments is detailed in the 450X Figure 46.

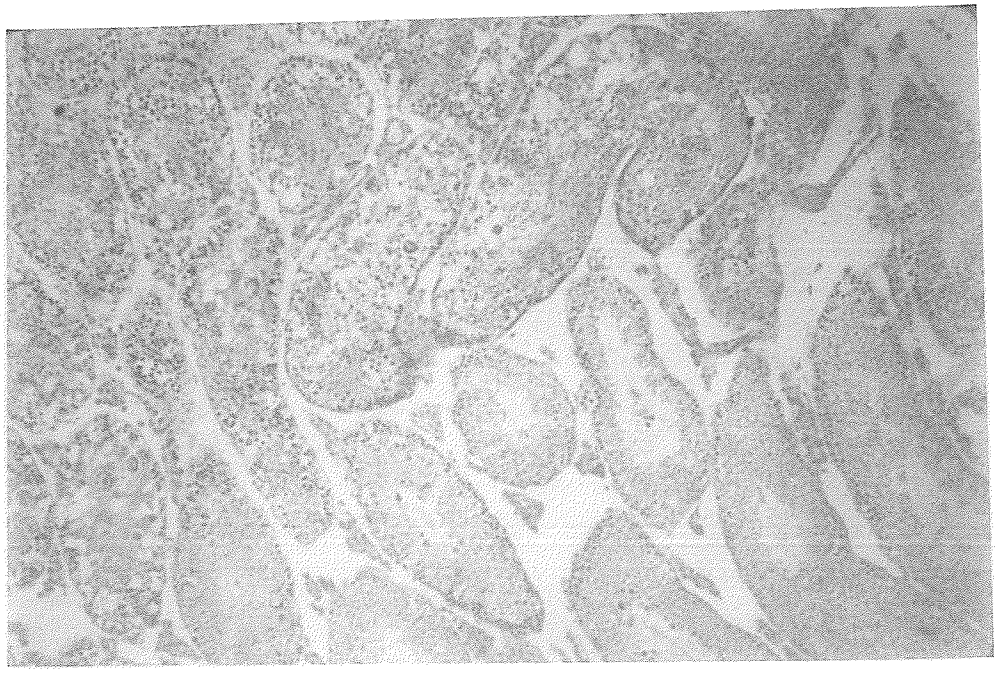

Fig. 45. A 100 Power Micrograph of Exposed Mouse Testis, 24 Hour Sacrifice, H&E Stain

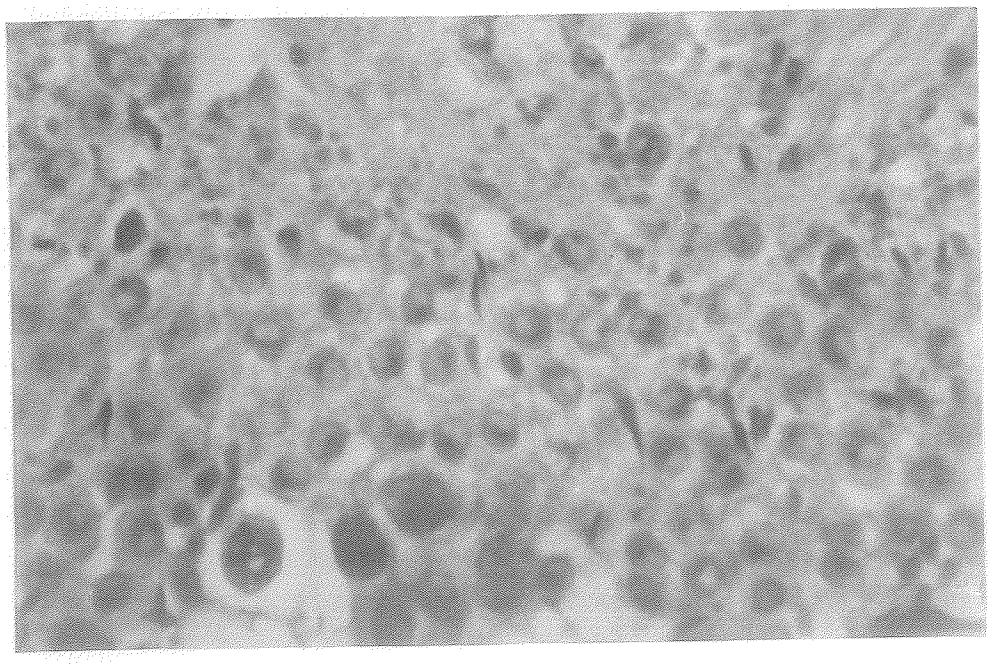

Fig. 46. A 450 Power Micrograph of Exposed Mouse Testis, 24 Hour Sacrifice, H&E Stain

The fragmentation of the germinal epithelium progresses rapidly during the next 24 hours (Figure 47, 40X) and is illustrated by the distinct thinning of the tubule walls as dead cells are sloughed off into the lumen.

Fig. 47. A 40 Power Micrograph of Exposed Mouse Testis, 48 Hour Sacrifice, H&E Stain

The progressive denudation is illustrated in Figures 48 and 49, 100 and 450X micrographs respectively, of a testicle section obtained six days after exposure. Stem cells, type B spermatogonia and Sertoli cells are all present, although the thickness of the germinal epithelium is only 1 to 3 cell diameters. The polymorphonuclear structure in the tubule lumen of Figure 49 is of particular interest since this only occurs in abnormal testicular tissue.

Fig. 48. A 100 Power Micrograph of Exposed Mouse Testis, 6 Day Sacrifice, H&E Stain

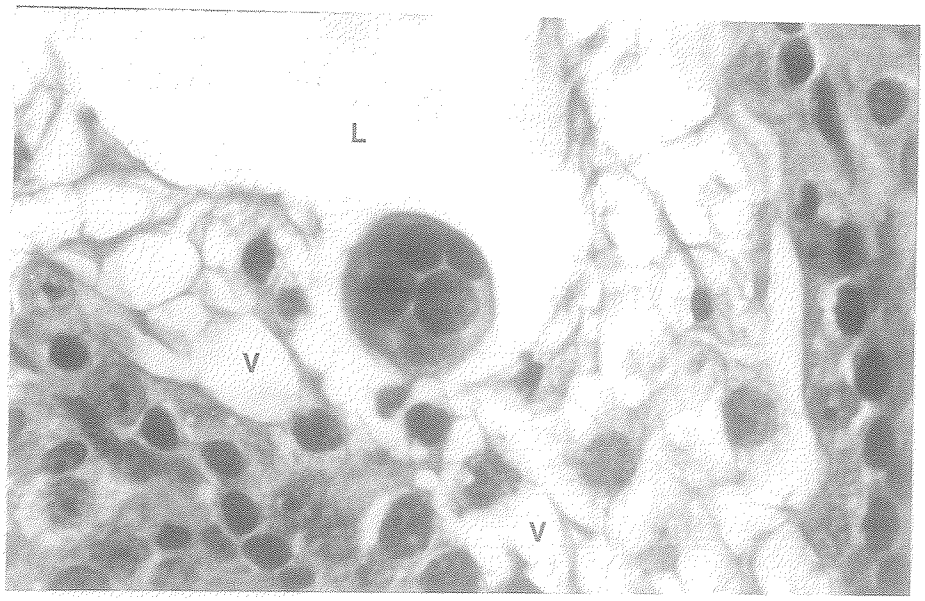

Fig. 49. A 450 Power Micrograph of Exposed Mouse Testis, 6 Day Sacrifice, H&E Stain

Figures 50 and 51 (100X) show adjacent H&E and PAS stained sections, respectively, of the same tubule 10 days post irradiation. Figure 50 shows virtually no interstitial tissue and tubules packed with dead cells and fluid. The luminal area of the tubules is surrounded by late spermatids, as evidenced by the dark stained acrosomes. The PAS section gives very similar appearance, but no acrosomal figures are visible.

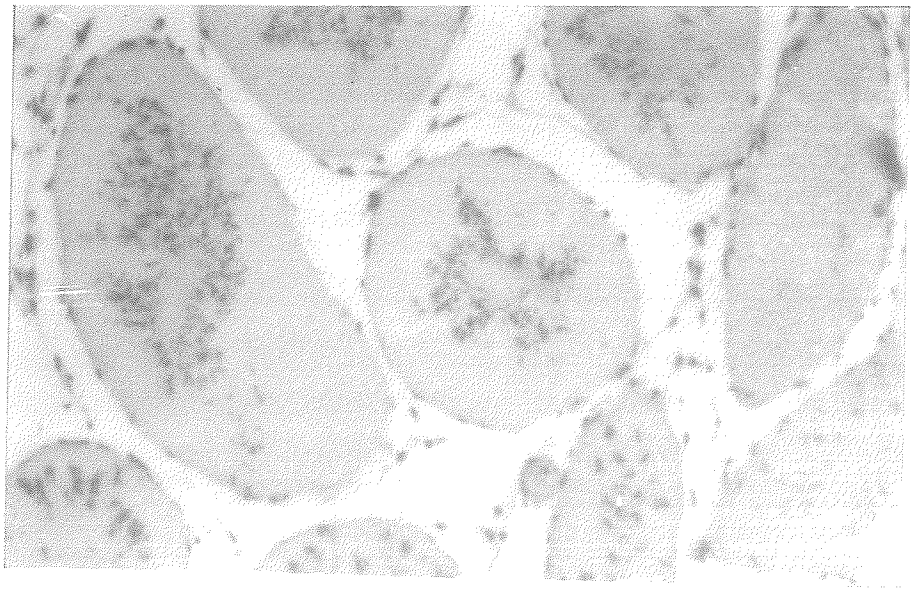

Fig. 50. A 100 Power Micrograph of Exposed Mouse Testis, 10 Day Sacrifice, H&E Stain

Fig. 51. A 100 Power Micrograph of Exposed Mouse Testis, 10 Day Sacrifice, PAS Stain

This anomalous stain configuration is shown in more detail in the 450X magnification of the same tubules in Figures 52, and 53 respectively, PAS and H&E stains of 6 micron paraffin sections. In each H&E section groups of abnormal spermatids may be seen surrounding the former lumen of the tubule, a matrix of dead cells occupying the remaining volume. The spermatid abnormalities consist primarily of pale staining acrosomal figures or acrosomes lacking the characteristic hooked tip. The matching PAS stained section shows no evidence of spermatids of any stage or configuration, and this inability to obtain a positive PAS reaction from the acrosomal cap of the spermatid implies a chemical change in the acrosomal structure.

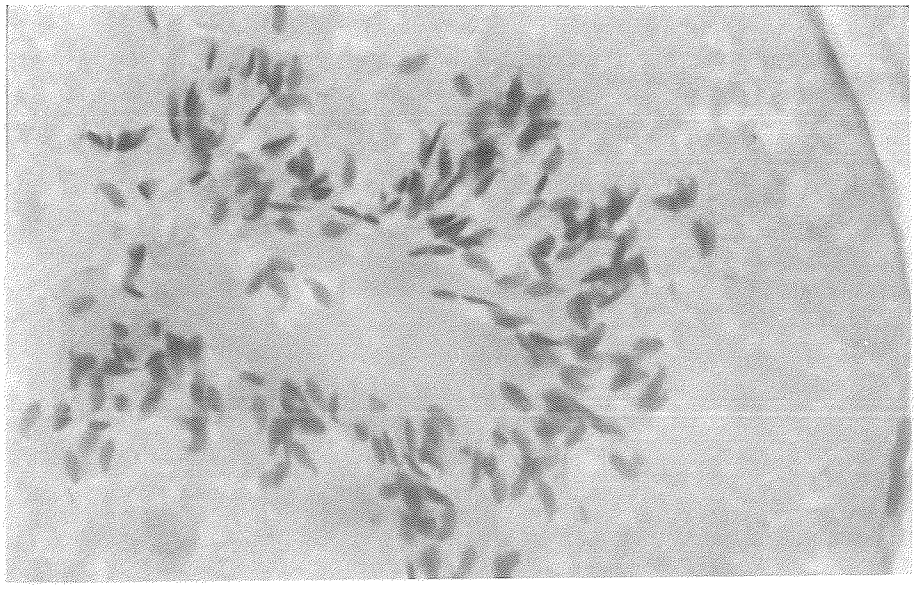

Fig. 52. A 450 Power Micrograph of Exposed Mouse Testis, 10 Day Sacrifice, H&E Stain

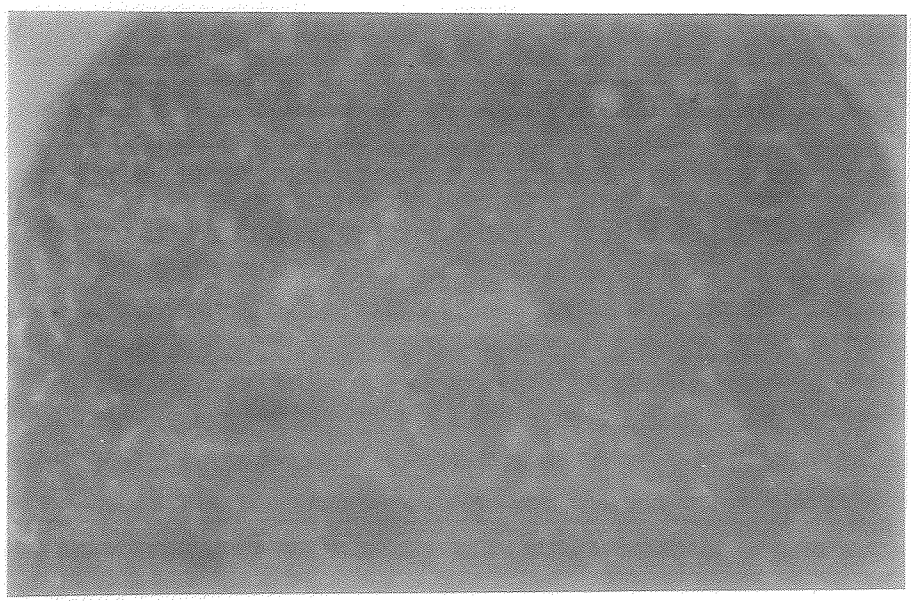

Fig. 53. A 450 Power Micrograph of Exposed Mouse Testis, 10 Day Sacrifice, PAS Stain

The appearance of the germinal epithelium is slightly altered at 19 days post exposure as shown in Figures 54 and 55 (100X), H&E and PAS, respectively. Figure 54 shows a definite, but still vacuolized and thin, germinal epithelium and Figure 55 shows no acrosomal figures. This is shown in greater detail for one tubule in Figures 56 and 57. The arrow, visible at the top of the figure identifies the tubule lumen in each figure. The H&E section shows many cell types associated with spermatogenesis, most abnormal morphologically and the entire cell mass separated from the basement membrane. The PAS section, as in Figure 53, shows a complete lack of spermatids.

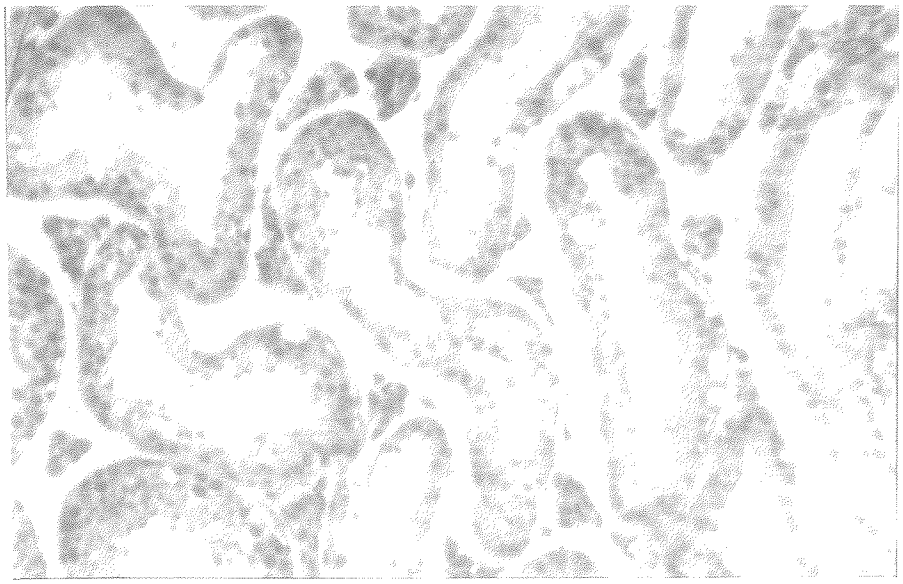

Fig. 54. A 100 Power Micrograph of Exposed Mouse Testis, 19 Day Sacrifice, H&E Stain

Fig. 55. A 100 Power Micrograph of Exposed Mouse Testis, 19 Day Sacrifice, PAS Stain

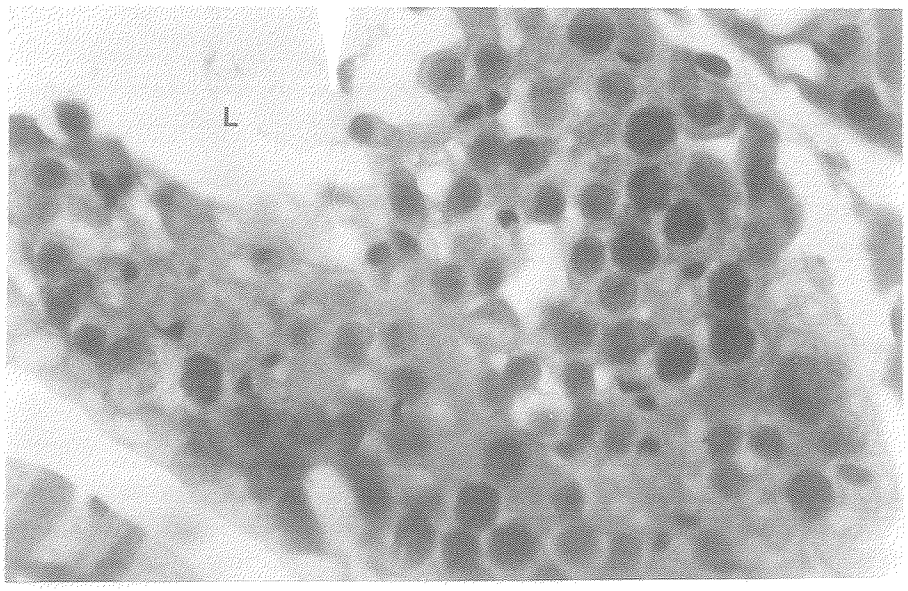

Fig. 56. A 450 Power Micrograph of Exposed Mouse Testis, 19 Day Sacrifice, H&E Stain

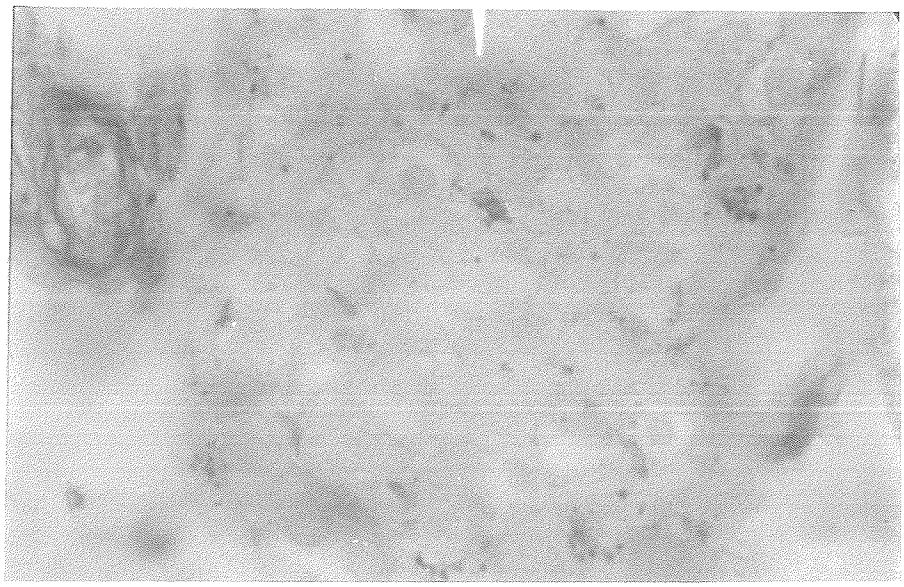

Fig. 57. A 450 Power Micrograph of Exposed Mouse Testis, 19 Day Sacrifice, PAS Stain

Figures 58 and 59, obtained 43 days after exposure, show a large number of the germ cells with morphologically normal appearance, the vacuolization of the germinal epithelium having disappeared. Adjacent to the lumen are what appear to be young spermatids. Again, the PAS section shows no evidence of spermiogenic activity.

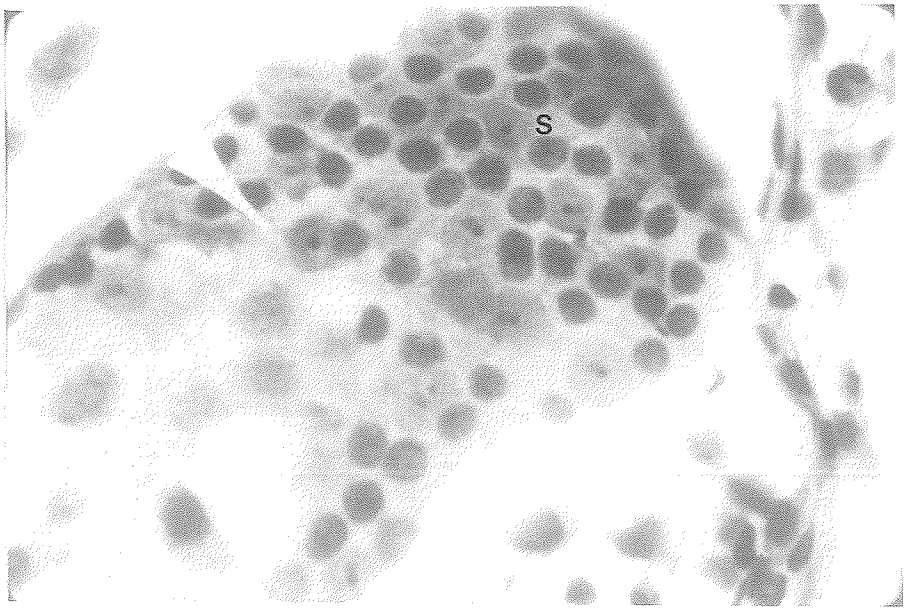

Fig. 58. A 450 Power Micrograph of Exposed Mouse Testis, 43 Day Sacrifice, H&E Stain

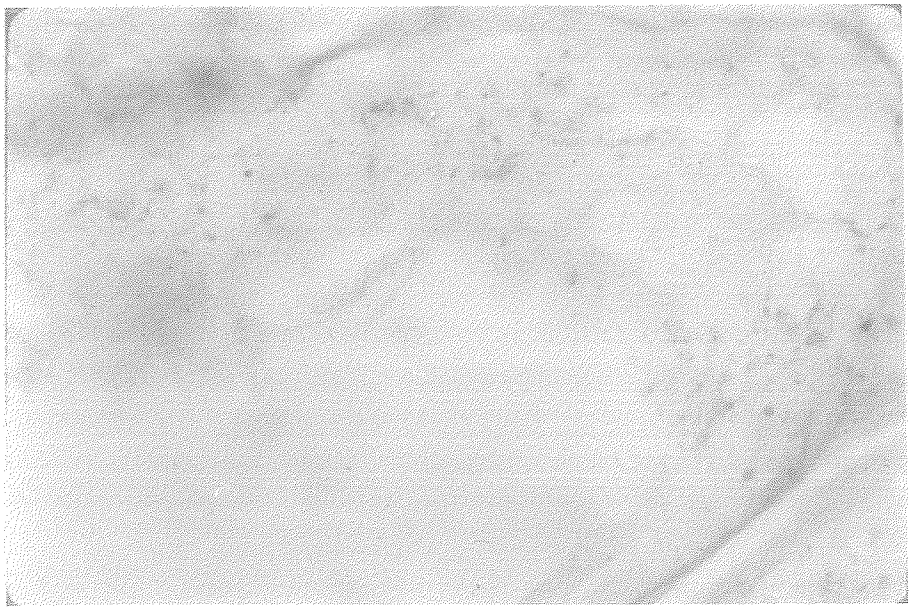

Fig. 59. A 450 Power Micrograph of Exposed Mouse Testis, 43 Day Sacrifice, PAS Stain

C. OVARIAN EXPOSURE

Two experimental series of ovarian exposures were performed. In the first series, the right ovary was exposed to one of the following intensities, 10, 20, 30, 40, 50 or 60 w/cm^2 for 10 seconds. The animals were sacrificed 24 hours later and both ovaries were collected. In the second series, a group of animals were exposed to 10 w/cm^2 for 30 seconds and the animals sacrificed at selected times after exposure from two to 19 days post irradiation.

Figure 60 shows a representative histological preparation. No damage or anomalous conditions were found in any of the preparations. The ovarian stroma, primordial follicles, graafian follicles, corpora lutea and corpora albicans all appear identical to those of a normal animal of the same age and parity.

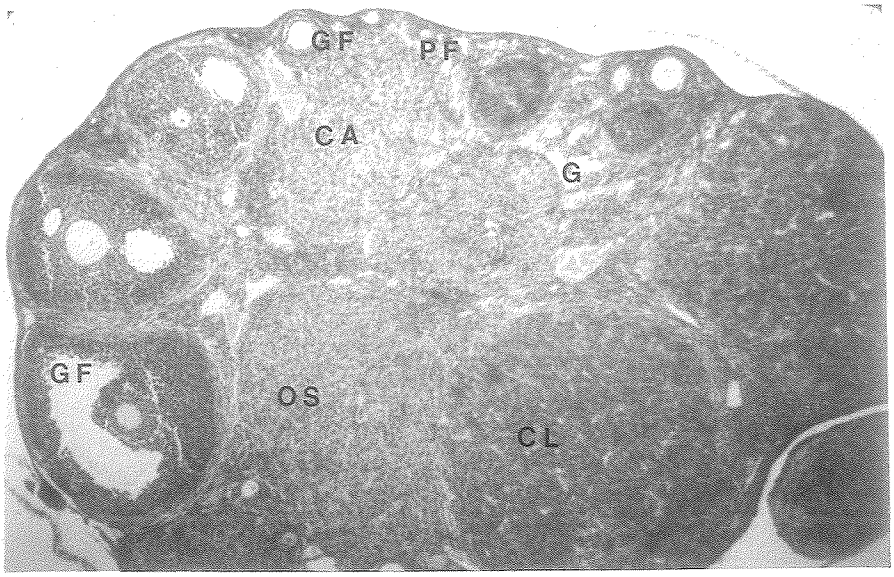

Fig. 60. A 40 Power Micrograph of the Mouse Ovary, H&E Stain

V. DISCUSSION

A. IN-UTERO EXPOSURES

The results of the statistical analysis of the in-utero ultrasonic exposures are summarized in Table 11, wherein entries are made only for statistical significances exceeding the 95% confidence level.

The variables are arranged according to frequency of appearance, i.e., the dependent variables list, from top to bottom, involves successively fewer independent variables, and the independent variables from left to right are significant for successively fewer dependent variables. Prior to discussing each dependent variable, a few general remarks are pertinent concerning the relationships in Table 12.

The following statements can be made: examination of the relations between the variables elucidates several important points. Differences between the exposed, sham exposed and control groups are significant only for the number of, and for a single type of anomaly, viz., subcutaneous hemorrhage. The possibility exists that the effect of the acoustic exposure manifests itself as damage to the fetal vascular system. (See discussion of testicular exposures for implications of other deleterious effects made manifest by observations of vascular system perturbations.)

TABLE 12 - RELATIONSHIP OF SIGNIFICANCE LEVELS OF DEPENDENT AND INDEPENDENT VARIABLES TO IN-UTERO EXPOSURES

	IT^2R	T^2	T	ITR^2	ITR	I^2TR	R	E/S	C	Cl	IM	GD	COSθ	RES	D	A	A^2
Pregnancy	.001	.01	.02	.01	.001										.05	.02	.01
Anomalies (No.)	.02	.01	.05				.02	.01	.001			.05					
Anomalies (Type)	.01	.02						.05	.01	.01							
Maternal Damage	.05	.001	.01			.001											
# Live Fetuses	.05		.001	.001						.001			.05				
Fetal Weight		.001	.01								.05						
Total Implants				.05						.001							
Proportions of Males											.001			.001			
Maternal Survival						.001											

KEY TO ABBREVIATIONS:

I - Acoustic Intensity
T - Time
R - Exposure Repetitions
E - Exposed Animals
S - Sham Animals
C - Control Animals
Cl - Corpora Lutea
IM - Implants
GD - Gestational Days
RES - Resorptions
D - Dip Constant
A - Age

As terms involving a quadratic function of time appear more often in Table 12, than those of intensity quadrature, the feasibility is increased of investigating toxic effects of lower intensities (1 w/cm^2), without the necessity of exposures lasting many hours.

The miticidal chemical application and progressive aging of the dams did not affect the results to a significant degree, except for the probability of pregnancy.

Differences between the uterine horns did not appear anywhere as a statistically significant variable. Though the correlation coefficients of Table 8 show that under certain conditions inter-uterine differences do exist, such correlations do not occur as a function of any of the independent variables considered here.

Maternal damage is a positive function of dose, incorporating both linear and guadratic terms of intensity, time and number of repetitions. Time alone appears in the regression equation as a negative quantity over the range of exposure times used.

Table 13, for R = 2, provides some examples of the probability of maternal damage for doses in which maternal damage is found.

TABLE 13- PROBABILITY OF MATERNAL DAMAGE

Intensity (W/cm^2)	Time (Sec.)	(P Mat. Damage)
5	10	0.18
6	10	0.44
8	5	0.60
10	5	1.08

Maternal damage in the pregnant animal is a result of exposure which virtually precludes the gathering of data concerning the toxicity of ultrasound for the reproductive functions. Animals suffering direct and observable damage from exposure to an acoustic field should not be included for other assay measures due to the possible interaction of the damage and physiological support of the developing pups.

Maternal death is an undesirable result for this study and survival of the dam was dependent only upon I^2TR. Only maternal damage and maternal survival appear to be dependent upon this independent variable. This relationship is of additional interest since acoustic intensity thresholds in brain tissue for observable histological lesions has produced the relation $IT^{\frac{1}{2}}$= Constant (68). The implication here is that similar physical mechanisms may be involved in the two situations. Thus, as the thermal mechanism is believed to be the dominant one for lesion production in mammalian brain, in this dosage region, gross

heating of the animal by absorption processes may account for the maternal damage and survival effects observed in this study.

The dependent variable of the probability of an animal being pregnant at the time of exposure, is related to most of the dependent variables and is the sole dependent variable significantly affected by the miticidal treatment. The constant term of the regression equation appears as a large negative quantity. Age is also a factor, as expected, but becomes negative after the dam is beyond one year of age. The linear and quadratic terms for time alone yield a positive quantity to 220 seconds, after which the combined terms cause the probability to decrease. Since no significant difference between exposed, sham and control was found, separation of this variable from the entire model may not be a valid procedure. As the temporal terms dominate, it is suggested that the method of animal handling plays an important role in the study.

Death and local damage to the dam has been found in other studies (26,42), and has been attributed to thermal effects. The damage reported here includes the possibility that heat may be a causative agent, but more work will be necessary to determine unambiguously the cause or causes of damage and death in the dam.

One type of fetal anomaly, viz., subcutaneous hemorrhages, exhibited a significant causal relation to the independent variables and a significant difference between the exposed, sham exposed and control group. These differences were significant for both number and type of abnormality. Terms involving exposure time and repetitions dominate the relation, and the gestational day of exposure becomes a factor for the number of anomalies since the probability of an hemorrhagic incident decreases with increasing gestational age at exposure. Hemorahagec and other effects on the vascular system due to acoustic exposure have been reported (Mannor, et. al.; Taylor & Pond), and have been ascribed to both thermal and mechanical damage to the vascular system. The determination of whether damage results from thermal mechanisms for the work of this study, will require further investigation involving knowledge of in-utero acoustic intensities and absorption coefficients of the embryonic tissues. The linear and quadratic terms of time alone change sign at approxiamtely 216 seconds exposure. The significance and frequency of the temporal terms, and the close agreement between the summed regression coefficients, suggests that low intensity, long exposure periods may be preferable for continued toxicity studies. The regression equation for type of anomaly lacks both the linear term of time and the significant term for gestational day. The presence of the latter term in number, but not type of anomaly equation is partly due to acceptance level, i.e., gestational day is significant at 0.10 for type of anomaly.

Total implants and number of live fetuses were the only two litter characteristics which were related significantly to independent variables and had standard estimates of error small enough to make the model meaningful. Significant correlations (> .50) between the dependent variables involved both the sum and difference of five of the experimental observations (See Table 8).

The sum of total implants is dependent upon a single independent variable, ITR^2, since there exists a necessary relationship between ova ovulated and total implants. The significant dose term enters the equation as a negative quantity which is offset at low doses by the positive linear term. All the dose related terms are dominated by the corpora lutea term due to its large positive regression coefficient.

The number of live fetuses is dependent upon dose in a more complex fashion. Three dose terms appear in the regression equation and quadratic terms of time or time-related variables, i.e., R, predominate. A cyclic phenomenon appears here with an amplitude of 0.66, which is large in comparison to the remaining regression coefficients, excepting the number of corpora lutea. Cyclicity is a well known factor in mammalian breeding situations (69), though, such behavior is thought to be either minimized or controlled in most laboratory rodents. The significance of the cyclic variable points to a definite yearly cycle in pup production.

The correlation coefficients listed in Table 8 provide confirmation of assumptions relating to reproductive variables in multiparous animals. The relatively high positive correlation between the sum of total implants and the sum of total resorptions, is referred to as a crowding effect, and is common among the litter bearing species. The last two relations for total implants supports the contention of minimal effect of one uterine horn on the other. Thus, as the difference in total implants between the horns increases, so too does the difference in total resorptions, with a correlation of +.69. This relation illustrates both the crowding effect and the extent of decoupling of the duplex uteri in the mouse. The correlation statements relating early resorptions to total resorptions, sum and difference, have the expected high positive associations. The sum of late resorptions is highly correlated to the differences of both late and total resorptions, the coefficients being -.89 and -.71, respectively. This is the same phenomenon discussed with respect to implants applied to one more variable, as is the next relation between the inter-uterine differences in late resorptions, a variable negatively correlated with the sum of total resorptions. The positive, high correlation between the difference of late and total resorptions, again stresses the functional separation of the two uterine horns.

Fetal weight is a relatively sensitive indicator of many factors (69), and as such may be used to assess the results of

various insults to the uterine environment. For a sample of 407 animals, this analysis shows fetal weight to be sensitive only to the time duration of exposure and the number of implants present. The last factor is a second example of the crowding effect. Quadratic and linear temporal terms appear with a sign change at approximately 93 seconds, becoming positive beyond this point. It is probable that the model exceeds the limits of confidence in the vicinity of this sign change.

The proportion of males in a given litter is not a function of the treatment. The regression equation shows that this proportion increases as the number of implants increases, and decreases as the number of resorptions increase. This decrease in males preferentially to females has been documented for other animals (67) and the results of this analysis implies a similar behavior for the mouse.

B. TESTICULAR EXPOSURES

The extensive morphological effects observed in testicular tissue after the 25 w/cm^2 - 30 second ultrasonic exposure are useful for delineating the time sequence for development of structural changes but of limited value for identification of the toxic levels of this agent. The similarity of the damage progression as seen in the epithelial dissolution, with that of the lower dose after the fifth day post irradiation provides a dose-effect correspondence which may be useful in dose selection procedures. A unique aspect of the high intensity exposure is the immediate visibility of the lesion. Although function alteration of tissue has been observed immediately following exposure to more intense ultrasonic fields, histological damage, using light microscopy is not apparent for some minutes (70).

Two well known mechanisms may be considered to account for the severe and immediate (60 seconds post irradiation) disruption of the germinal epithelium, viz., cavitation and a thermal mechanism. Although the damage observed in the immediately sacrificed animals' organs is severe and pervasive, it is not clear that it could be the result of a cavitation process, i.e., either transient or stable cavitation. The fact that the damage does not extend to the interstitial tissue or basement membranes, as would be expected of a non-selective mechanical mechanism, also mitigates against cavitation being the only physical mechanism present.

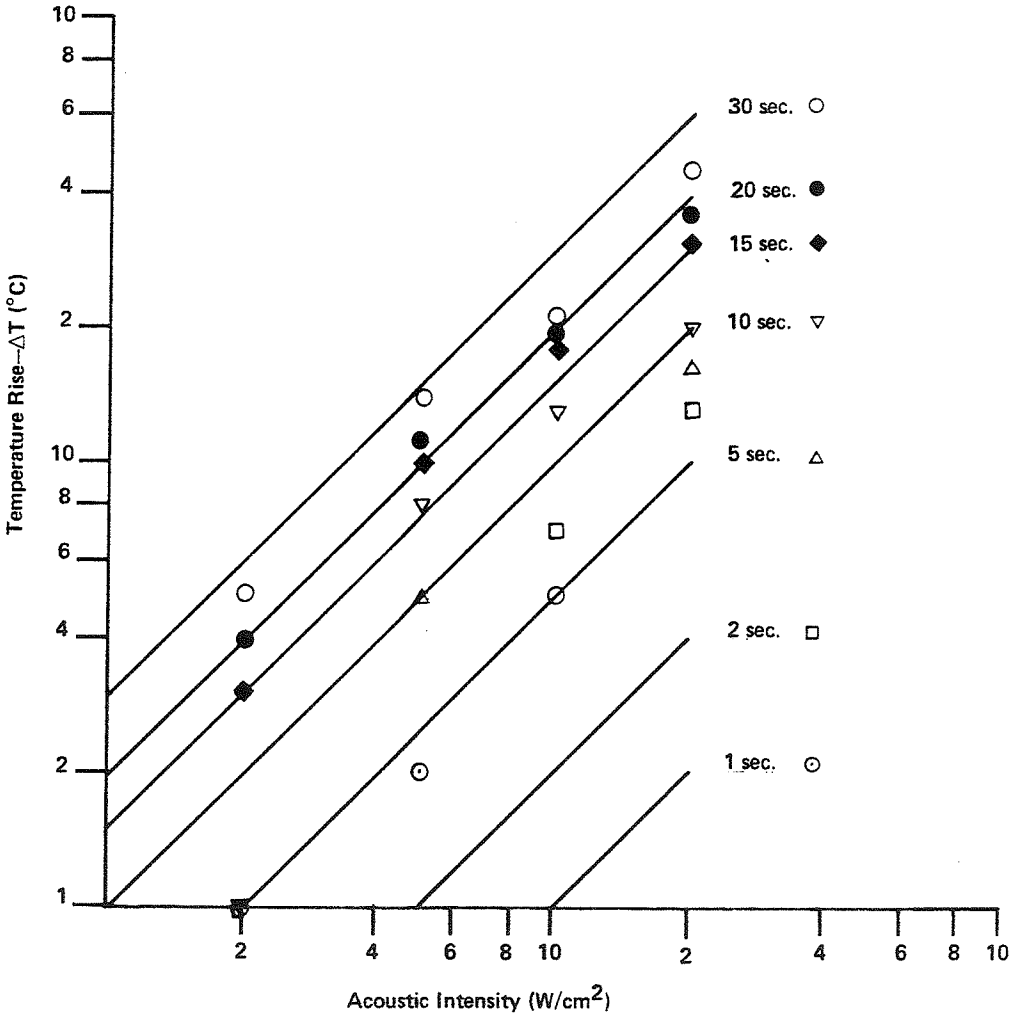

Fig. 61. Acoustic Intensity vs. Tissue Temperature Rise

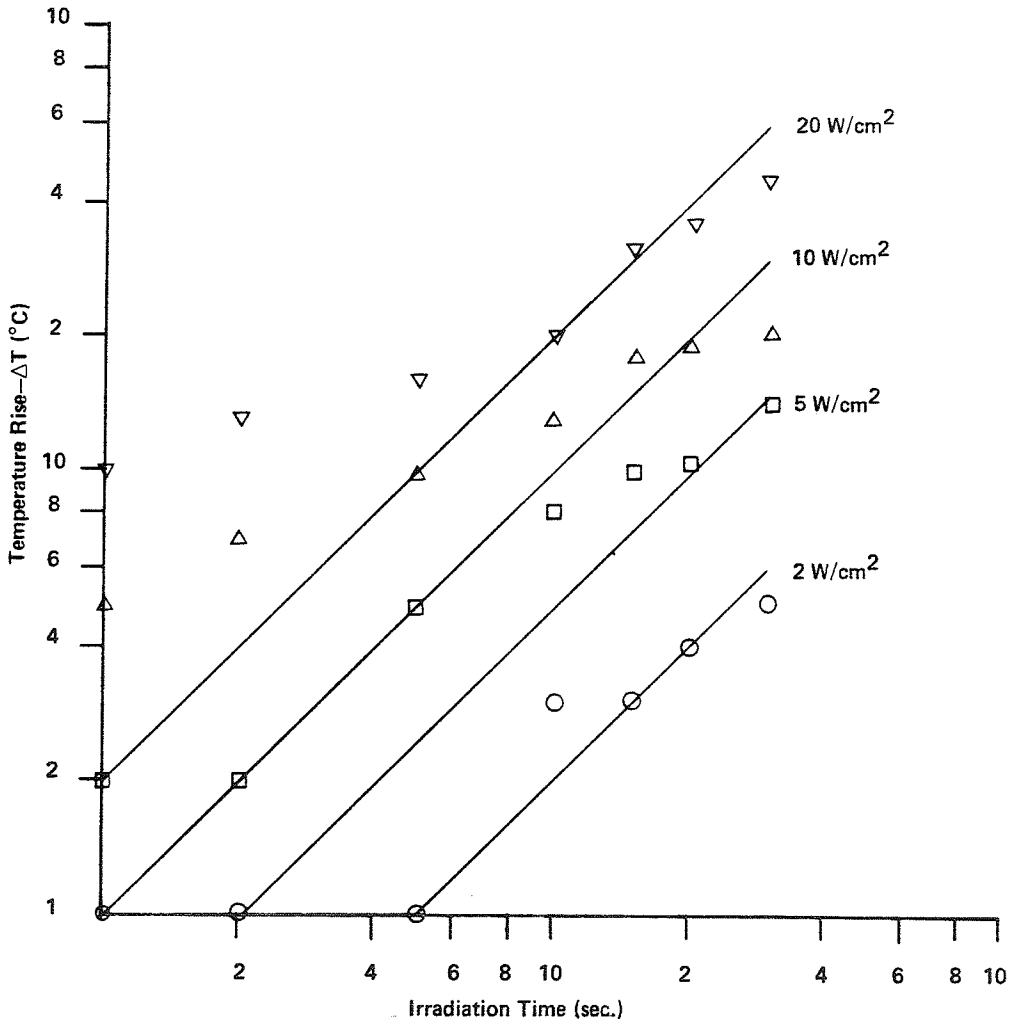

Fig. 62. Irradiation Time vs. Tissue Temperature Rise

A thermal mechanism of damage may be more easily involved. Figures 61 and 62 show the relation between the rise in testicular, or intrascrotal, temperature and the acoustic intensity of exposure for various times. The dashed lines in the figure are computed for the situation where heat conduction processes are ignored, from Equation 12:

$$\frac{dT^\circ}{dt} = \frac{2\alpha I}{\rho CK}$$

EQUATION 12

where α is the acoustic pressure absorption coefficient per unit path length, obtained by independent measurement (49); I is the acoustic intensity, PC is the heat capacity per unit volume of the tissue and K is the mechanical equivalent of heat. The plotted points are measurements of intrascrotal temperatures made by inserting a small copper-constantan thermocouple under the scrotal skin of the mouse and recording, from a digital telethermometer, the peak temperatures obtained within the scrotum for exposures of various intensities and durations in the intact animal.

It is seen that for a 25 w/cm^2, 30 second exposure, the terminal temperature within the testicular tissue may be as high as 44-45^o C., based on a 37^o C. ambient, initial temperature. Assuming that thermal equilibrium is very nearly reached after 10-15 seconds of irradiation (55), it may be considered that the intratesticular temperature for the high intensity exposure was in the neighborhood of 45^o C. for many seconds prior to the end of the irradiation period and could account for the severe and immediate damage observed in the testes in this series of exposures. However, the long term progression of damage observed for many days after exposure is not so easily accounted for by this process.

The thermal mechanisms, as a direct effect acting on the germinal epithelium of the testes, is difficult to support for the lower dose. Reference to Figure 61 shows the temperature rise in this situation, to be only 2 degrees C. at the end of the exposure period, which is in correspondence with the histological preparations showing minimal if any damage. Increased temperature may still play a significant role in accounting for the observed effects: 1) as localized damage to specific cells and structures, 2) as indirect action on testicular components, or 3) as thermal-time stress, i.e., dT^o/dt as opposed to simple T.

Thermal damage to the testes, especially through natural or induced cryptorchidism, is well documented (67,71). Scrotal

testes maintained at normal body cavity temperatures for extended periods of time, exhibit a progressive maturation depletion and eventually appear as senile organs. This requires 20 to 30 days of temperatures maintained at 37^{o} to 39^{o} C. to halt irreversibly spermatogenesis. If the testes are allowed to cool in the scrotal sac the damage is reversible since some stem and Sertoli cells survive. The time course of damage to the germinal epitheluim induced in the cryptorchid testes appears similar to that observed in the testes of the low dose animals, with the main difference being in the slightly accelerated degeneration in the acoustic case. A point of major agreement between the thermal and acoustic insult is the morphologically apparent insensitivity of the spermatogonia.

Heat is known to cause losses in meiosis, and for the mouse, this has been proposed as a natural mechanism to minimize birth anomalies (67,71). In this regard it is interesting to note that for both the tenth and the forty third day post-irradiation animals, no normal post-meiotic cells were present.

The damage to germinal tissue caused by X-ray and other ionizing radiation is probably the best characterized, if not completely understood, of all injurious agents (72,73). Though there are no a priori reasons to believe that damage produced by ionizing radiation is in any way the same as that produced by

an acoustic or other mechanical insult, similarities do exist and should not be overlooked (71). For example, following X-ray exposure, the existance of a normal tubule adjacent to one exhibiting extensive deterioration may appear, and it is postulated that differences in tubular sensitivity occur as a function of mitotic and meiotic activity in the tissue volume at that instant of time (72). Considering the different sensitivities of various germinal cells in relation to DNA synthesis and cell division, this result is expected. In the acoustic case evidence to support the view that different stages of spermatogenesis are also attended by different mechanical properties, such as values for the elastic constants, is lacking, though the idea provides interesting speculation.

Primarily due to the similarities of acoustic effects on testes and that from other agents and processes, the following is included. A deficiency of zinc will induce degenerative changes in the mammalian testes (71) similar to that observed in thermal or acoustic insult. This deficiency may lead to the complete and irreversible halt of spermatogenesis if allowed to continue. Of even greater interest is the effect of cadmium on the germinal epithelium. This highly toxic metal displaces zinc in the testes and causes a progressive degeneration very similar to that seen following an acoustic exposure. One of the first signs of cadmium poisoning is an intratubular edema, occuring within the first twelve hours following administration. This edema is caused by

injury to the testicular vascular bed, particularly the venous return. The circulatory system of the testes is unique in several ways; the capillaries of the testicle are particularly rich in zinc, and the walls allow nutrients and macromolecules transit which normally are contained within the vessels (71). Secondly, and possibly most important, the spermatic artery - pampiniform plexus, designed to aid in testicular temperature regulation, has no counterpart anywhere else in mammalian anatomy. Within hours changes take place in testicular enzymes, particulary zinc metallo-enzymes. Twenty four hours after cadmium administration, all tubular elements are in the process of degenerating. The degeneration processes are virtually complete within seven to ten days and are at this point accompanied by a marked thickening of the tunica albugnea. All these effects are related to either damage to the temperature regulatory aspects or enzymatic relationships of the specialized testicular vasculature. This relation is further emphasized by the fact that the cadmium is not toxic to the testes of the chicken, an intra-abdominal organ.

Although acoustic damage shows many similarities to the above, no gross vasculature damage has been observed, even less the mass hemorrhagic effects described for cadmium poisoning. Nor is the interstitial tissue morphologically disrupted as in the metal effects.

The ability of cadmium to destroy the germinal epithelium is not universal. Some animals, even of the same species, are resistant to the toxic effects. In particular, among the resistant strains of mice is the A/HeJ mouse, and among the susceptible is the C57L/J mouse. The F1 hybrid from these two animals is the LAF/J mouse, used in this study. It has been reported that a cross between an insensitive strain and a sensitive strain produces susceptible offspring (74), and if a parallel exists, a question may be raised as to how far the acoustic similarity may be pursued. The completely denuded appearance of some tubules in the testes of acoustically irradiated animals find exact counterparts in the tissue of the hypophysectionized animal (67). The uninterrupted hypothalamic-pituitary-testicle pathway is essential to the maintenance of spermatogenesis. Since this is a feedback network, the alteration by insult to any element may be injurious to the output: spermatogenesis (69).

C. OVARIAN EXPOSURE

Ovaries exposed to lethal doses of ionizing radiation undergo degenerative morphological changes easily recognized and are well characterized in the literature (72). The cumulus cells are the first to respond to this insult with pyknosis or rhexis. Oocytes do not show gross changes at low X-ray doses, but weeks later the number of developing follicles are significantly decreased. At high doses, the oocytes become pyknotic and degenerate. The resopnse of oocytes is highly variable both with respect to species and deveopmental stage, making generalizations difficult.

Contrary to that observed with ionizing radiation (72), ultrasound did not produce any recognizable changes in the mouse ovaries at the exposure regimes employed in this study. This seeming resistance to structural damage may be explained by the following two organ features. Preliminary measurements of the acoustic amplitude absorption coefficient of ovary shows that the value at 1 MHz lies between 0.007 N/cm and 0.01 N/cm and is therefore about one-tenth that of most other soft tissues. The range of this quantity may be due to acoustic property differences between the ovarian stroma, follicles, corpora lutea and corpora albicans, as observed by placement of the small thermocouple detector, respectively, in each of these structures. This low value of the absorption coefficient may well eliminate thermal mechanisms as a damaging agent and use of equation 12 shows that a

maximum temperature rise of only 3^{o} C. is to be expected for exposure to 60 w/cm^2 for 10 seconds.

A second feature of the mouse ovary concerns the physical dimensions of this organ, from histological preparations, yields a mean diameter of 1.56 mm. As the wavelength of a 1 MHz sinusoidal wave in water is 1.5 mm, and there is little reason to believe that the acoustic impedance of ovarian tissue is significantly different from that of water; the organ may be involved in a transmission medium-wave interaction which results in virtually all the acoustic energy being transmitted with little or no loss. This loss has transmission, i.e. without the phenomena of refraction, reflection, diffraction, etc., occuring, may account for the absence of structural changes.

The report by Garrison and co-workers on the functional characteristics of rat ovaries showing no response to pulsed, (10 msec. on, 190 msec. off) acoustic fields of intensities up to 100 w/cm^2 for 10 minutes may help in providing guidelines for continued investigation into this area.

VI. CONCLUSIONS

A. IN-UTERO FETAL EXPOSURES

Toxic effects of ultrasound, for the irradiation conditions in this study, may be absent as in the instance of sex partition of the fetuses and fetal weight, or rely on a single irradiation variable as the maternal survival or dependent upon many acoustic and procedural related variables such as in the probability of pregnancy.

A multiplicative combination of linear terms involving acoustic intensity, time of exposure, and repetitions of the procedure does not adequately characterize the deleterious effects on reproductive function and fetal viability. Quadratic terms at least must be included in any effective model relating toxic effects on pregnant animals to ultrasonic exposures. In particular, non-linear effects of time, and time-related variables, may be important as by the presence of quadratic temporal terms, alone and/or multiplied by intensity, in eight of the nine dependent variables.

The absence of significant differences between the three experimental groups of animals may be attributed to the interaction of procedural effects alone with effects induced by the

acoustic exposure. This view is further supported by the presence of linear and quadratic terms of time in five of the nine regression equations.

Significant correlations between the chosen dependent variables have been established, and these aid in minimizing unsupported assumptions necessary to the analysis of experimental data.

The regression surfaces outlined in these models, may now be filled by careful planning of future experiments. In particular, the effects of repetitive exposure to the experimental regimen should prove fruitful in assessing the extent of temporal effects.

Further manipulation of the statistical models constructed may aid in reducing the error function and increase the predictive capacity.

B. TESTICULAR EXPOSURES

The toxic effects of ultrasound on the testicular tissue of the mouse are severe and irreversible for the acoustic intensities and exposure times used in this study. The effects observed are not unique in that some chemical and radiative toxic agents discussed in Section V cause anomalies with one or more points of similarity to those induced acoustically. The effects of ultrasound on the germinal epithelium of the mouse mimic two of the toxic agents, viz., heat and cadmium poisoning. The similarities here are in the halt of spermatogenic activity at meiosis and a characteristic degeneration of the germinal epithelium. Both non-acoustic modalities act on the same tissue systems, viz., the vascular system and the enzyme systems necessary to germ cell maturation and renewal. A relationship between the two non-acoustic toxic agents exists within the avian reproductive systems, wherein cadmium is not toxic to the testicular tissue and these organs reside within the abdominal cavity at normal body temperature. This fact may be exploited to examine the site of acoustic interaction with reproductive tissue.

A further parallel between acoustic damage and ionizing radiation is evident in the pattern of damage, where a relatively normal germinal epithelium may be seen in a tubule adjacent to a second tubule exhibiting gross disruption of the cellular

morphology. This, again, supports the view that an indirect effect, mediated possibly by vascular or enzymatic dysfunction, is operative. A multiplicity of techniques are available to assess damage to the target organ if mediated by vascular or enzymatic changes, including monitoring the differential temperatures of arterial and venous blood supplies in the spermatic blood vessels, and radioimmunoassay techniques of circulating hormones. The above procedures are means of assessing quantitatively the morphological alteration or the functional change of a target organ. Functional considerations are also necessary points for examination, but difficult to determine in reproductive organs. It is not known how much of the germinal epithelium must remain to provide a mammal with "normal" fertility. Sperm counts and determination of abnormal spermatozoa have proved misleading in the assessment of fertility (71). Thus, toxicity acquires an ambiguous meaning when germinal tissue is the target organ. The resolution of this ambiguity lies in the careful definition of what criteria are to be assessed in determining that a toxic reaction has occurred.

C. OVARIAN EXPOSURES

The combination of a relatively low acoustic absorption coefficient for the ovary and particular physical dimensions comparable to one acoustic wave length may serve to render the ovary relatively acoustically transparent. The exposure of the ovary to ultrasonic fields of other frequencies chosen such that the diameter is not an integral number of wave lengths, should provide answers to questions of mechanisms and dimensional dependencies. Most soft tissues have absorption coefficients which are a function of the frequency to a power covering the range of 1 to 2 (75,76). If a similar behavior is exhibited by ovarian tissues, a higher frequency acoustic field will provide both higher tissue temperatures per unit time of exposure.

Though considerable caution needs to be exhibited until more details become available, it appears from this study that ovaries may be fairly resistive to CW ultrasonic insult which may include the doppler fetal monitor employed clinically. It remains an important point to determine whether a similar statement can be made for repeated pulse exposures, particularly as they are used in clinical medicine.

LIST OF REFERENCES

1 Erikson, K.R., Fry, F.J. and Jones, J.P. "Ultrasound in Medicine." IEEE Trans. Sonics and Ultrasonics. SU-21, 3, pp. 144-170, 1974.

2 Dunn, F. and Fry, F.J. "Ultrasonic Threshold Dosages for the Mammalian Central Nervous System." IEEE Trans. Bio-Med. Engin. BME-18, 4, pp. 253-256, 1971.

3 Fry, F.J., Kossoff, G., Eggleton, R.C. and Dunn, F. "Threshold Ultrasonic Dosages for Structural Changes in the Mammalian Brain." J. Acoust. Soc. Am., 48, 6 (Pt. 2), pp. 1413-1417, 1970.

4 Dunn, F. "Effects of Ultrasound on Tissues and Organs: Session Summary." Proc. of a workshop at Battelle Seattle Res. Center, Seattle, Wash., Nov. 8-11, 1971. D.H.E.W. pub. (FDA) 73-8008 BRH/DBE 73-1, pp. 103-108, 1972.

5 Gavrilov, L.R. "Physical Mechanism of the Lesion of Biological Tissues by Focused Ultrasound." Sov. Phys. Acoust., 20, 1, pp. 16-18, 1974.

6 Lele, P.P. "Ultrasound in Biology and Medicine." Biomedical Physics and Biomaterials Science. Stanley, H.E. (ed.), MIT Press, Cambridge, Mass., pp. 257-300, 1972.

7 Robinson, T.C. and Lele, P.P. "An Analysis of Lesion Development in the Brain and in Plastics by High-Intensity Focused Ultrasound at Low-Megahertz Frequencies." J. Acoust. Soc. Am., 51, 4(2), 1972.

8 Fields, S. and Dunn, F. "Correlations of Echographic Visualizability of Tissue with Biological Composition and Physiological State." J. Acoust. Soc. Am., 54, 3, pp. 809-812, 1973.

9 Pond, J.B. "The Role of Heat in the Production of Ultrasonic Focal Lesions." J. Acoust. Soc. Am., 47, 6 (Pt. 2), pp. 1607-1611, 1970.

10 Von Micsky, L.I. "Ultrasonic Tomography in Obstetrics and Gynecology." Diagnostic Ultrasound. Grossman, C.C., Holmes, J.H., Joyner, C. and Purnell, E.W. (ed.), Plenum Press, New York, pp. 348-368, 1966.

11 Meyers, R., Fry, W.J., Fry, F.J., Dreyer, L.L., Schultz, D.F. and Noyes, R.F. "Early Experiences with Ultrasonic Irradiation of the Pallidofugal and Nigral Complexes in Hyper-Kinetic and Hypertonic Disorders." J. Neurosurg., 16, 1, pp. 32-54, 1959.

12 Fry, F.J., Heimburger, R.F., Gibbons, L.V. and Eggleton, R.C. "Ultrasound for Visualization and Modification of Brain Tissue." IEEE Trans. on Sonics and Ultrasonics, SU-17, 3, pp. 165-169, July, 1970.

13 Somer, J.C. "Electronic Sector Scanning in Cerebral Diagnostics." Proc. 2nd World Congress on Ultrasonics in Med., Rotterdam, Netherlands, pp. 304-308, 4-8 June, 1973.

14 Freund, H.J. "Electronic Sector Scanning in Cerebral Diagnostics. III Visualization Intracranial Structures and Brain Arteries." Proc. 2nd World Congress on Ultrasonics in Med., Rotterdam, Netherlands, pp. 314-317, 4-8 June, 1973.

15 Fairbanks, Jr., W.M. and Scully, M.O. "A New Technique for Cardiac Pressure Measurement: Resonant Scattering of Ultrasound from Bubbles." IEEE Trans. of Biomed. Engr., BME-24, 2, pp. 107-110, March, 1977.

16 Jacobs, J.E. "Ultrasound as a Diagnostic Tool." Advances in Biomedical Engineering. Vol. 2, Brown, J.H.U. and Dickson, J.F. (ed.), Academic Press, New York, pp. 219-282, 1972.

17 Buschmann, W. "Biomedical Applications of Ultrasound. Advances in Biomedical Engineering. Vol. 1, Kenedi, R.M. (ed.), Academic Press, New York, pp. 1-76, 1971.

18 Fry, E.K., Kossoff, G. and Hindman, H.A. "The Potential of Ultrasound Visualization for Detecting the Presence of Abnormal Structures Within the Female Breast." IEEE Ultrasonic Symposium Proc. IEEE Group on Sonics and Ultrasonics, pp. 25-30, 1972.

19 Kossoff, G., Fry, E.K. and Jellins, J. "Average Velocity of Ultrasound in the Human Female Breast." J. Acoust. Soc. Am., 53, pp. 1730-1736, 1973.

20 Jellins, J., et. al. "Ultrasonic Grey Scale Visualization of Breast Disease." Ultrasound Med. Biol., 1, No. 4, pp. 393-404, 1975.

21 Kossof, G., Wadsworth, J.R. and Dudley, P.F. "The Round Window Ultrasonic Technique for Treatment of Menieres Disease." Arch. Otoloryng., 86, pp. 535-542, 1967.

22. Kossoff, G. "Current Status of Ultrasonic Treatment of Meniere's Disease." Proc. of a workshop at Battelle Seattle Res. Ctr., Seattle, Wash., Nov. 8-11, 1971. D.H.E.W. pub. (FDA) 73-8008 BRH/DBF 73-1, pp. 293-294, 1972.

23 Thompson, H.E. "The Future Role of Ultrasound in Obstetrical Care." Proc. of a workshop at Battelle Seattle Res. Center, Seattle, Wash., Nov. 8-11, 1971. D.H.E.W. pub. (FDA) 73-8008 BRH/DBE 73-1, pp. 103-108, 1972.

24 Holmes, J.H. "Diagnostic Applications of Ultrasound for the Kidney and Genitourinary Tract." Proc. 2nd World Congress Ultrasonics in Med., Rotterdam, Netherlands, pp. 180-185, 4-8 June, 1973.

25 Thompson, H.E. "Studies of Fetal Growth by Ultrasound." Diagnostic Ultrasound. Grossman, C.C., Joyner, C., Holmes, J.H. and Purnell, E.W. (ed.), Plenum Press, New York, pp. 416-427, 1966.

26 Mannor, S.M., Serr, D.M., et. al. "The Safety of Ultrasound in Fetal Monitoring." Am. J. Obstet. Gynecol., 113, 5, pp. 653-661, July, 1972.

27 Christie, A.D. "Diagnostic Procedures in Obstetrics. A Review of Commonly Accepted Scanning Techniques with Associated Limitations and Errors." Proc. 2nd World Congress on Ultrasonics in Medicine, Rotterdam, Netherlands, 4-8 June, 1973. deVlieger, M., White, D.N., McCready, V.R. (ed.), Am. Elsevier Pub. Co., Inc., N.Y., 1974.

28 Hochberg, H.M. "Accurate Noninvasive Measurement of Blood Pressure in Neonates, Infants and Children by Ultrasonic Techniques." Pediatrics Digest, 15, pp. 33-39, July, 1973.

29 Albright, R.J. and Harris, J.H. "Diagnosis of Urethral Flow Parameters by Ultrasonic Backscatter." IEEE Trans. Biomed. Engin., BME-22, pp. 1-11, 1975.

30 Miskin, M. and Bain, J. "B-Mode Ultrasonic Examination of the Testes." J. Clin. Ultrasound, 2, 308-311, 1974.

31 Fahim, M.S., Fahim, Z., Der., R., Hall, D.G., Harmon, J. "Heat in Male Contraception (Hot Water 60°C., Infrared, Microwave and Ultrasound)." Contraception, 11, 5, pp. 549-562, May, 1975.

32 Nicholas, D. "The Application of Acoustic Scattering Parameters to the Characterization of Human Soft Tissue." (abs.) IEEE Trans. on Sonics and Ultrasonics, SU-24, 2, p. 123, March, 1977.

33 Myers, G.H. "Diagnostic Medical Applications of Ultrasound." Proc. of a workshop at Battelle Seattle Res. Center, Seattle, Wash., Nov. 8-11, 1971. D.H.E.W. pub. (FDA) 73-8008 BRH/DBE 73-1, pp. 237-240, 1972.

34 Shore, M.L., O'Brien, W.D., Fred, R.K. and Leach, W.M. "On the Assessment of Risks from Ultrasound." (abs.) IEEE Trans. Sonics and Ultrasonics, p. 54, 1973.

35 Taylor, K.J.W. "Current Status of Toxicity Investigations." J. Clin. Ultrasound, 2, pp. 148-156, 1974.

36 Ulrich, W.D. "Ultrasound Dosage for Nontherapeutic Use on Human Beings--Extrapolations From a Literature Study." IEEE Trans. on Biomed. Eng., pp. 48-51, Jan., 1974.

37 Bell, E. "Action of Ultrasound on Adult and Embryonic Organ Systems." Am. J. Physical Med., 37, 4, pp. 184-191, August, 1958.

38 Smyth, M.G. "Animal Toxicity Studies with Ultrasound at Diagnostic Power Levels." Diagnostic Ultrasound. Grossman, C.C., Joyner, C., Holmes, J.H. and Purnell, E.W. (ed.), Plenum Press, N.Y., pp. 296-299, 1966.

39 Taylor, K.J.W. and Dyson, M. "Toxicity Studies on the Interaction of Ultrasound on Embryonic and Adult Tissues." Proc. 2nd World Congress on Ultrasonics in Medicine, Rotterdam, Netherlands, 4-8 June, 1973. deVlieger, M., White, D.N., McCready, V.R. (ed.), American Elsevier Pub. Co., Inc., pp. 353-359.

40 Ziskin, M.D. "Survey of Patient Exposure to Diagnostic Ultrasound." Proc. of a workshop at Battelle Seattle Res. Center, Seattle, Wash., Nov. 8-11, 1971. D.H.E.W. pub. (FDA) 73-8008 BRH/DBE 73-1, pp. 203-206, 1972.

41 McClain, R.M., Hoar, R.M. and Saltzman, M.B. "Teratologic Study of Rats Exposed to Ultrasound." Am. J. Obs. and Gyn., 144, 1, pp. 39-42, 1972.

42 Kirsten, E.B., Zinsser, H.H., Reid, J.M. "Effect of 1 mc Ultrasound on the Genetics of Mice." IEEE Trans. on Ultrasonics Engr., UE-10, pp. 112-116, 1963.

43 Mengoli, Henry F. "Effects of Ultrasonic Irradiation on the Cytochemistry of the Rat Testes." Ph.D. Thesis. The Catholic University of America Biological Studies, No. 43. The Catholic University of Am. Press, Washington, D.C., 1957.

44 Warrick, R., Pond, J.B., Woodward, B. and Connolly, C.C. "Hazards of Diagnostic Ultrasonography - A Study with Mice." IEEE Trans. on Sonics and Ultrasonics, SU-17, 3, pp. 158-164, 1970.

45 Sikov, M.R. and Hildebrand, B.P. "Effects of Ultrasound on the Prenatal Development of the Rat. Part 1. 3.2 MHz Continuous Wave at Nine Days of Gestation." J. of Clin. Ultrasound, 4, pp. 357-363, 1976.

46 Garrison, B.M., et. al. "The Influence of Ovarian Sonication on Fetal Development in the Rat." J. of Clin. Ultrasound, 1, 4, Dec., 1973.

47 Brunk, H.D. "An Introduction to Mathematical Statistics." Xerox College Publishing, 3rd. ed., Lexington, Mass., 1975.

48 Remington, R.D., Schork, M.A. "Statistics with Applications to the Biological and Health Sciences." Prentice Hall, Inc., N.J., 1970.

49 Brady, J.K., Goss, S.A., Johnston, R.L., O'Brien, W.D. and Dunn, F. "Ultrasonic Propagation Properties of Mammalian Testes." J. Acoust. Soc. Amer., 60, 1407-1409, 1976.

50 Bo, W.J., et. al. "Influence of Ultrasound on the Corpus Luteum." Exerpta Medica, International Congress Series, 2nd World Congress on Ultrasonics in Medicine, 277:26 (abs.), 1973.

51 Dunn, F. and Fry, F.J. "Ultrasonic Field Measurement Using the Suspended Ball Radiometer and Thermocouple Probe." Proc. of a workshop at Battelle Seattle Res. Center, Seattle, Wash., Nov. 1971. D.H.E.W. pub. (FDA) 73-8008 BRH/DBE 73-1, pp. 173-176, 1972.

52 W.J. Fry, R.B. Fry. "Determination of Absolute Sound Levels and Acoustic Absorption Coeff. By Thermocouple Probes--Experiment." TASA, Vol. 26, #3, pp. 311-317, May, 1954.

53 _____ "Determination of Absolute Sound Levels and Acoustic Absorption Coeff. By Thermocouple Probes--Theory." TASA, Vol. 26, #3, pp. 294-310, May, 1954.

54 King, L.V. Proceedings of the Royal Society. London, A137, 212, 1935.

55 Fox, F.E. "Sound Pressure on Spheres." JASA, Vol. 12, p. 147, 1940.

56 Hasegawa, T., Yosioka, K. "Acoustic Radiation Force on a Solid Elastic Sphere." JASA, Vol. 4C, No. 5, pp. 1139-1143, Nov., 1969.

57 Dunn, F., Averbuch, A.J. and O'Brien, W.D. "A Primary Method for the Determination of Ultrasonic Intensity with the Elastic Sphere Radiometer." Acoustics, 37, 1977. In Press.

58 Breazeale, M.A. and Dunn, F. "Comparison of Methods for Absolute Calibration of Ultrasonic Fields." J. Acoust. Soc. Am., 55, 3, pp. 671-672, March, 1974.

59 Goodman, L.S. and Gilman, A., (ed.). The Pharmocological Basis of Therapeutics. The MacMillan Co., New York, 4th Edition, pp. 42-92; 98-120, 1970.

60 Hall, L.W. Wrights Veterinary Anesthesia and Analgesia. William and Wilkins Co., Baltimore, Maryland, 7th Ed., p. 181, 1971.

61 Humason, G.L. "Animal Tissue Techniques." W.H. Freeman & Co., London, pp. 130-131, 1962.

62 Thompson, S.W. "Selected Histochemical and Histopathological Methods." Charles C. Thomas, Springfield, Ill., 1966.

63 Ham, A.W. Histology. J.B. Lippincott Co., Phil., Pa., pp. 874-962, 1969.

64 Oakberg, E.F. "A Description of Spermiogenesis in the Mouse and Its Use in Analysis of the Cycle of the Seminiferous Epithelium and Germ Cell Renewal." Am. J. Anat., 99, (3), pp. 391-413, 1956.

65 Rugh, R. The Mouse: Its Reproduction and Development. Burgess Publishing Co., Minn., pp. 1-43, 1968.

66 Monesi, V. "Spermatogenesis and the Spermatozoa." Reproduction in Mammals, Vol. I, Ch. 3. Austin, C.R. & Short, R.V. (ed.), Cambridge Univ. Press, 1972.

67 Nalbandov, A.V. Reproductive Physiology of Mammals and Birds. Third Edition. W.H. Freeman & Co., San Francisco, 1976.

68 Dunn, F., Lohnes, J.E., and Fry, F.J. "Frequency Dependencies of Threshold Ultrasonic Dosages for Irreversible Structural Changes in Mammalian Brain." J. Acoust. Soc. Am., 58, 2, pp. 512-514, August, 1975.

69 Liggins, G.C. "The Fetus and Birth." Reproduction in Mammals: 2 Embryonic and Fetal Development. Austin, C.R. and Short, R.V. (ed.), Cambridge University Press, pp. 72-109, 1972.

70 Dunn, F. "Interaction of Ultrasound and Tissue." Ultrasound Graphia Medica. Verlag Der Wiener Medizinischen Akademie, p. 452, 1969.

71 Johnson, A.D., Gomes, W.R., & VanDemark, N.L. The Testis. Vol. III, Academic Press, New York and London, 1970.

72 Mandl, A.M. "The Radiosensitivity of Germ Cells." Biological Reviews, 39, pp. 288-371, 1964.

73 Kotetsky, S. "The Pathological Effects of Radiation Injury." Radiation Biology and Cancer. University of Texas Press, Austin, Texas, pp. 71-89, 1959.

74 Chiquoinc, A.D., Suntzeff, V. "Sensitivity of Mammals to Cadmium Necrosis of the Testis." J. Reprod. Fertility, 10, 455, 1965.

75 Dunn, F., Edmonds, P.D. & Fry, W.J. "Absorption and Dispersion of Ultrasound in Biological Media." Biological Engineering. Chp. 3, Herman P. Schwan (ed.), McGraw-Hill, pp. 205-332, 1969.

76 Goldman, D.E. & Heuter, T.F. "Tabular Data of the Velocity and Absorption of High-Frequency Sound in Mammalian Tissues." J. Acoust. Soc. Am., 28, 1, pp. 35-37, Jan., 1956.

APPENDIX A

Listing of SOUPAC Statistical Program used in the Analysis of the Results of the In-Utero Exposures.

```
TRA (C)
          OUT (T8)(201, 227).
     First.
          PER (1) (2,27) (1).
          EBC (1) (1).
          REC (1) "EQ"*14*(101)*1*.                    EXPOSED
          REC (1) "EQ"*12*(101)*-1*.                   CONTROL
          REC (1) "EQ"*-0*(102)*-2*(102)*1*.           NEG CONTROL
          IF  (101)"-""0""+".
      "+" MUL (2) (3) (26) (103).                      TOTAL DOSE
          MUL (2,3) (103) (104,105).
          MUL (26) (103) (106).
          GO  "0".
      "-" MUL (3,26,23) (3) (141,142).
          MOV (3,26,23) (139,140).
      "0" MUL (4)*30*(90).                             DAY OF THE YEAR
          REC (4) "EQ"*3*(91)*-2*.
          REC (4) "EQ"*4*(91)*-1*.
          REC (4) "EQ"*5*(91)*-1*.
          REC (4) "EQ"*8*(91)*1*.
          REC (4) "EQ"*9*(91)*2*.
          REC (4) "EQ"*10*(91)*2*.
          REC (4) "EQ"*11*(91)*3*.
          REC (4) "EQ"*12*(91)*3*.
          ADD (90) (91) (5)*-29*(92).
          DIF (6)*76*"R""L""R".
      "L" DIF (4)*2*"*+2""*+2""*+1".
          ADD (92)*1*(92).
          DIV (92*366*(93).
          GO  "*+2".
      "R" DIV (92)*365*(93).
          MOV (93) (94).
          ADD (94) (94,98) (95,99).
          CON (71,72) (94) (1).
      DO(70)*1,6*.
          MOV (71F) (73).
          SUB (73)*1*(73).
          IF  (73)"*+1""+2""*-1".
          ADD (73)*1*(73).
          MOV (73) (71F).
```

```
        XAD (71) (72) (71).
LOOP.   MUL (94,99)*6.283185*(94,99).
        COS (94,99) (151,161,2).
        SIN (94,99) (152,162,2).
        CON (99)*0*.
        DIF (6)*76*"B""*+1""E".
        DIF (92)*180*"B""A""C".
  "A"   OUT (P) (1,140).
        ABORT.
  "C"   SUB (92)*136*(115).
        GO  "D".
  "E"   ADD (92)*230*(115).
  "D"   CON (114)*1*.
        MUL (115) (115) (116).
  "B"   REC (7)"EQ"*6*(117)*-1*(117)*1*.
        SQU (25) (30).
        OUT ( T1) (101,106) (139,142)(151,162) (114,117) (25) (30).
        EBC (8) (8).
        REC (8) "EQ:*13*(118)*0*(118)*1*.
        OUT ( T2) (101,106)(139,142)(151,162)(114,118).
        IF  (118) "NO""NO""*+1".
        REC (*) "EQ"*23*(118)*0*(118)*1*.
        OUT ( T3) (101,106)(139,142)(151,162)(114,118).
        IF  (8) "NO""*+1""NO".
        EBC (21,22)(21,22).
        REC (22) "EQ"*14*(119)*1*.
        REC (22) "EQ"*14*(125)(20).
        DIF (22) *15*"G""*+1""G".
        DIF (21)*13*"*+1""*+1""H".
        OUT ( T9) (1,27).
        GO  "*+3".
  "H"   REC (22) "EQ"*15*(120)*1*.
        REC (22) "EQ"*15*(126) (20).
  "G"   REC (22) "EQ"*18*(121)*1*.
        REC (22) "EQ"*18*(127) (20).
        REC (22) "EQ"*28*(122)*1*.
        REC (22) "EQ"*28*(128) (20).
        REC (22) "EQ"*29*(123)*1*.
        REC (22) "EQ"*29*(129) (20).
```

"AGE"

DIP CONST

DAY OF GESTATION

MATERNAL DAMAGE

MORTALITY
MORTALITY

PREGNANCY
PREGNANCY

14,15,18,28,29,33
HEMORRHAGE

EYELID NONFUSION

GIANT

UNSPECIFIED

STUNTED

```
        REC (22 "EQ"*33*(124)*1*.
        REC (22)"EQ"*33*(130)(20).                                  EXENCEPHALY
        SQU (125,130)(131,136).
        OUT ( T4) (101,106)(139,142)(151,162)(114,117)(119,136)     ANOMALIES
        IF  (11)"A""*+1""*+4".                                      CL'S RECORDED?
        IF  (12)"A""*+1""*+3".
        OUT ( T9(1,27).
        GO  "T"
"J"     ADD (11)(12)(118).                                          CL'S
        SUB (11)(12)(119).
        IF  (9)"A""*+1""V".
        IF  (10)"A""*+1""V".
        IF  (13)""A""*+1""V".
        IF  (14)""A""*+1""V".
        IF  (15)""A""*+1""V".
        IF  (16)""A""*+1""V".
        IF  (17)""A""*+1""V".
        IF  (18)""A""*+1""V".
        OUT ( T9)(1,27).
        GO  "T"
"V"     ADD (9)(13)(15)(17)(31).
        ADD (10)(14)(16)(18)(32).
        ADD (31)(32)(120).                                          IMP'S (TOTAL)
        SUB (31)(32)(121).
        ADD (9)(10)(122).                                           FETUSES
        SUB (9)(10)(123).
        ADD (13)(14)(124).                                          IMP'S (EMPTY)
        SUB (13)(14)(125).
        ADD (15)(16)(126).                                          RESORP. EARLY
        SUB (15)(16)(127).
        ADD (17)(18)(128).                                          RESORP. LATE
        SUB (17)(18)(129).
        ADD (126)(128)(130).                                        RESORP. TOTAL
        ADD (127)(129)(131).
        MOV (133)(132).
        IF  (99)"A""*+1""*+5.
        CON (99)*1*.
        SQU (9,18)(9,18).
        DIV (19)(122)(133)*0*
        OUT ( T5)(101,106)(139,142)(151,162)(114,131).              AV. WGT.
```

```
          GO  "V".
          OUT (T15)(101,106)(139,142)(151,162)(114,131).
          IF  (19)"A""*+1*+3".
          OUT ( T9)(1,27).
          GO  "NO".                                                    FETUS
    "T"   IF  (122)"A""NO""*+1".
          OUT ( T6)(101,106)(139,142)(151,162)(114,117)(132)(122).
          IF  (23) "A""*+1""*+4".                                      MALES RECORDED?
          IF  (24) "A""*+1""*+3".
          OUT ( T8)(1,27).
          GO  "NO".
          DIV (23)(122)(42).                                           PROP OF MALES
          OUT (T 7)(101,105)(139)(141)(151,162)(114,117)(120)(130)(42)(132)(122).
    "NO"  NOO.
          END P

MAT.      SIN (T1)(T2)(T3)(T4)(T5)(T6)(T7)(T8)(T9)(T10)(T15).
          PRI (T9)"(',2F4.0,F5.0,15F4.0,F6.2,7F4.0,F8.0)".
          PRI (T8)"(',2F4.0,F5.0,15F4.0,F6.2,7F4.0,F8.0)".
          PRI (T1)"(',2F3.0,2F5.0,F6.0,3F4.0,F6.0,F4.0,12F5.2,2F4.0,F6.0,2F3.0,F5.2)".
          PRI (T2)"(',2F3.0,2F5.0,F6.0,3F4.0,F6.0,F4.0,12F5.2,2F4.0,F6.0,2F3.0)".
          PRI (T3)"(',2F3.0,2F5.0,F6.0,3F4.0,F6.0,F4.0,12F5.2,2F4.0,F6.0,2F3.0)".
          COL (T4)(T10)(5,26).
          PRI (T10)"(',2F4.0,2F8.0,6F4.0,6F5.0,6F6.3)".
          COL (T5)(T10)(5,22).
          PRI (T10)"(',2F4.0,4F8.0,2F7.0,14F5.0)".
          COL (T15)(T10)(5,23).
          PRI (T10)"(',2F3.0,3F5.0,F7.0,F3.0,14F7.3)".
          PRI (T 6)"(',2F3.0,2F5.0,F6.0,3F4.0,F6.0,F4.0,12F5.2,2F4.0,F6.0,F3.0,F5.2,F4.0)".
          COL (T7)(T10)(7,16).
          PRI (T10)"(',2F3.0,F5.0,2(F5.0,F7.0),2F4.0,F6.0,3F4.0,2F5.3,F4.0)".
          PRI (T10)"(',2F3.0,2(2F5.0,F7.0),4F5.0,2F8.3,F5.0)".
          END P

  REG (T1)(P)(T10).
          VAR (1,20)23,28).
          MUL (24)(P)(P)()()(P)(P)(P)(P).
          VAR (1,18)(23,28).
          MUL (22)(P)(P)()()(P)(P)(P)(P).
          END P
```

```
REG (T2)(P)(T10).
        VAR (1,20)(23,27).
        MUL (24)(P)(P)()()(P)(P)(P)(P).
        VAR (1,18)(23,27).
        MUL (22)(P)(P)()()(P)(P)(P)(P).
        END P

REG (T3)(P)(T10).
        VAR (1,20)(23,27).
        MUL (24)(P)(P)()()(P)(P)(P)(P).
        VAR (1,18)(23,27).
        MUL (22)(P)(P)()()(P)(P)(P)(P).
        END P

REG (T4)(P)(T10).
        VAR (1,20)(23,29)(31)(33,35)(37)(39,41)(43).
        MUL (24)(P)(P)()()(P)(P)(P)(P).
        VAR (1,18)(23,29)(31)(33,35)(37)(39,41)(43).
        MUL (22)(P)(P)()()(P)(P)(P)(P).
        END P

REG  (T5)(P)(T10).
        VAR (1,20)(23,40).
        MUL (26)(P)(P)()()(P)(P)(P)(P).
        VAR (1,18)(23,40).
        MUL (24)(P)(P)()()(P)(P)(P)(P).
        END P
REG (T15)(P)(T10).
        VAR (1,20)(23,40).
        MUL (26)(P)(P)()()(P)(P)(P)(P).
        VAR (1,18)(23,40).
        MUL (24)(P)(P)()()(P)(P)(P)(P).
        END P

REG (T6)(P)(T10)()()()(1).
        VAR (1,20)(23,27).
        MUL (24)(P)(P)()()(P)(P)(P)(P).
        VAR (1,18)(23,27).
        MUL (22)(P)(P)()()(P)(P)(P)(P).
        END P
```

APPENDIX B

Experimental Animal Data

KEY TO MOUSE DATA COLUMNS

Column No.	Explanation
1	Maternal Effects: A = Delivered early; D = Died prior to necropsy; N = Not pregnant at necropsy
2	Number of live fetuses - Left uterine horn
3	Number of live fetuses - Right uterine horn
4	Number of corpora lutea - Left uterine horn
5	Number of corpora lutea - Right uterine horn
6	Empty implantation sites - Left uterine horn
7	Empty implantation sites - Right uterine horn
8	Early fetal resorptions - Left uterine horn
9	Early fetal resorptions - Right uterine horn
10	Late fetal resorptions - Left uterine horn
11	Late fetal resorptions - Right uterine horn
12	Litter weight (grams)
13	Number of fetal anomalies in litter
14	Type of fetal anomaly: ST = Stunted; GI = Giant; HE = Hemorrhage; EX = Exencephaly; EF = Eye fusion
15	Number of males in litter
16	Number of females in litter
17	Number of maternal damage sites

PREGNANT FEMALE MOUSE DATA - CONTROLS

Control Animal	1	2	3	4	5	6	7	8	9	10	11	12	13	14	15	16	17
0001		06	01	06	01							0905					
0002		00	04	01	04							0521				04	
0003		03	06									1006					
0004		01	02									0374					
0006		02	07	02	07							0972	01	ST	03	06	
0007		05	03	06	06			00	03	01	01	0978					
0008		05	00	05	01							0768			01	04	
0009		03	07	03	08			00	01			1207					
0010		00	02	02	05			00	03			0250	01	GI		02	
0011		05	05							00	01	1330	01	GI	06	04	
0012		04	00	05	03			01	00			0478			02	02	
0013		07	04	08	04			01	00			1416	01	GI			
0014		04	08									1425					
0015		04	05	04	05							0980					
0016		04	03	04	03							1030	07	GI			
0017		07	03	07	03							1203	01	HE			
0018		00	02	02	02							0251			02		

Control Animal	1	2	3	4	5	6	7	8	9	10	11	12	13	14	15	16	17
0019				04	03			04	03						03	02	
0020		04	00	04	00							0496					
0021		03	04	06	04			03	00			0847					
0022		06	02	06	04							0879					
0023		04	05	05	05			01	00			1092	01	ST			
0024		03	02	03	03							0781					
0025		07	04									1245	01	ST			
0026		05	04					00	01			1109					
0027		04	07	06	07					02	00	1456					
0028		03	07									1178					
0029		02	04									0784					
0030		05	05	06	05							1212					
0031		02	01	03	05							0436	01	GI			
0032		05	01									0732					
0033		01	00	02	03			02	00			0142					
0034		05	03	06	04			01	01			0920					
0035		02	04									0824					
0036		02	04	03	04							0827					
0037		04	03					02	00			0835					

PREGNANT FEMALE MOUSE DATA - GESTATION DAY 10

EXPOSURE PARAMETERS: 1 w/cm^2; 100 sec. - 1 Exposure

a) Exposed Animals	1	2	3	4	5	6	7	8	9	10	11	12	13	14	15	16	17
0304		07	04	07	05			00	01			0187					
0305		06	04	06	05				01			0190					
0307		03	07	04	07				01			0711					
0308		03	07	04	07							0992					
0330	D																
0331		06	06	05	04							0975	02	HE			
0332		05	07	05	06							1007	12	HE			
0334		08	05	05	04							1187	08	HE			
0335		07	04	06	04							1107	02	HE			
0337		05	04	04	04						01	0702					
0338		06	03	04	07							1085					
0339	D																
0340	N																
0341	N																
0342				03	04	00	04										

a) Exposed Animals	1	2	3	4	5	6	7	8	9	10	11	12	13	14	15	16	17
0344		05	06	05	05					01		0888					
0345		03	10	03	10							0998	01	HE			
0379	D																
0380		03	04	04	04							0530	01	HE			
0381		01	02	02	02							0261					
0382	N																
0383		03	06	03	06					01		0887					
0385		02	03	04	04		02	02				0471					
0390		03	05	05	04							0735	02	HE			
0408	N																
0409		06	05	06	07				01			0795					
0411		08	04	08	04							0430					
0447		04	04	04	07						02	0740					
0448	N																
0449	A																
0451		02	04	03	05						01	0180					
0469		01	08	03	06				01			1271	02	EF			
0471		04	08	05	06							1425					

a) Exposed Animals	1	2	3	4	5	6	7	8	9	10	11	12	13	14	15	16	17
0472		06	03	07	04							0998					
0473		07	02	07	04							1216					
0475		05	06	05	06			01		01		1535					
0476	D																
0477		03	08	03	07							1145					
0478		06	04	06	04							1135					
0480		03	05	03	04							0925					
b) Sham Exposed																	
0306		03	05	04	07			01	01			0721					
0333		00	03	03	03							0353	01	HE			
0343		06	00	03	04							0460					
0386		06	05	07	05							0983					
0391		06	04	03	04					00	01	1170	01	HE			
0450		04	06	05	08					00	01	0870	01	HE			
0474				03	01					04	01						
0479				04	02	00	02										

PREGNANT FEMALE MOUSE DATA - GESTATION DAY 6

EXPOSURE PARAMETERS: 2 w/cm^2; 100. sec. - 2 Exposures

a) Exposed Animals	1	2	3	4	5	6	7	8	9	10	11	12	13	14	15	16	17
0808	N																
0809		04	04	05	05							0890					
0810	N																
0812	N																
0813		05	06	06	08							0127					
0820				04	05			04	05								
0822		02	04	03	05				01			0800					
0824	D																
0825	N																
0832	D																
0834	A																
0840	D																
0841		06	03	06	03							0971					
0842	A																
0844		02	06						02			0979					
0852	D																
0853		05	05	05	05							1215					

a) Exposed Animals	1	2	3	4	5	6	7	8	9	10	11	12	13	14	15	16	17
0855		00	02	04	04			04	02			0239					
0856		03	00	04	03			01	03			0278					
0857	D																
0863	A																
0864		02	06	02	06							0930	01	HE			
0865		04	07	05	07							1208	02	HE			
0866	D																
0875		07	05	07	05							1407					
0876				03	02	02	00										
0878	N																
0879	N																
0880				02	00	01	00										
0887		05	05	06	06			01	01			1187					
0888		05	05									1121					
0889	N																
0891		07	05	07	05							1307	02	HE			
0892	06	04	07	05							01	1102	01	ST			
0902		05	03	05	03							0977	02	HE			
0903	D																
0905		02	08	03	08			01				1002					

a) Exposed Animals	1	2	3	4	5	6	7	8	9	10	11	12	13	14	15	16	17
0907		06	02	06	03				01			0900					
0918		06	02	06	04					01	01	1001					
0919	N																
0920	N																
0921	N																
0922		05	02	07	04			02	02			0830					
0930		05	04	04	04				01			1120					
0931	N																
0932	N																
0935	N																
0942	D																
0944		05	05	06	05			01	01				02	HE			
0946		05	07	06	07			01				1180					
0947		04	05	05	05							0860					
0954				02	02			02	01								
0955		06	05	06	05							1320					
0956				02	00			02									
0958	N																
0959	N																

a) Exposed Animals	1	2	3	4	5	6	7	8	9	10	11	12	13	14	15	16	17
0991		03	02	05	07			02	03	00	01	0613			01	04	
0994		06	03	06	04					00	01	0790			04	05	
0995	N																
b) Sham Exposed																	
0811	N																
0821	N																
0823	N																
0833		04	06	04	07				01			0108	01	HE			
0843		02	05	02	06				01			0830					
0845		03	04	03	04							0901					
0854		03	05	03	05							1020					
0867		01	00	02	00							0115					
0868	N																
0877	N																
0890		01	05						01			0870	01	HE			
0904		08	03	08	03							1206					
0906		04	00					01				0581					
0923	N																
0933		02	06	03	07				01			1126	03	GI			

b) Sham Exposed	1	2	3	4	5	6	7	8	9	10	11	12	13	14	15	16	17
0934		01	07	02	08				01	01		0712	02	ST			
0943		04	05	04	05			01				0860	01	HE			
0945		05	05	05	05							0930	03	HE			
0957		00	02	00	02							0207	02	ST			
0966	D																
0968		07	06	07	06							1120					
0993	N																

PREGNANT FEMALE MOUSE DATA - GESTATION DAY 10

EXPOSURE PARAMETERS: 5 w/cm^2; 10. sec. - 2 Exposures

a) Exposed Animals	1	2	3	4	5	6	7	8	9	10	11	12	13	14	15	16	17
1103				03	02	03	02						01				
1107	N												01	GI			
1108		00	01	00	02							0165	01	ST		01	
1109		01	01	01	02							0276	03	ST	01	01	
1114				03	02			03	00								
1115		06	04	06	05							1081			04	06	
1117		01	00	03	00			02	00			0122			01		
1122	N																
1124		06	03	06	03							1095			05	04	
1126				02	03			01	03								
1127		00	06	04	06			02	00			0819			02	04	
1128		07	03	08	04				01	01		1180			04	06	
1129		05	04	06	04				01	00		1130			03	06	
1131		06	04	07	04				01	00		1192			05	05	
1141	N																
1142	N																
1145		02	01	04	06							0412			01	02	

a) Exposed Animals	1	2	3	4	5	6	7	8	9	10	11	12	13	14	15	16	17
1147		05	07	07	07			01	00			1411			05	07	
1148				03	02	01	00										
1152		00	02	03	04							0248				02	
1159		01	02	05	06			01	04			0241			02	01	
1162		01	00	03	02							0085			01	00	
1164				00	04	00	03										
1172	N																
1174				00	02	00	01										
1175		03	08	03	07				01			1303			05	06	
1179		05	05	05	05							1128			06	05	
1180		00	06	02	06	02	00					0708			03	03	
1181		00	02	03	02			03	00			0236				02	
1184	N																
1191		00	02	03	03			03	00			0252			02	00	
1193	D																
1195		00	04	01	07				03			0504				04	
1196		03	00	04	04	01	00					0342			01	02	
1208				02	02			02	01								

a) Exposed Animals	1	2	3	4	5	6	7	8	9	10	11	12	13	14	15	16	17
1211		02	04	03	05				01			0656			03	03	
1214		05	07	06	07							1324			05	07	
1215		04	06	05	06			01	00			1204			04	06	
1241	A																
1242	A																
1244	D																
1247				04	05			03	02								
1290		00	04	04	05			02	00			0418			01	03	
1293	N																
1294		03	05	04	05							0935			04	04	
1297		00	03	02	05							0303			02	01	
1299		02	03	05	04			03	00			0582			02	04	
1303				06	04			04	02								
1305		03	01	03	03				02						02	02	
1315		01	02	04	03				01			0329			03		
1317				05	04			05	04								
1224		01	06	03	08				02			0743			03	04	
1227				03	05			01	05								
1229				03	03			03	01								

b) Sham Exposed	1	2	3	4	5	6	7	8	9	10	11	12	131	14	15	16	17
1102		03	00	03	02							0520					
1105				01	02			01	02								
1106		01	00	01	02							0151	01	GI			
1112		05	02	06	04			01				0831					
1116	N																
1123		03	01	04	04			01	01			0437					
1125		04	03	04	05							0962					
1130		06	04	07	06						02	1316					
1132		03	07	04	07							1132					
1143		04	05	04	05				01			1075					
1144				03	02	01	02										
1146	N																
1150		03	08	03	08				01			1268					
1160		01	00	04	02			01				0087					
1161		02	04	05	05	00	01	03				0480					
1171	N																
1173	N																
1182		07	03	07	04				01			0879					
1183		08	03	08	04				01			1207					

b) Sham Exposed	1	2	3	4	5	6	7	8	9	10	11	12	13	14	15	16	17
1192		03	05	05	08			01	03	01		0721					
1194	N																
1209		02	01	02	01							0441	03	GI	01	02	
1210		03	00	03	05							0423	01	HE	02	01	
1212				05	04	05	04										
1213				01	01			01	01								
1240				05	04	03	00										
1243	A																
1245	A																
1246		03	04	04	05			01				0946			03	04	
1291		04	05	04	05							0873			04	05	
1292		00	05	03	05							0675			02	03	
1295		01	03	02	03							0404			02	00	
1296		03	03	05	03			02				0517			01	05	
1298		04	01	04	03							0401	01	ST	03	02	
1300		03	05	05	05							0792	01	HE	03	05	
1301		01	01	06	03	05	00					0153	01	ST		02	
1302	N																

b) Sham Exposed	1	2	3	4	5	6	7	8	9	10	11	12	13	14	15	16	17
1304	D																
1314		02	03	04	04			01	01			0398	02	ST	01	04	
1316				02	04					02	01						
1225				04	03			02									
1226				02	04				04								
1228	N																

PREGNANT FEMALE MOUSE DATA - GESTATION DAY 10

EXPOSURE PARAMETERS: 6 w/cm^2; 10. sec. - 2 Exposures

a) Exposed Animals	1	2	3	4	5	6	7	8	9	10	11	12	13	14	15	16	17
1342		03	04	04	05				01			0730	01	ST	02	05	
1344		02	02	04	02							0378	01	ST	02	02	
1347				01	00			01	00								
1350				02	01			02	01								
1351		02	02	04	03			00	01			0384			01	03	
1352				03	02	03	02										
1353				03	03			02	01								01
1357				05	04			03	04								
1358				03	03	03	03										
1360	N																
1364		01	03	04	03			02	00			0428			02	02	
1367		03	00	03	04			00	04			0315			02	01	
1368				01	03	01	00										01
1369		04	04	05	05			01	01			0939			03	05	
1371		06	03	06	03			01	00			0993			04	05	
1372				04	04			04	02								01

a) Exposed Animals	1	2	3	4	5	6	7	8	9	10	11	12	13	14	15	16	17
1374				04	00			01									
1376	N							01									01
1377				01	02	01	02										
1377				01	02	01	02										
1381		02	01	05	03			02	02			0261			01	02	
1384	N																01
1385		03	00	03	00			01	00			0371			01	02	02
3187		00	03	05	05					05	00	0366			02	01	
1389	N																
1394		05	02	05	03							0737			04	03	
1395		05	03	05	04							1031			04	04	
1396	N																
1398	N																
1400				02	00			02	00								
1401		04	01	06	03			02	00			0461	01	ST	02	03	
1403	D																
1404				04	02	03	00	00	02								
1405	D																

a) Exposed Animals	1	2	3	4	5	6	7	8	9	10	11	12	13	14	15	16	17
1410				01	02			00	02								01
1411	N																02
1441		00	01	02	03			02	00			0103			01		
1442	D																
1443	N																01
1444		02	01	08	02			02	00			0381				02	
1449		01	00	03	00			02	00			0103				01	02
1450		03	00	05	03			01	01			0282				02	01
1451	D																
1452	N																
1454	N																03
1456	N																
1458	N																01
1460	D																
1462				01	03			00	01								01
1482	N																01
1487	N																01
1488		01	01	02	03							-206			01	01	01
1489				02	02			02	01								
1490				02	00	02	00										

b) Sham Exposed	1	2	3	4	5	6	7	8	9	10	11	12	13	14	15	16	17
1343		00	03	03	03	00	00	00	01			0332			01	02	
1345		05	05	075	07	00	00	00	02			0960	02	ST	03	07	
1346		05	05	05	05	00	00	00	00			1018	01	ST	04	06	
1348		02	02	02	05	00	00	00	03			0404			01	03	
1349		00	00	02	01	00	00	02	00								
1354		00	00	00	04	00	00	00	04								
1355	N																
1356		03	08	03	08	00	00	00	00			1213			04	07	
1359		00	00	03	03	02	03	00	00								
1361		05	03	05	03	00	00					0829	01	HE	02	06	
1362		00	00	02	01	00	00	00	01								
1363		02	06	03	08	00	00	01	02			1030			03	05	
1365		00	00	02	03	00	00	02	03								
1366		00	04	01	04	00	00					0297	04	ST	01	03	
1370	N																
1373		00	00	02	01	00	00	02	01								
1375		05	04	05	05	00	00	00	01			0966			03	06	
1378		00	00	04	04	00	00	03	04								
1379		02	05	03	05	00	00	01	00			0661			03	04	

b) Sham Exposed	1	2	3	4	5	6	7	8	9	10	11	12	13	14	15	16	17
1380		01	00	03	05	00	00	02	00			0124			01	00	
1383	N																01
1386	N																
1388		03	04	05	06	00	00	00	01			0798			04	03	
1390	N																01
1391	N																
1392	N																
1393		02	03	02	04	00	00					0562			02	03	
1397	N																
1399		00	00	02	00	00	00	02	00								
1402	N																01
1406		02	05	04	05	00	00	01	00			0586	02	HE	03	04	
1407		02	00	02	04	00	00	00	00			0207			02	00	
1408		00	00	04	05	04	02	00	00								01
1409	N																02
1412	N																03
1440		00	00	02	01	00	00	02	00								

b) Sham Exposed	1	2	3	4	5	6	7	8	9	10	11	12	13	14	15	16	17
1445		01	01	02	03	00	00	01	01			0189					
1446	N																
1447		01	01	02	04	00	00	00	00			0205			01	01	02
1448		01	00	01	01	00	00	00	00			0103			00	01	
1453	N																
1455		01	00	02	04	00	00	00	01			0066	01	ST	00	01	
1457		00	00	01	04	00	00	01	05								
1459		00	00	00	02	00	00	00	01								
1461	N																
1482		03	03	00	00	00	00	01	01			0590			03	03	
1484	N																
1485	N																
1486	N																

VITA

John K. Brady was born in Flushing, New York on the 28th of April, 1943. He graduated from Blue Island Community High School, Blue Island, Illinois in 1961. In 1970 he obtained the Bachelor of Science degree from the University of Illinois, Urbana, in Electrical Engineering; and the Master of Science in 1972 from the same institution. The field of specialization for the graduate work was biological engineering, and the master's thesis is titled "Ultrasonic Dosage Studies as a Function of Frequency for the Mammalian Central Nervous System Tissue." The doctoral thesis research subject is also in the field of ultrasonic toxicity; viz., the potentially toxic effects of ultrasound as applied to the mammalian reproductive system.

Experience as a teaching assistant includes two electrical engineering laboratory courses in fundamental circuit theory and one laboratory course in electron microscopy for the Biology Department.

He is a member of the Institute of Electrical and Electronics Engineers and the Acoustical Society of America.

A list of publications follow.

1. "Ultrasonic Propagation Properties of Mammalian Testes," Brady, J.K., Goss, S., Johnston, R., Dunn, F., O'Brien, W.D. JASA, 60, 1407-1409 (1976).

2. "Ultrasonic Properties of Mammlian Testes," Brady, J.K., Goss, S., Johnston, R., Dunn, F., O'Brien, W.D. Paper presented to the 91st Meeting of the Acoustical Society of America, Washington, D.C., April 1976. Abstract: JASA, 59, Supp. #1, 1976.

3. "Ultrasonic Toxicity Study of the Mouse Reproductive System and the Pregnant Uterus," Fry, F.J., Dunn, F., Brady, J.K., Erdman, W.D., Strang, P., Kohn, R., Baird, I., and Cobb, J. Paper presented to the AIUM Meeting, Winston-Salem, North Carolina, October 1975.

4. "Ultrasonically Produced Functional Alterations in Biological Systems," J.K. Brady and F. Dunn. Paper presented to the 87th Meeting of ASA, September 1974. Abstract: JASA, 55, Supplement, April 1974.

5. "Absorption of Ultrasound in Biological Media," F. Dunn, J.K. Brady. Biofizika, 18, No. 6, 1063-1066 (1973).

6. "Temperature and Frequency Dependence of Ultrasonic Absorption in Tissue," F. Dunn, J.K. Brady. Paper presented to the 8th International Congress on Acoustics, London, 1974.

7. Masters Thesis - 1972

   "Ultrasonic Dosage Studies as a Function of Frequency for the Mammalian Central Nervous System Tissue."

8. Ph.D. Thesis - 1977

   "A Preliminary Investigation of the Toxicological Effects of Ultrasound As Applied to the Gonads and In-Utero Fetus of the Mouse."